

INVESTIGATION OF SUBHARMONIC  
OSCILLATIONS IN  
NONLINEAR SECOND ORDER SYSTEMS

By

Emerson Carag Tangan



# United States Naval Postgraduate School



## THESIS

INVESTIGATION OF SUBHARMONIC  
OSCILLATIONS IN  
NONLINEAR SECOND ORDER SYSTEMS

by

Emerson Carag Tangan

December 1970

*This document has been approved for public release and sale; its distribution is unlimited.*

T138225



Investigation of Subharmonic Oscillations  
in  
Nonlinear Second Order Systems

by

Emerson Carag Tangan  
Lieutenant Commander, Philippine Navy  
B.S., Philippine Military Academy, 1958

Submitted in partial fulfillment of the  
requirements for the degree of

MASTER OF SCIENCE IN ELECTRICAL ENGINEERING

from the

NAVAL POSTGRADUATE SCHOOL  
December 1970



## ABSTRACT

A nonlinear control system sometimes oscillate at a frequency that is an integral submultiple of the driving frequency in response to a sinusoidal input. Such a response is undesirable. An analog computer study is undertaken to investigate the occurrence of subharmonic oscillation in second order systems with nonlinearities characterized by saturation and hysteresis effects.





## TABLE OF CONTENTS

I.	INTRODUCTION -----	10
	A. NONLINEAR SYSTEMS -----	10
	B. SUBHARMONIC OSCILLATIONS -----	11
II.	DUAL-INPUT DESCRIBING FUNCTION -----	13
III.	SYSTEM NONLINEARITIES -----	21
	A. SATURATION -----	21
	B. NON-IDEAL RELAY -----	21
	C. BACKLASH -----	23
IV.	SUBHARMONIC GENERATION -----	30
V.	DISCUSSION -----	32
	A. SYSTEM WITH SATURATION NONLINEARITY -----	32
	B. SYSTEM WITH NON-IDEAL RELAY -----	50
	C. SYSTEM WITH TWO NONLINEARITIES -----	60
VI.	CONCLUSIONS -----	68
	APPENDIX A: PROGRAM SYMBOLS -----	71
	APPENDIX B: ANALOG SIMULATION -----	73
	COMPUTER OUTPUTS -----	79
	LIST OF REFERENCES -----	102
	INITIAL DISTRIBUTION LIST -----	103
	FORM DD 1473 -----	104



## LIST OF TABLES

### Table

V-1a	Range of input frequencies that sustain subharmonic oscillation. Data obtained from results of analog computer simulation. -----	36
V-1b	Range of input frequencies for subharmonic oscillation for input amplitude = 22 volts, 30 volts, and 40 volts. -----	37
V-2	Output amplitude of system with saturation; $\zeta=0.02$ -	38
V-3	Amplitude of system response and error signal for system with saturation level $\pm 1$ -----	48
V-4	Simulation data for non-ideal relay; $a = 1$ , $c = 0.2$ -	55
V-5	Simulation for non-ideal relay (continuation) -----	56
V-6	Domains of subharmonic for system with two nonlinearities; $\zeta = 0.283$ , $\omega_n = 14.14$ -----	63
V-7	Range of input frequencies for subharmonic oscillation data (two nonlinearities) $\omega_n = 10$ -----	64



## LIST OF ILLUSTRATIONS

Figure		
III-1	System block diagrams. -----	22
III-2	Simulation output for nonlinearities. -----	25
III-3a	Block diagram of second order system with saturation. -----	26
III-3b	Analog simulation using digital logic for simulation of saturation. -----	26
III-4a	Second order system with non-ideal relay.-----	27
III-4b	Analog simulation of system with relay. -----	27
III-5a	Second order system with two nonlinearities. ---	28
III-5b	Analog simulation of system with two nonlinearities. -----	29
V-1	The 28-Degree Criterion. -----	33
V-2	Area for occurrence of 1/3 subharmonic for symmetric saturation. -----	35
V-3	Domain of 1/3 subharmonic oscillation for symmetrical saturation; $\zeta = 0.02$ . -----	39
V-4	Output amplitude for 1/3 subharmonic due to saturation. Input amplitude = 3 volts. -----	41
V-5	Output amplitude for 1/3 subharmonic due to saturation. Input amplitude = 16 volts. -----	42
V-6	Domains of subharmonic for asymmetrical saturation. Input amplitude = 6 volts. -----	44
V-7a	Describing function loci for $A = 4$ . -----	46
V-7b	Describing function loci for $B = 8$ . -----	47
V-8	Amplitude of 1/3 subharmonic oscillation for saturation level = $\pm 1$ . -----	49
V-9	Describing function for relay with hysteresis. -	52



V-10	Bode plot of $G(s) = \frac{1}{s^2 + s + 1}$ -----	53
V-11	Domain of subharmonic output for system with relay; $a = 1$ , $c = 0.2$ . -----	57
V-12	Domain of subharmonic output. -----	59
V-13	Domains of subharmonic oscillation for system with saturation and backlash; $\zeta = 0.212$ , $\omega_n = 7.07$ . -----	65
V-14	Domains of subharmonic oscillation for system with saturation and backlash; $\zeta = 0.2$ , $\omega_n = 10.0$ . -----	66
V-15	Domains of subharmonic oscillation for system with two nonlinearities; $\zeta = 0.141$ , $\omega_n = 14.14$ -	67
B-1a	Saturation characteristic curve. -----	74
B-1b	Analog simulation for saturation. -----	74
B-2a	Characteristic curve of relay with hysteresis.-	76
B-2b	Analog simulation of relay with hysteresis. ---	76
B-2c	Analog circuit of track-track (T/T) unit. -----	76
B-3a	Backlash characteristic curve. -----	78
B-3b	Analog simulation for backlash. -----	78
C-1	1/2 subharmonic oscillation due to asymmetric saturation. -----	79
C-2	Fundamental to 1/2 subharmonic due to asymmetric saturation. -----	80
C-3	1/3 subharmonic oscillation due to symmetrical saturation. -----	81
C-4	1/3 subharmonic oscillation to fundamental oscillation. -----	82
C-5	1/3 subharmonic oscillation due to saturation.-	83





C-6	Fundamental oscillation to 1/3 subharmonic oscillation for relay. -----	84
C-7	1/3 to 1/4 subharmonic oscillation due to relay with hysteresis; $a = 1$ , $c = 0.3$ . -----	85
C-8	1/3 to 1/5 order subharmonic for system with relay; $a = 1$ , $c = 0.1$ . -----	86
C-9	Change of input frequency from 1.5hz to 1.3hz to 1.2hz resulting in change of subharmonic oscillation from 1/5 to 1/4 to 1/3; $a = 1$ , $c = 0.1$ . -----	87
C-10	1/5 subharmonic oscillation to fundamental oscillation; $a = 1$ , $c = 0.01$ . -----	88
C-11	1/5 to 1/7 subharmonic oscillation for relay; $a = 1$ , $c = 0.1$ . -----	89
C-12	1/7 to 1/5 subharmonic oscillation. -----	90
C-13	Change of input frequency from 3.2 hz to 3.4 hz causing change of subharmonic oscillation from 1/7 to 1/9. -----	91
C-14	1/9 to 1/7 subharmonic for Relay, $a = 1$ , $c = 0.1$ . -----	92
C-15	1/11 to 1/9 subharmonic oscillation. -----	93
C-16	Output oscillating at two different subharmonic 1/11 and 1/13 at same input frequency of 5.5 hz-	94
C-17	Singal waveforms of system with two nonlinearities; $\zeta = 0.387$ . -----	95
C-18	Signal waveforms for 1/5 subharmonics oscillation. -----	96
C-19	Fundamental oscillation to 1/3 subharmonic oscillation for systems with saturation and backlash. -----	97
C-20	1/3 subharmonic oscillation build up with input $9 \sin 6.6 \pi t$ for saturation and backlash. -----	98
C-21	Build up of 1/7 subharmonic. -----	99



C-22	1/3 subharmonic oscillation fading to fundamental oscillation due to change of input frequency from 1.3 hz to 1.4 hz. -----	100
C-23	Signal waveforms showing change of subharmonic mode from 1/4 to 1/5. -----	101



## ACKNOWLEDGEMENT

The author wishes to express his sincere appreciation and indebtedness to Doctor George J. Thaler for the topic, guidance, and assistance which he provided during the pursuit of this study and the preparation of this thesis.



## I. INTRODUCTION

### A. NONLINEAR SYSTEMS

A system is said to be linear if its performance obeys the "Principle of Superposition". The "Principle of Superposition" states that if  $C_1(t)$  and  $C_2(t)$  are the responses of a system when it is separately subjected to two inputs  $R_1(t)$  and  $R_2(t)$ , respectively, then for all  $a$  and  $b$ , the response of the system to the input  $aR_1(t)+bR_2(t)$  is  $aC_1(t)+bC_2(t)$  and this must hold for all inputs. In other words, once the response to one type of signal is known, the response to any other signal can be deduced directly.

On the other hand, any system is said to be nonlinear if the "Principle of Superposition" does not hold. The term nonlinear systems applies to varied types of systems which have practically nothing in common with one another. As a consequence, there is no way of generalizing the responses of nonlinear systems for a class of inputs to the response for any other inputs. The response to one type of input does not necessarily contain sufficient information about the response to some other input. Even two inputs which are of the same waveshape but different in amplitude can give responses that are entirely different. This makes the study of nonlinear systems quite difficult. Even with this difficulty, there is little choice except to tackle the problem in some way because nonlinear systems occupy a very important role in practical systems.





There is a great variety of possible nonlinear characteristics, and there are different ways by which nonlinear systems are classified. One classification is of a mathematical kind based on the equations involved, however the study of nonlinear systems on a mathematical basis is extremely difficult. In this study, types of nonlinearities encountered in servo systems are considered, namely saturation and hysteresis effects. The consideration of nonlinear elements in the operation of control systems have practical significance because it takes linear theory nearer to reality.

#### B. SUBHARMONIC OSCILLATIONS

A linear system when subjected with a sinusoidal input produces a steady-state output which is also a sinusoid and oscillates at a frequency equal to the input frequency but may differ from the input in amplitude and phase. This is true for all frequencies. However, for a system with suitable nonlinear characteristic when subjected to a sinusoidal input, there is no guarantee that the steady-state output is also a sinusoid. In the usual case, the output wave contains frequency components which are integral multiples of the input frequency. Also, the system can produce a response which oscillates at a frequency which is an integral submultiple of the input frequency. This frequency response phenomenon is known as "subharmonic resonance". When the frequency of the output is  $1/n$  times the driving frequency, where  $n$  is an integer, then the output



oscillation may be called the  $1/n$  order subharmonic oscillation. When the output oscillates with the input frequency, the output oscillation is called the fundamental oscillation.

The subharmonic phenomenon is of a resonant nature and because of this, the subharmonic component is often of large amplitude which causes the system output to bear little resemblance to a sinusoid of the input frequency. The output is considerably different from that obtained when the subharmonic phenomenon does not occur. For systems in which the output is intended to reproduce the input as closely as possible, as in the motion of a loudspeaker cone or of a servo motor, this phenomenon can cause a distortion that cannot be tolerated. In the field of feedback control systems, it is interesting to know the conditions under which subharmonic oscillations may occur. Subharmonic oscillations can give false information which can be troublesome, so it is desirable to eliminate the possibility of the occurrence of subharmonic oscillations. This is true in the case of recording seromechanisms which are frequently subjected to periodic inputs. The possibility of the occurrence of the subharmonic oscillations reduces the reliability of the systems.



## II. DUAL-INPUT DESCRIBING FUNCTION

The requirement that a nonlinearity be described by an equation in the frequency domain and that this equation be compatible for use with the transfer function of the linear components gave rise to approximating the effects of the nonlinear component by using a linear "approximate transfer function" or describing function. The approximation is made by defining the describing function in terms of the Fourier series for the component response to a sinusoidal input.

The describing function is defined as the ratio of the magnitude of the fundamental term in the Fourier series for the output wave to the magnitude of the input sinusoid at a phase angle which is the angle between the two sine waves and for all permissible amplitude and frequency of the input wave [Ref. 9]. In mathematical form, let the input be  $A\sin\omega t$  and the fundamental frequency term in the Fourier series for the output waveform is

$$F(A,\omega)\sin[\omega t + \phi(A,\omega)],$$

then the describing function for the nonlinear component is

$$DF = \frac{|F(A,\omega)|}{|A|} \quad / \phi(A,\omega)$$



Therefore, the describing function is but a mathematical linearization of a nonlinearity in the presence of a sinusoidal input. In analysis this sinusoid is physically identified as the system limit cycle and the describing function is used to predict its amplitude and frequency. The use of the describing function is based on the assumption that harmonics generated by the nonlinear characteristics are sufficiently filtered before being fed as input to the nonlinear element.

An extension of the describing function technique is the consideration of a more complex signal fed to the nonlinear element. The first extension is the use of dual-frequency signal,

$$v_i = a \cos(\omega t + \phi) + b \cos n\omega t$$

as input signal to the nonlinearity with the restriction that  $a$ ,  $b$ , and  $n$  must be real. The dual-input describing function can be defined as the ratio of the amplitude of the desired frequency component in the output waveform to the amplitude of the component of the same frequency in the input waveform. Therefore, in the determination of the dual-input describing function it is necessary to find the output waveform of the nonlinear element for an input composed of two sinusoidal signals and analyze the output to find the components of a particular frequency. In the systems considered here, these signals are composed of that component due to the input signal at a fixed frequency





and the component due to the fed back signal which may be of different frequency from the input signal. It is again assumed that the harmonics of the signal fed back are adequately filtered. The concept of the describing function is thus extended to allow for an input signal composed of two sinusoidal signals of different amplitudes and frequencies.

To illustrate the derivation of the dual-input describing function, consider the cubic characteristic,

$$y = x^3$$

Let the input be of the form

$$x = A \sin n\omega t + B \sin (\omega t + \theta)$$

where

A and B are independent amplitudes,

$\omega$  and  $n\omega$  are any two values of frequencies, and

$\theta$  is an independent phase angle.

Substituting the value of x in the nonlinear equation, the result is,

$$\begin{aligned} y &= [A \sin n\omega t + B \sin (\omega t + \theta)]^3 \\ &= A^3 \sin^3 n\omega t + 3A^2 B \sin^2 n\omega t \sin(\omega t + \theta) \\ &\quad + 3AB^2 \sin n\omega t \sin^2(\omega t + \theta) + B^3 \sin^3(\omega t + \theta) \end{aligned}$$



Using trigonometric identities to express the above expression as a series of sine waves of fundamental and harmonic frequencies results in

$$\begin{aligned}
 y = & A^3 \left[ \frac{3}{4} \sin n\omega t - \frac{1}{4} \sin 3n\omega t \right] \\
 & + 3A^2B \left[ \frac{1}{2} \sin(\omega t + \theta) - \frac{1}{4} \sin\{(2n+1)\omega t + \theta\} \right. \\
 & \quad \left. + \frac{1}{4} \sin\{(2n-1)\omega t - \theta\} \right] \\
 & + 3AB^2 \left[ \frac{1}{2} \sin n\omega t - \frac{1}{4} \sin \{(n+2)\omega t + 2\theta\} \right. \\
 & \quad \left. - \frac{1}{4} \sin \{(n-2)\omega t - 2\theta\} \right] \\
 & + B^3 \left[ \frac{3}{4} \sin (\omega t + \theta) - \frac{1}{4} \sin 3(\omega t + \theta) \right]
 \end{aligned}$$

or

$$\begin{aligned}
 y = & \frac{3A}{4} (A^2 + 2B^2) \sin n\omega t - \frac{A^3}{4} \sin 3n\omega t \\
 & + \frac{3B}{4} (B^2 + 2A^2) \sin(\omega t + \theta) - \frac{B^3}{4} \sin 3(\omega t + \theta) \\
 & + \frac{3A^2}{4} \left[ \sin\{(2n-1)\omega t - \theta\} - \sin\{(2n+1)\omega t + \theta\} \right] \\
 & - \frac{3AB^2}{4} \left[ \sin\{(n+2)\omega t + 2\theta\} + \sin\{(n-2)\omega t - 2\theta\} \right]
 \end{aligned}$$



By inspection of the above expression, the sum of the first and third terms is the fundamental input function equation,  $x$  multiplied by the factors  $\frac{3}{4}(A^2+2B^2)$  and  $\frac{3}{4}(B^2+2A^2)$ . For the other terms, there are values of  $n$  which have to be considered as will be explained in succeeding paragraphs. Consider the following cases:

(1). Non-harmonically related input sinusoids. In this case  $n$  is irrational, i.e.,  $n$  is not expressible as a ratio of two integers. In the problem being considered,  $n \neq 1/3, 1, \text{ or } 3$ . For the frequency  $n\omega/2\pi$ , the dual-input describing function is:

$$N_A(A,B) = \frac{\frac{3}{4} A(A^2+2B^2) \sin n\omega t}{A \sin n\omega t}$$

$$N_A(A,B) = \frac{3}{4} (A^2+2B^2)$$

and for frequency  $\omega/2\pi$ , the dual-input describing function is:

$$N_B(A,B) = \frac{\frac{3}{4} B(B^2+2A^2) \sin(\omega t+\theta)}{B \sin(\omega t+\theta)}$$

$$N_B(A,B) = \frac{3}{4} (B^2+2A^2)$$

The resulting dual-input describing functions,  $N_A(A,B)$  and  $N_B(A,B)$  are both independent of the phase angle,  $\theta$  but dependent on the input signal amplitudes  $A$  and  $B$ .

The dual-input describing function is modified if  $n$  assumes a value such that the other terms in the series



have the frequency of either of the input signals  $\omega/2\pi$  or  $n\omega/2\pi$ , i.e.,  $n = 1/3, 1$ , or  $3$ .

(2). Harmonically related input sinusoids.

(a)  $n = 3$ . For this case there are two additional terms in the output waveform,  $y$  that is considered, i.e., the fourth and eight terms, such that the dual-input describing function becomes

$$N_A(A, B, 3, \theta) = \frac{\frac{3A}{4} (A^2 + 2B^2) \sin 3\omega t - \frac{B^2}{4} \sin(3\omega t + 3\theta)}{A \sin 3\omega t}$$

The above expression shows that varied phase angles are associated with the terms, so the phasor representation is utilized, then

$$N_A(A, B, 3, \theta) = \frac{\frac{3}{4} A (A^2 + 2B^2) e^{j3\omega t} - \frac{B^2}{4} e^{j(3\omega t + 3\theta)}}{A e^{j3\omega t}}$$

$$N_A(A, B, 3, \theta) = \frac{3}{4} (A^2 + 2B^2) - \frac{B^2}{4A} e^{j3\theta}$$

Similarly for

$$N_B(A, B, 3, \theta) = \frac{\frac{3B}{4} (B^2 + 2A^2) e^{j(\omega t + \theta)} - \frac{3AB^2}{4} e^{j(\omega t - 2\theta)}}{B e^{j(\omega t + \theta)}}$$

$$N_B(A, B, 3, \theta) = \frac{3}{4} (B^2 + 2A^2) - \frac{3AB}{4} e^{-j3\theta}$$

The resulting dual-input describing functions are complex and dependent on  $A$ ,  $B$ , and  $\theta$ . The resulting DIDFs for the other two cases,  $n=1$  and  $n=1/3$  as shown in the succeeding derivations are also complex and dependent on  $A$ ,  $B$ , and  $\theta$ .





(b)  $n=1$ . For this case,  $N_A$  and  $N_B$  combine to give terms of frequency  $\omega/2\pi$ . Proceeding in the same manner as for the case  $n=3$ ,

$$N_A(A, B, 1, \theta) = \frac{\frac{3}{4} A(A^2 + 2B^2) e^{j\omega t} + \frac{3B}{4} (B^2 + 2A^2) e^{j(\omega t + \theta)}}{A e^{j\omega t}} + \frac{\frac{3A^2 B}{4} e^{j(\omega t - \theta)} + \frac{3AB^2}{4} e^{j(\omega t + 2\theta)}}{A e^{j\omega t}}$$

$$N_A(A, B, 1, \theta) = \frac{3}{4} (A^2 + 2B^2) + \frac{3B^2}{4A} (B^2 + 2A^2) e^{j\theta} + \frac{3B^2}{4} e^{-j\theta} + \frac{3B^2}{4} e^{j2\theta}$$

$$N_B(A, B, 1, \theta) = \frac{\frac{3}{4} A(A^2 + 2B^2) e^{j\omega t} + \frac{3B}{4} (B^2 + 2A^2) e^{j(\omega t + \theta)}}{B e^{j(\omega t + \theta)}} + \frac{\frac{3A^2 B}{4} e^{j(\omega t - \theta)} + \frac{3AB^2}{4} e^{j(\omega t + 2\theta)}}{B e^{j(\omega t + \theta)}}$$

$$N_B(A, B, 1, \theta) = \frac{3A}{4B} (A^2 + 2B^2) e^{-j\theta} + \frac{3}{4} (B^2 + 2A^2) + \frac{3A^2}{4} e^{-j2\theta} + \frac{3AB}{4} e^{j\theta}$$

(c)  $n = 1/3$ . This case is identical with the case for  $n=3$ .



$$N_A(A, B, 1/3, \theta) = \frac{\frac{3A}{4} (A^2 + 2B^2) e^{j(\omega t/3)} - \frac{3A^2 B}{4} e^{j(\omega t/3 + \theta)}}{A e^{j(\omega t/3)}}$$

$$N_A(A, B, 1/3, \theta) = \frac{3}{4} (A^2 + 2B^2) - \frac{3AB}{4} e^{j\theta}$$

$$N_B(A, B, 1/3, \theta) = \frac{-\frac{A^3}{4} e^{j\omega t} + \frac{3B}{4} (B^2 + 2A^2) e^{j(\omega t + \theta)}}{B e^{j(\omega t + \theta)}}$$

$$N_B(A, B, 1/3, ) = -\frac{A^3}{4B} e^{-j\theta} + \frac{3}{4} (B^2 + 2A^2)$$



### III. SYSTEM NONLINEARITIES

In most practical feedback systems, the nonlinear element is in the forward path. The basic system considered in this study is shown in Figure III-1a, where  $N$  is the nonlinear element whose gain depends on the magnitude of the input to this element and  $G(s)$  is the linear frequency dependent portion.

#### A. SATURATION

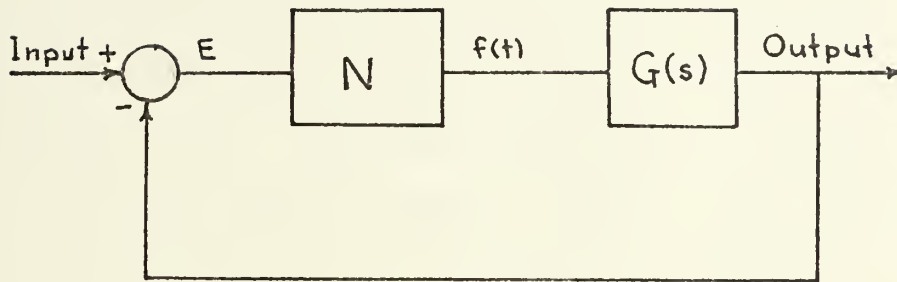
The nonlinearities considered here are saturation, relay with hysteresis and backlash. Most physical systems contain certain nonlinearities. The most common nonlinear phenomenon is characterized by a saturating or limiting characteristic. Limiting is almost universally present in control systems since most instrumented signals can take values only in a bounded range. Many error detectors, such as a resolver or synchro differential have a restricted range of linearity. The saturation phenomenon is also present in amplifiers, whether electron tubes, transistors, magnetic amplifiers or other devices are used. The input-output characteristic is shown in Figure III-1b.

#### B. NON-IDEAL RELAY

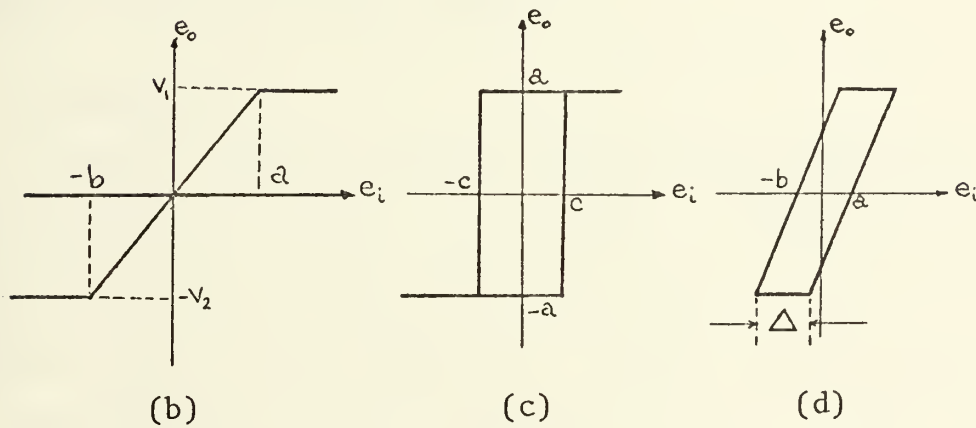
The other nonlinearity is the relay with hysteresis which is characterized by the curve shown in Figure III-1c. The hysteresis delays the switching operation until the



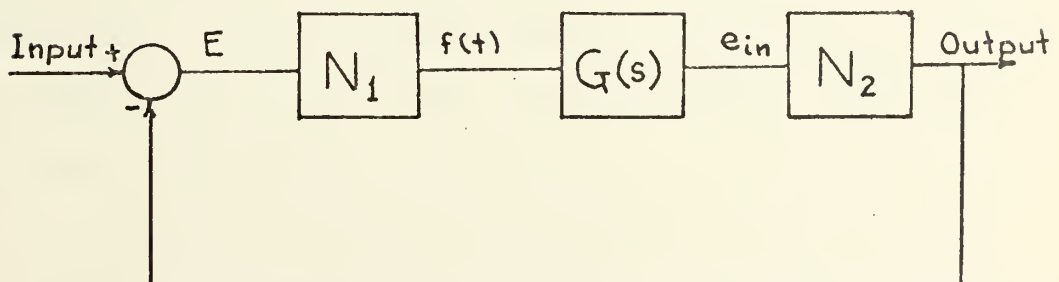
NONLINEAR ELEMENT      LINEAR ELEMENT



(a) Block diagram of basic system.



NONLINEAR      LINEAR      NONLINEAR



(e) Basic system with two nonlinear elements.

FIGURE III-1: System block diagrams.





output is past the desired zero point. A system using this type of relay must have a limit cycle in steady state.

The relay is a device to apply the power which drives the load. In a relay control system, the power amplifier is a relay device. The relay amplifier is desirable because it can be simple, rugged, compact, and relatively cheap, while meeting high load power requirements. Examples where relay control systems are typically applied are in space vehicle attitude control and aircraft and missile adaptive control systems.

### C. BACKLASH

Another commonly encountered nonlinear phenomenon in most mechanical linkages is backlash. In control systems these are present in most mechanical gears. This is true even for new ones and with use, the backlash increases. In simple physical terms, backlash in gears is the free space between adjacent teeth. It occurs whenever there is inexact linkage between mechanical parts, i.e., when there is slack between mating gears. The backlash characteristic is shown in Figure III-1d, where  $\Delta$  represents the amount of backlash.

In one way or another, linear and nonlinear systems will encounter the backlash problem if they have a gear train. In the field of control systems, a system is included in the class of unstable systems if it continuously oscillates with constant amplitude and zero input (limit

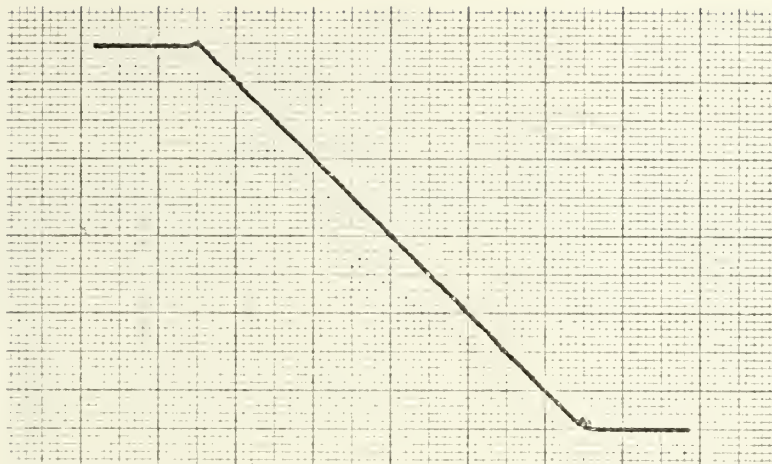


cycle). Thaler and Pastel [Ref. 9] show that for a second order servo with backlash, the existence of the limit cycle depends on the value of the damping factor,  $\zeta$ . For  $\zeta \geq 0.29$ , the system is stable so that for  $\zeta < 0.29$  the effect of backlash is to cause an unstable character. If the phase portrait is drawn for the system, the phase portrait will show the backlash effect near the origin. For systems where it is desired to have the phase trajectories terminate at the origin, the backlash effect causes serious trouble.

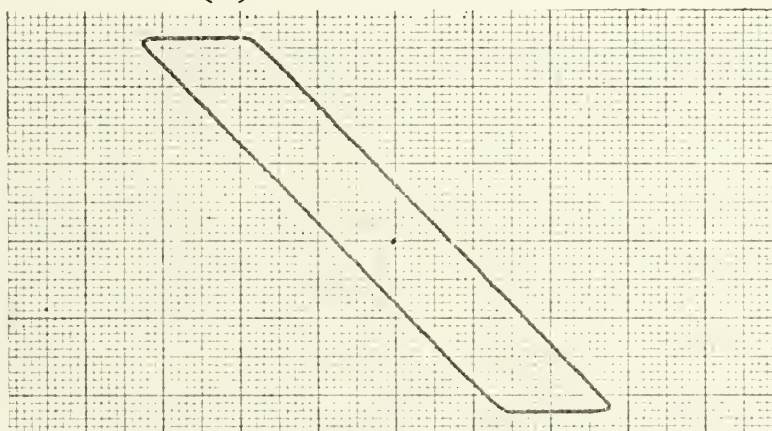
The three nonlinearities discussed above were simulated on the electronic analog computer. The operation of the simulators for the nonlinearities are explained in Appendix B. The characteristics of the nonlinearities were produced very nicely as shown in Figure III-2.

Figures III-3, III-4, and III-5 show the block diagrams of the second order systems with the indicated nonlinearity which were simulated on the analog computer.

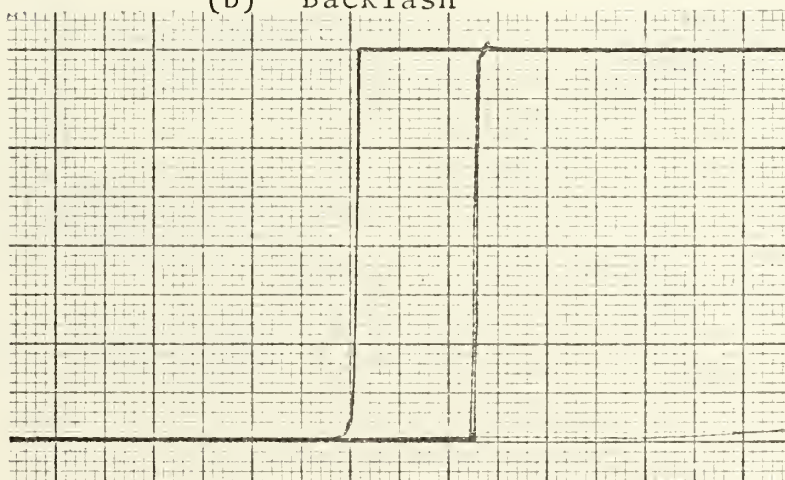




(a) Saturation



(b) Backlash



(c) Relay with Hysteresis

FIGURE III-2: Simulation output for nonlinearities.



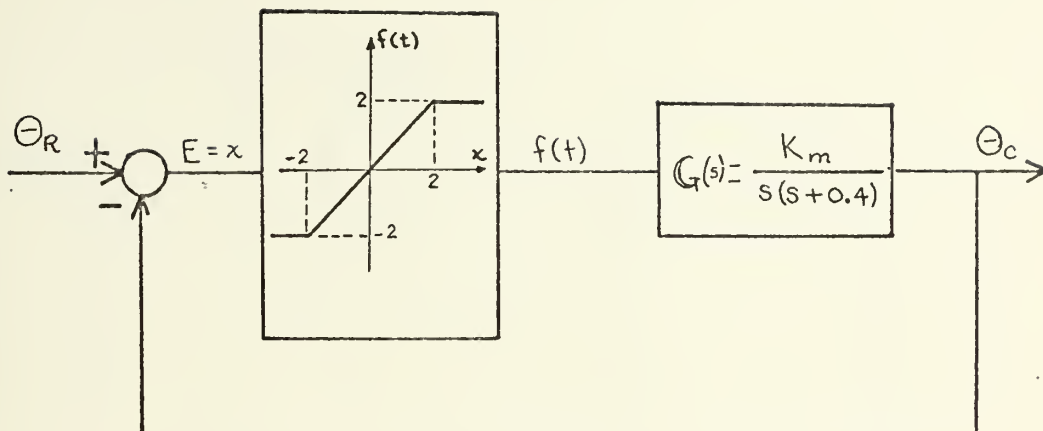


FIGURE III-3a: Block diagram of second order system with saturation.

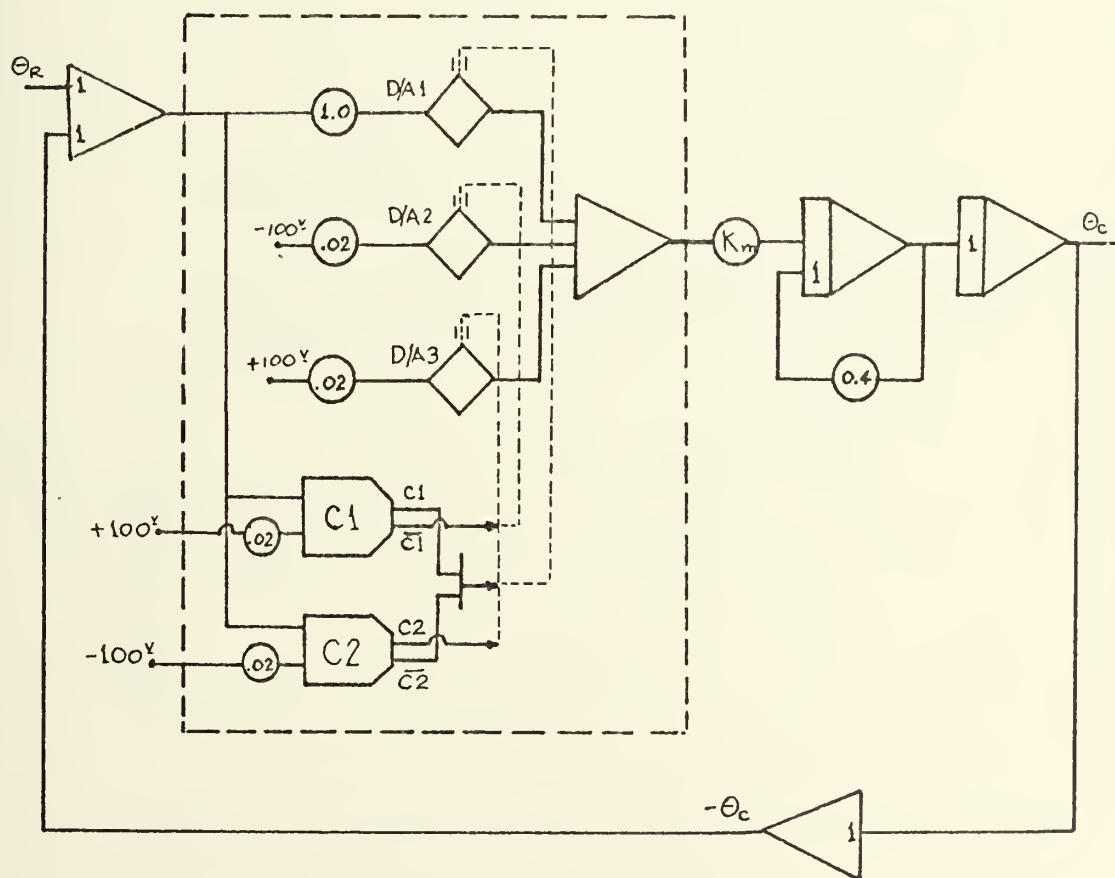


FIGURE III-3b: Analog simulation using digital logic for simulation of saturation.





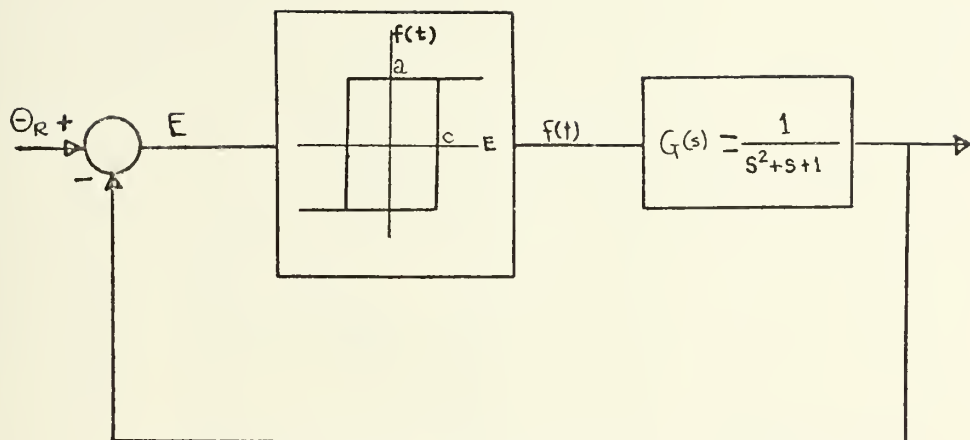


FIGURE III-4a: Second order system with non-ideal relay.

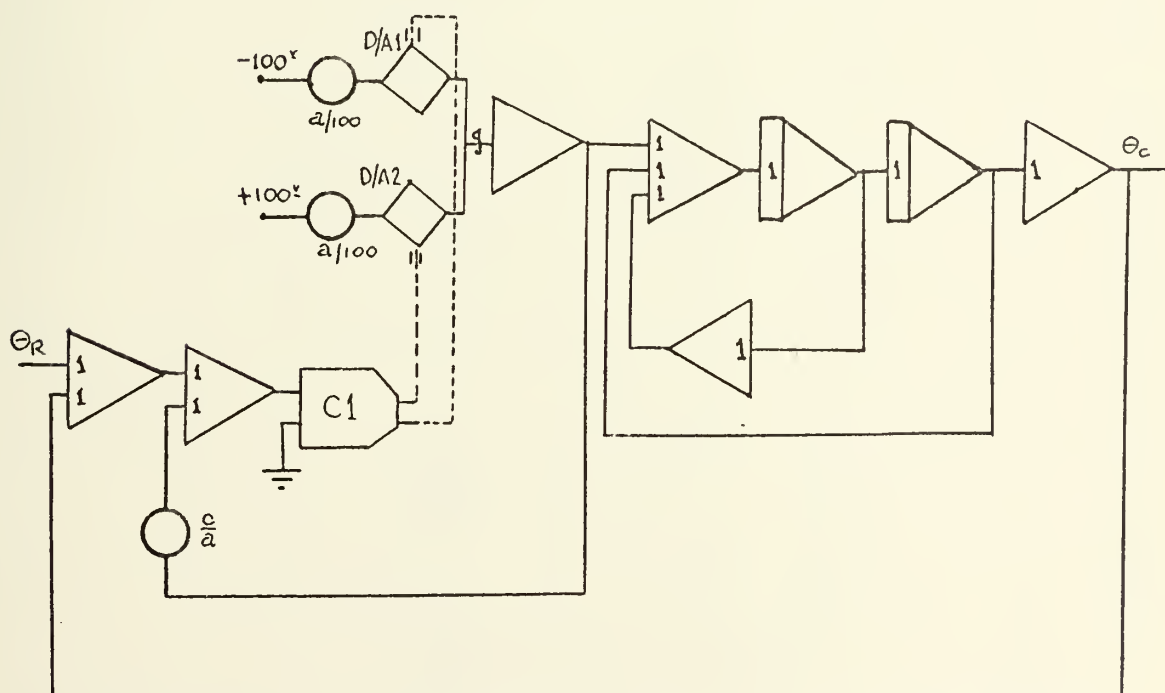


FIGURE III-4b: Analog simulation of system with relay.



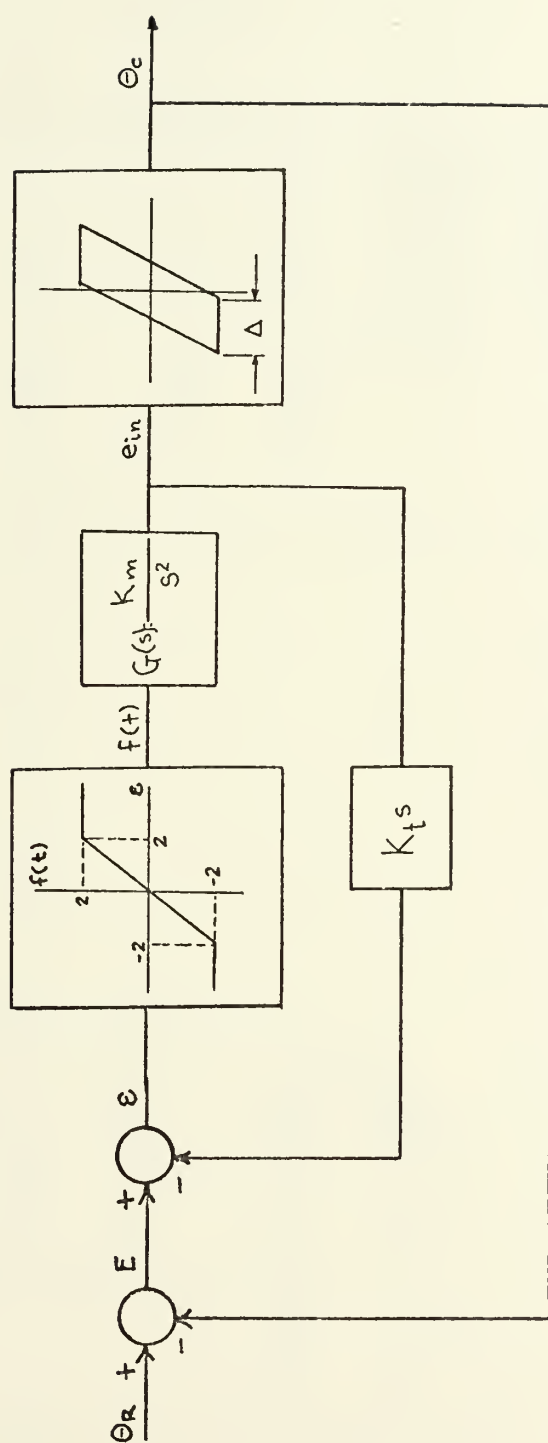


FIGURE III-5a: Second order system with two nonlinearities.



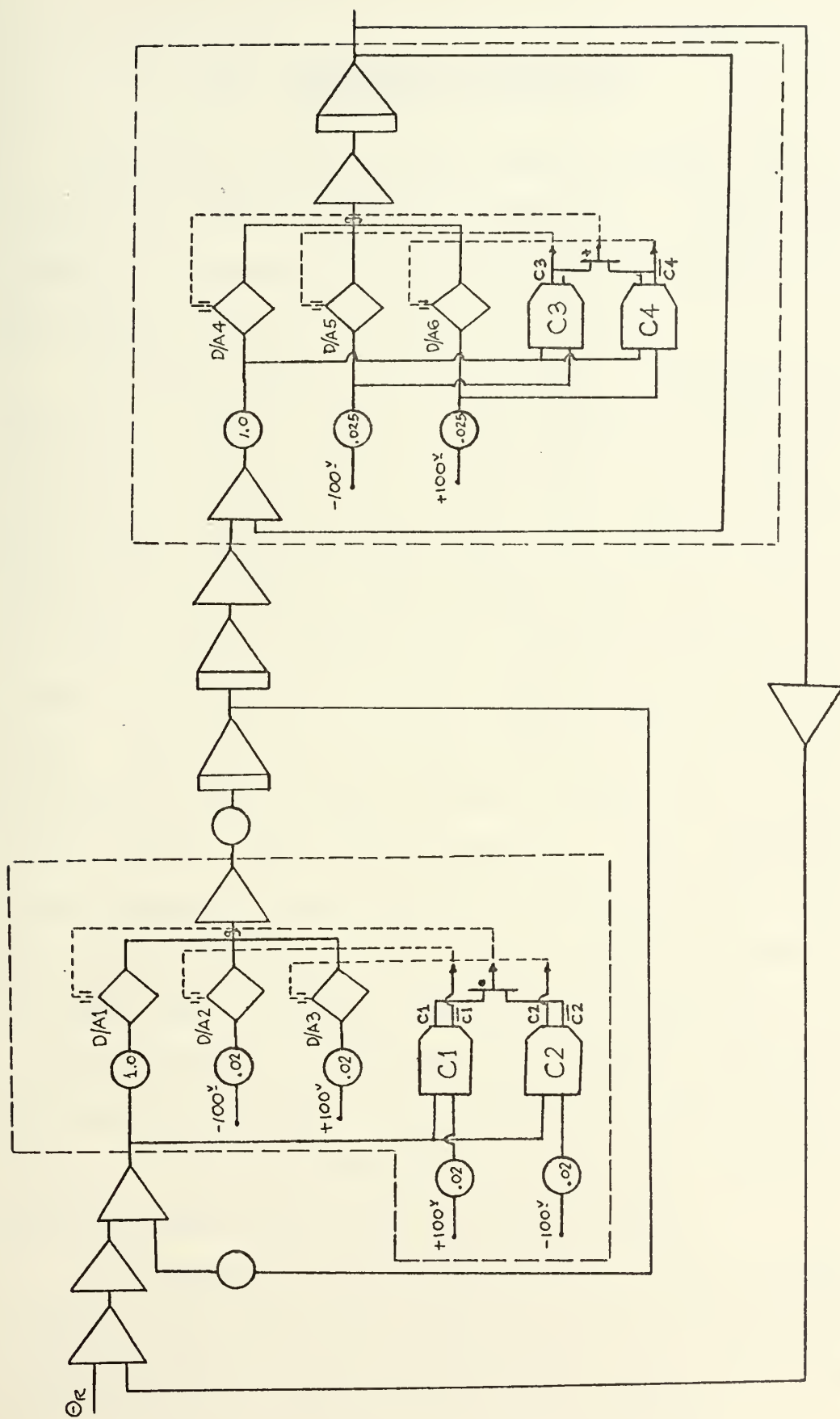


FIGURE III-5b: Analog simulation of system with saturation and backlash.



#### IV. SUBHARMONIC GENERATION

Consider the basic system shown in Figure III-1a with a nonlinear element in the forward path. If the nonlinear element is replaced by an element of unity gain, the resulting linear system is assumed to be stable.

As stated earlier, the "Principle of Superposition" applies to linear systems. The response of the closed loop system to a given signal is independent of any other signal which may be applied at the same time. When a nonlinear element is included in the feedback loop this is no longer the case. The response of the nonlinear element to a given signal is modified if another signal is applied at the same time. The effect of the other signal may be considered as varying the gain of the nonlinear element for the primary input signal. The case of interest is when the additional signal input is also sinusoidal with a frequency that is an integral multiple of the primary input frequency. In this case, the output component of the angular frequency,  $\omega$  may be modified in amplitude and phase by the presence of the additional input. This modifies the loop gain of the system. The phase change is caused by the intermodulation products generated by the nonlinear element.

The stability of the closed loop system is affected by varying the gain of the nonlinear element since the nonlinear element is a part of the feedback loop. For a range of





sinusoidal inputs, the response of the nonlinear element may be so modified that the closed loop is rendered oscillatory. Where the system is such that the open-loop frequency response plotted on the complex plane do not intersect with the negative real axis, the nonlinear elements have to introduce an adequate phase change in order that stable oscillation can occur. This implies that the frequency of the oscillation must be related to the input frequency. What is of interest here is where the frequency of the oscillation is an integral submultiple of the primary input frequency in which case subharmonic oscillation is generated.



## V. DISCUSSION

The systems shown in Figures III-3, III-4, and III-5 with the indicated nonlinearities were simulated to investigate the occurrence of subharmonic oscillations and to observe the effect of changing the variable parameters in the systems such as, the damping factor,  $\zeta$  and forward linear gain,  $K_m$  in Figures III-3 and III-5 and the amount of hysteresis,  $2c$  in Figure III-4, in the generation of subharmonic oscillation.

### A. SYSTEM WITH SATURATION NONLINEARITY

Figure III-3a shows a second order system with a saturation nonlinearity. The nonlinear characteristic is defined as:

$$\begin{aligned}e_o &= e_i & -2 < e_i < 2 \\e_o &= 2 & e_i > 2 \\e_o &= -2 & e_i < -2\end{aligned}$$

and the gain of the linear portion of the saturation is unity. The transfer function of the linear part is,

$$G(s) = \frac{K_m}{s(s + 0.4)}$$

Considering the linear part, the closed loop transfer function is

$$\frac{\theta_c}{\theta_R} = \frac{K_m}{s^2 + 0.4s + K_m}$$



with characteristic equation

$$s^2 + 0.4s + K_m = 0$$

The natural frequency,  $\omega_n$  and the damping factor,  $\zeta$  is determined from the following relationships:

$$\omega_n = \sqrt{K_m}$$

$$\zeta = \frac{0.4}{2\omega_n} = \frac{0.2}{\sqrt{K_m}}$$

In the simulation of the system in the electronic analog computer,  $K_m$  was varied from 1 to 100 giving a variation in  $\zeta$  from 0.2 to 0.02. Typical results obtained by the simulation are shown in Figures C-1 through C-5.

Ogata [Ref. 6] discussed an analysis of subharmonic responses in systems with a nonlinear element whose input-output characteristic curves shows saturating or limiting characteristics and showed that for nonlinear characteristic curves that are skew symmetric, odd-order subharmonic oscillations can occur.

The "28-degree criterion" for predicting responses of saturating feedback systems was introduced by Douce [Ref. 1]. In the complex plane, two lines are drawn from the point  $s = -1$  on each side of the negative real axis and each line makes an angle of  $28^\circ$ . This is illustrated in Figure V-1. The region bounded by the two lines represent the critical region for a system with saturation nonlinearity. Utilizing this, the Nyquist diagram of the linear part of the system



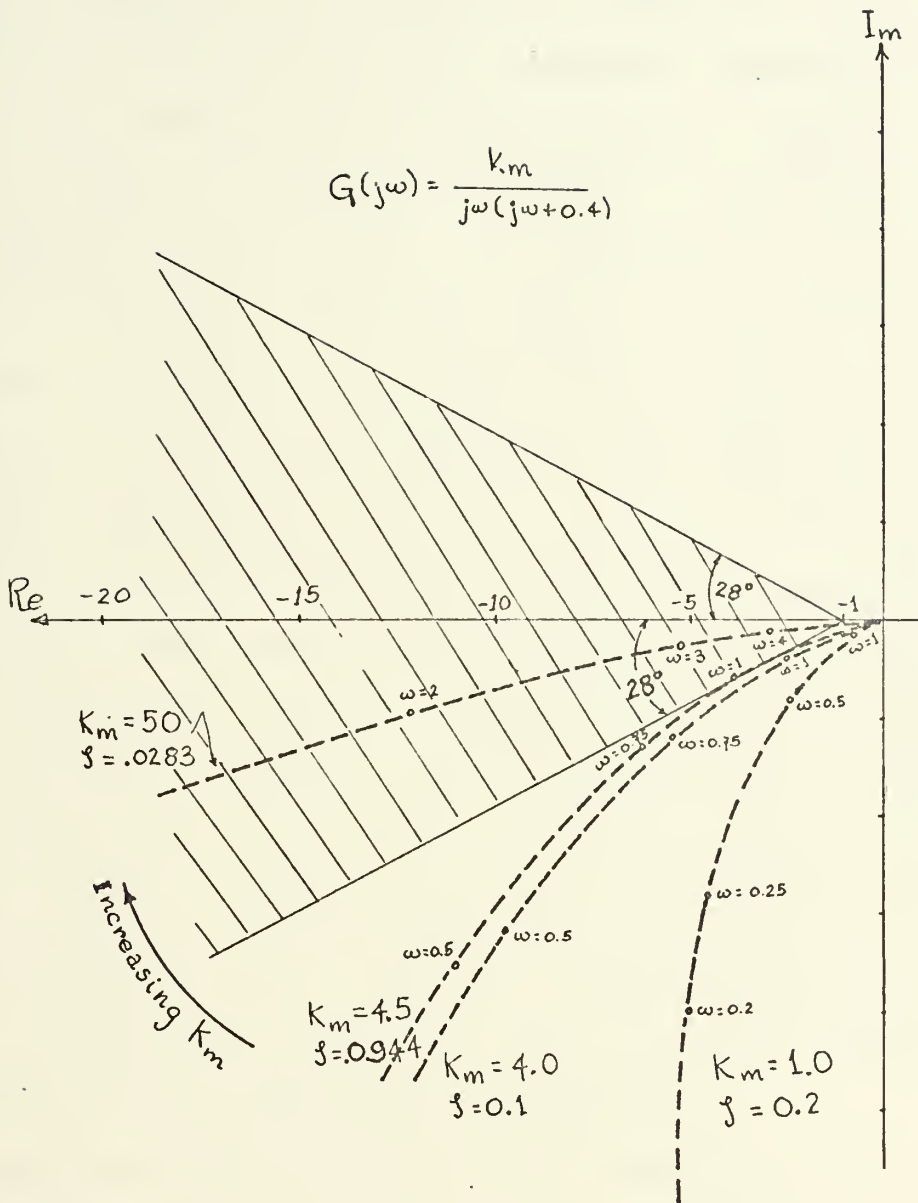


FIGURE V-1: The 28°-Criterion (Douce [Ref. 1]). Shaded area shows region where 1/3 subharmonic can be generated in systems containing a limiter. Dotted lines represent open loop frequency response of linear system with indicated value of  $K_m$ .





provides sufficient information to predict possible occurrence of subharmonic oscillations. Subharmonic resonance is possible when the open loop frequency response of the linear portion enters the critical region. Figure V-1 shows the open loop frequency response of the linear part for different values of  $K_m$ . Also indicated is the damping factor. The figure shows that for  $K_m < 4.5$  ( $\zeta > 0.0944$ ), the open loop frequency response of the linear portion lies outside the critical region so that subharmonic oscillation cannot occur. For  $K_m > 4.5$ , for example  $K_m = 50$ , the linear open loop frequency response is inside the critical region. The results of the analog computer study agree accurately with the "28-degree criterion" as can be seen in Figure V-2 which shows the domain of 1/3 subharmonic oscillation as a function of input frequency and damping factor,  $\zeta$ . The figure also shows the effect of input amplitude, i.e., for greater input amplitude, the domain decreases and the system has to be more lightly damped to sustain subharmonic oscillation.

Subharmonic oscillation of 1/3 order was the only one observed for the system with skew symmetric saturation non-linearity. Figure V-3 shows the domain of 1/3 subharmonic as a function of input amplitude and input frequency. It can be seen that the range of input frequency where subharmonic oscillation is sustained decreases with increasing input amplitude. The same observation can be seen in Figure V-2. It can be deduced that subharmonic oscillation



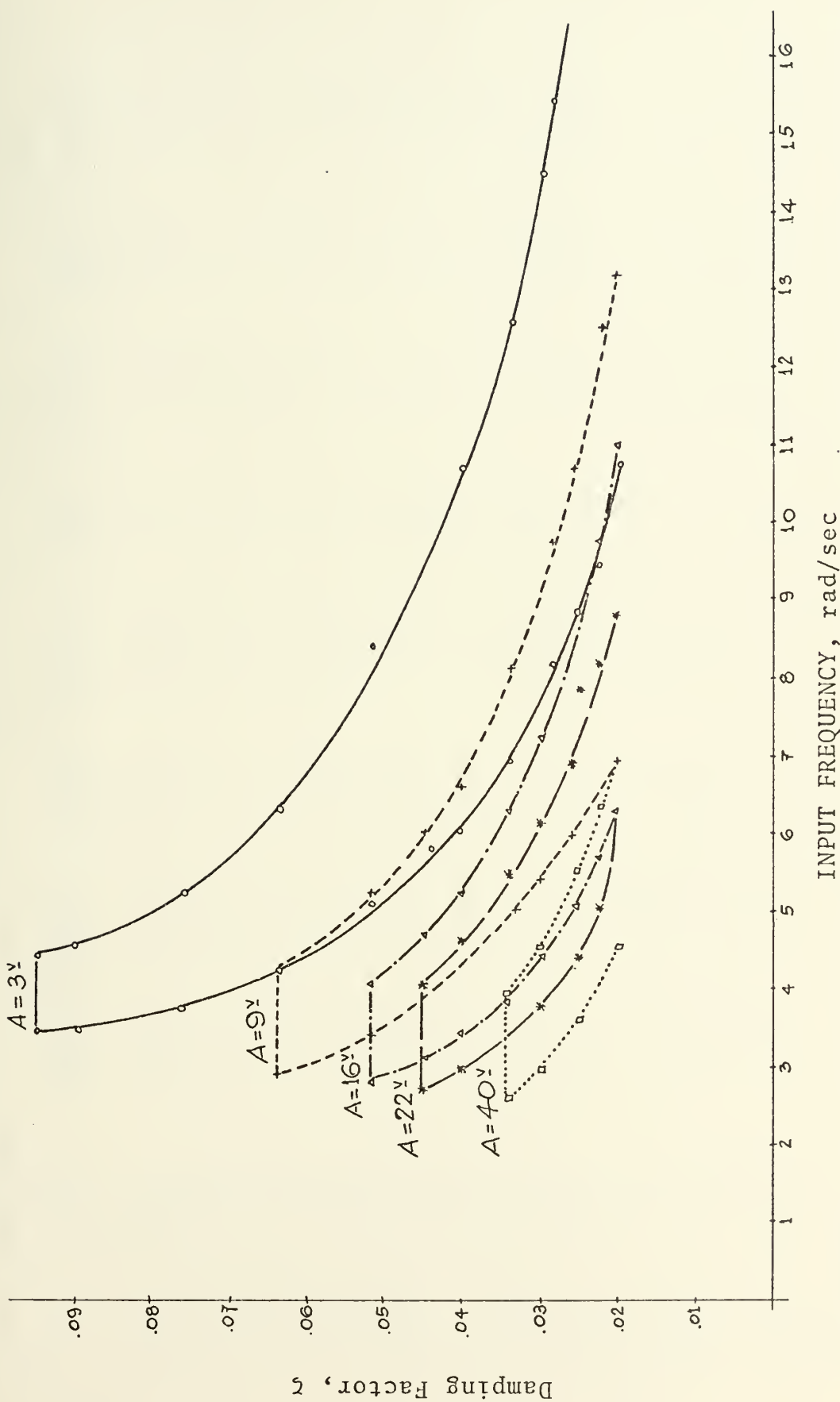


FIGURE V-2: Area for occurrence of  $1/3$  subharmonic for symmetric saturation. Graph shows relationship between input frequency and damping factor and input amplitude. Darkened marks are obtained by experiment.



INPUT AMPLITUDE		3 volts		6 volts		9 volts		16 volts	
$\tau$	$\omega_n$ rad/sec	Input Range.	Frequency rad/sec	Input Range.	Frequency rad/sec	Input Range.	Frequency rad/sec	Input Range.	Frequency rad/sec
0.02	10.00	10.68	21.67	8.16	16.64	6.91	13.19	6.28	10.99
0.0224	8.94	9.42	19.47	7.54	14.44	6.28	12.56	5.65	9.73
0.0249	8.36	8.79	18.21	7.54	13.82	6.28	11.30	5.02	9.11
0.0283	7.07	8.16	15.39	6.28	11.93	5.34	9.73	4.71	7.54
0.0298	6.70	8.16	14.44	5.97	10.68	5.41	9.11	4.4	7.22
0.0338	5.91	6.91	12.56	5.34	9.73	5.02	8.16	3.77	6.28
0.4	5.00	6.0	10.68	5.02	8.16	4.39	6.59	3.45	5.21
0.0448	4.46	5.81	9.73	4.4	7.22	3.96	6.0	3.09	4.7
0.0517	3.87	5.1	8.4	4.4	6.28	3.39	5.21	2.76	4.08
0.0633	3.16	4.2	6.28	3.39	5.02	2.89	4.14	----	----
0.0757	2.64	3.7	5.20	2.89	4.14	----	----	----	----
0.0896	2.236	3.45	4.58	----	----	----	----	----	----
0.0944	2.12	3.39	4.4	----	----	----	----	----	----
0.10	----	----	----	----	----	----	----	----	----

Table V-1a: Range of input frequencies that sustain subharmonic oscillation. Data obtained from results of analog computer simulation.



Input Amplitude	22 volts		30 volts		40 volts	
$\zeta$	$\omega_n$ rad/sec	Input Frequency Range. rad/sec	Input Frequency Range. rad/sec	Input Frequency Range. rad/sec	Input Frequency Range. rad/sec	Input Frequency Range. rad/sec
0.02	10.00	6.0	8.79	5.34	7.54	4.58 6.91
0.0224	8.94	5.02	8.16	5.02	6.59	4.02 6.03
0.0249	8.36	4.4	7.85	4.08	6.4	3.6 5.59
0.0283	7.07	4.4	6.91	3.64	6.03	3.01 4.71
0.0298	6.7	3.83	6.34	3.39	5.4	2.89 4.52
0.0338	5.91	3.77	6.1	3.26	5.15	2.6 3.89
0.04	5.00	3.33	5.46	2.89	4.58	-----
0.0448	4.46	2.95	4.58	2.57	3.7	-----
0.0517	3.87	2.7	4.02	2.45	3.2	-----
0.0633	3.16	-----	-----	-----	-----	-----
0.0757	2.64	-----	-----	-----	-----	-----

Table V-1b: Range of input frequencies for subharmonic oscillation  
for input amplitudes = 22 volts, 30 volts, and 40 volts.





Input Amplitude	3	6	9	16	22	30	40
<u>Input Frequency</u>							
4.4							
4.58							80.0
5.02						75.0	75.0
5.65						67.5	68.75
6.28				57.5	57.5	55.0	53.75
6.91			48.0	46.5	47.5	47.5	47.5
7.53			38.0	40.0	39.0	40.0	
8.16		34.0	34.0	32.5	33.75		
8.79		29.0	29.0	30.0	30.0		
9.42		25.0	24.5	27.5			
10.68	20.0	19.5	18.75	20.0			
10.99	17.0	17.0	16.0	17.5			
11.93	16.0	16.0	15.5				
12.56	14.25	13.75	14.0				
13.19	13.0	12.75	12.5				
15.7	9.12	9.0					
16.64	7.75	7.75					
18.84	6.25						
20.1	5.5						
21.35	4.5						
21.66	4.0						

Table V-2 : Output amplitude of system with saturation  
 $\zeta = 0.02$ .



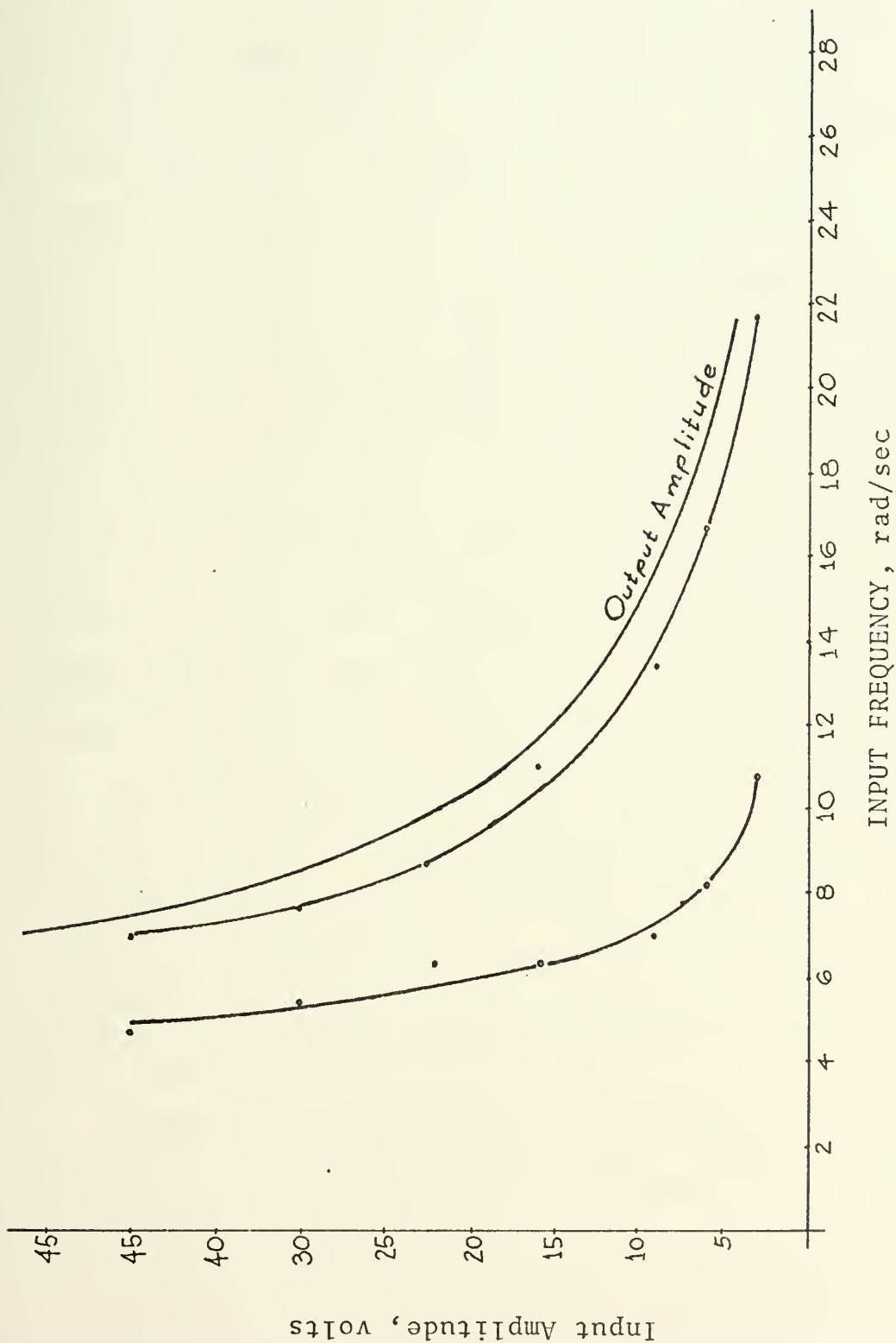


FIGURE V-3: Domain of 1/2 subharmonic oscillation for symmetrical saturation  
 $\zeta = 0.02$



can occur only for a range of input amplitude. For a small input amplitude such that the error signal to the nonlinear element is less than the saturation level, no subharmonic oscillation can possibly occur because the system will just be linear. Also shown in the figure is the variation of output amplitude. For a particular damping factor, the example  $\zeta = 0.02$  in Figure V-4, the output amplitude varies as shown by the curve irregardless of the input amplitude. The output amplitude is dependent on the range of input frequency that the subharmonic oscillation is "locked on". Figures V-4 and V-5 show the output amplitude variation for different values of  $\zeta$ . Ogata [Ref. 6] concluded that subharmonic oscillations do not occur as response of the output of the nonlinear feedback control system when the output-input amplitude ratio for a given amplitude of a sinusoidal input is 2 ~ 3 db or less. This is equivalent to a ratio of 1.256 ~ 1.41. The results of the simulation study do not agree with this criterion as can be seen in Figures V-4 and V-5 where the lowest output-input amplitude ratios are 1.25 and 1.125, respectively. The possibility of subharmonic oscillation is greater for greater output-input ratio.

Subharmonic oscillation of 1/2 order was observed when the saturation nonlinearity is skew asymmetric. The saturation characteristic is

$$\begin{aligned} e_o &= e_i & -2 < e_i < 4 \\ e_o &= -2 & e_i < -2 \\ e_o &= 4 & e_i > 4 \end{aligned}$$



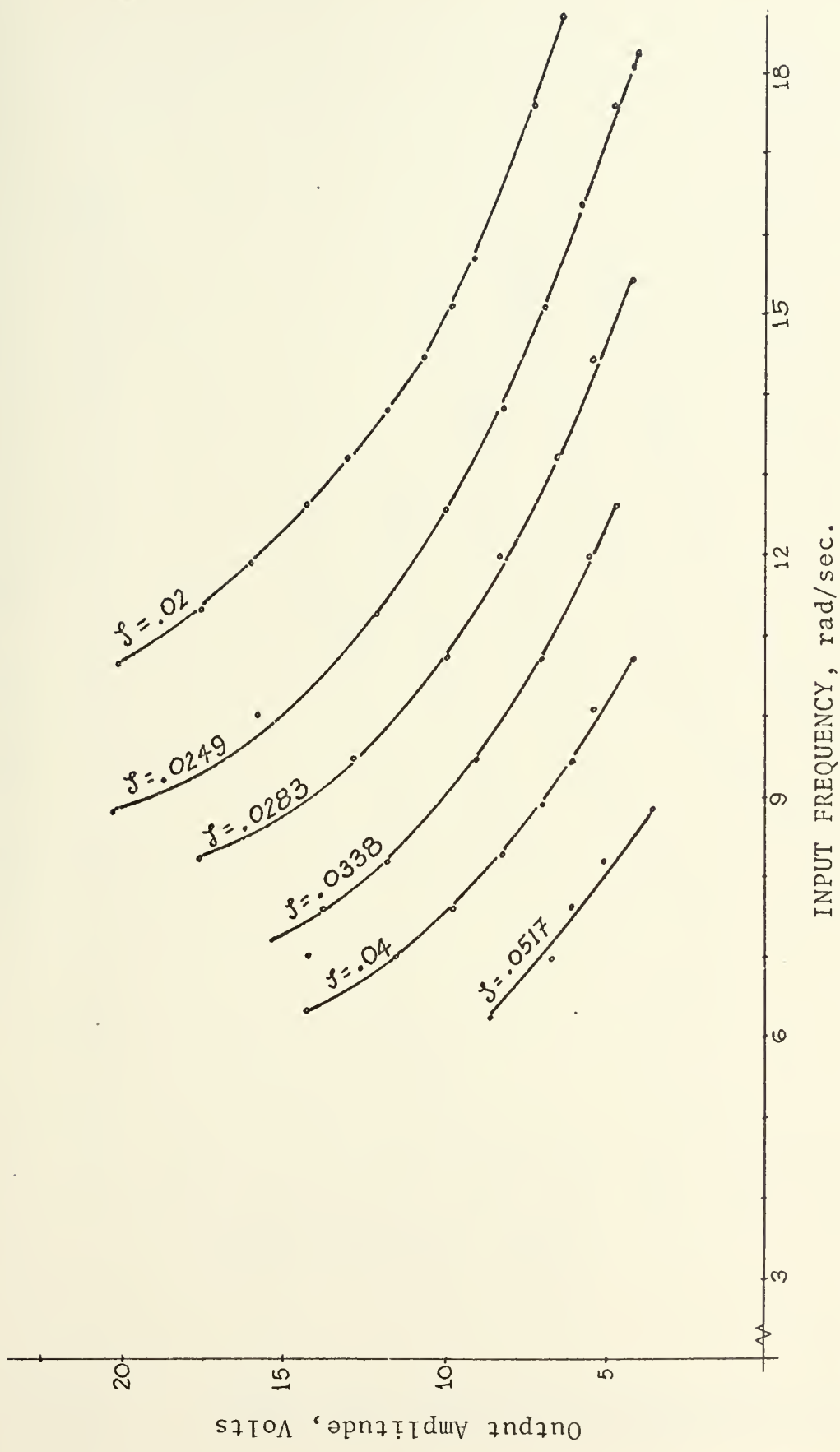


FIGURE V-4. Output amplitude for 1/3 subharmonic due to saturation. Amplitude of input = 3 volts.





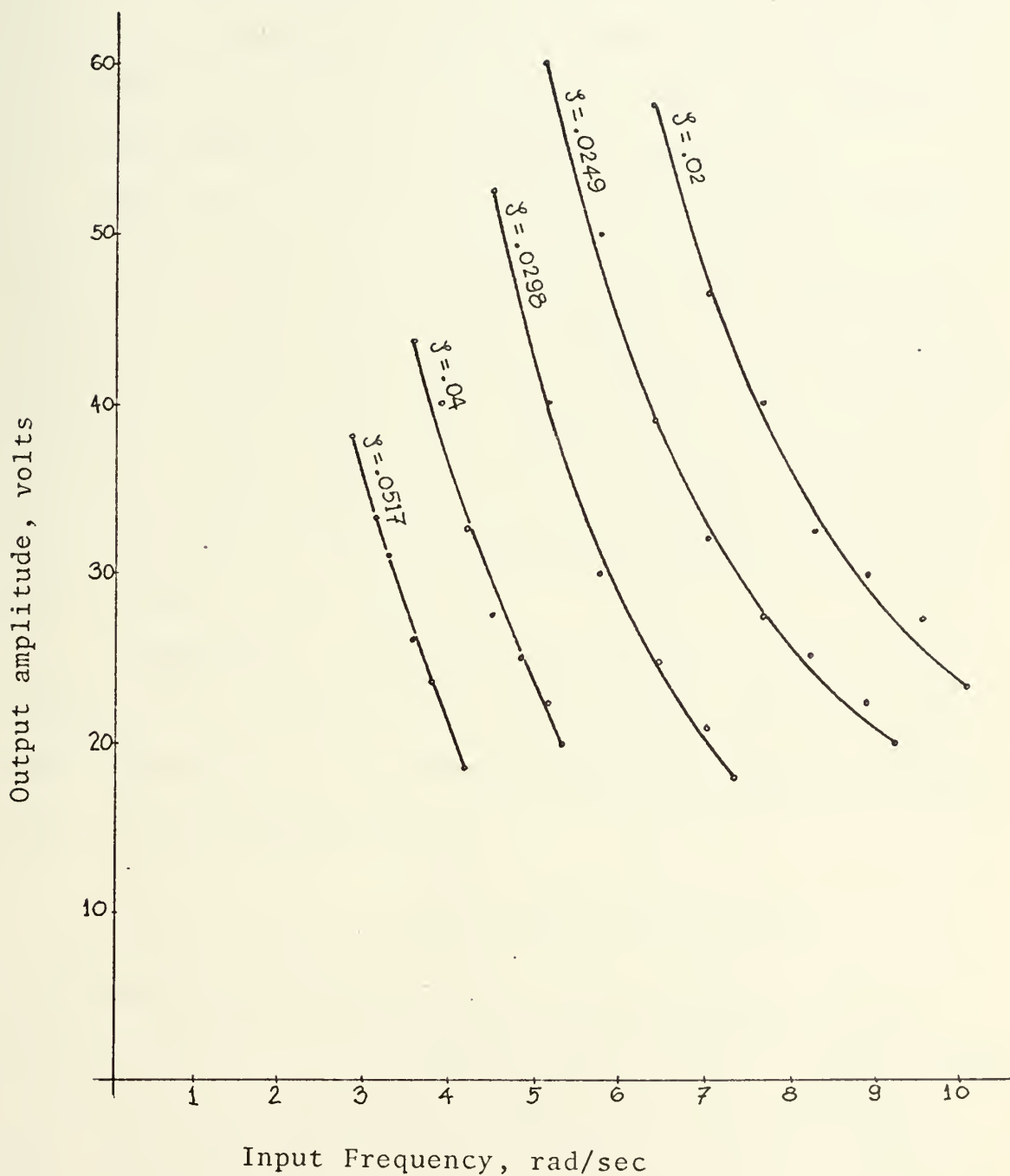


FIGURE V-5: Output amplitude for 1/3 subharmonic due to saturation. Input amplitude = 16 volts.



The domain of  $1/2$  subharmonic is shown in Figure V-6. Figures C-1 through C-5 show the signal waveforms for  $1/2$  and  $1/3$  orders subharmonic oscillations and also the waveforms of the error signals. Figure C-2 shows the build up of  $1/2$  order subharmonic and Figure C-4 shows the decay of  $1/3$  order subharmonic to fundamental oscillation.

West, Douce and Livesly [Ref. 12] presented a method of using the dual-input describing function technique to study subharmonic oscillation. Figure V-7 is the describing function loci which shows the response of a saturation nonlinearity to a sinusoidal signal of amplitude  $B$  and of a signal at three times this frequency and of amplitude  $A$ . Ref. 12 tabulates other describing function loci for different values of amplitude  $B$ .

A subharmonic oscillation of  $1/n$  order where  $n$  is an integer will oscillate at a frequency that is  $1/n$ th of the input frequency. To investigate this subharmonic, let the input to the nonlinearity be

$$A \cos n\omega t + B \cos (\omega t + \theta)$$

The signal  $A \cos n\omega t$  is assumed to be known and the describing function for the signal  $B \cos (\omega t + \theta)$  is superimposed on the open loop frequency response locus of the linear part. The value of  $B$ , such that the describing function cuts the frequency response locus for a frequency,  $\omega$  is the amplitude that corresponds to an overall open loop gain of unity. So this gives a possible steady-state amplitude of the resultant subharmonic oscillation.



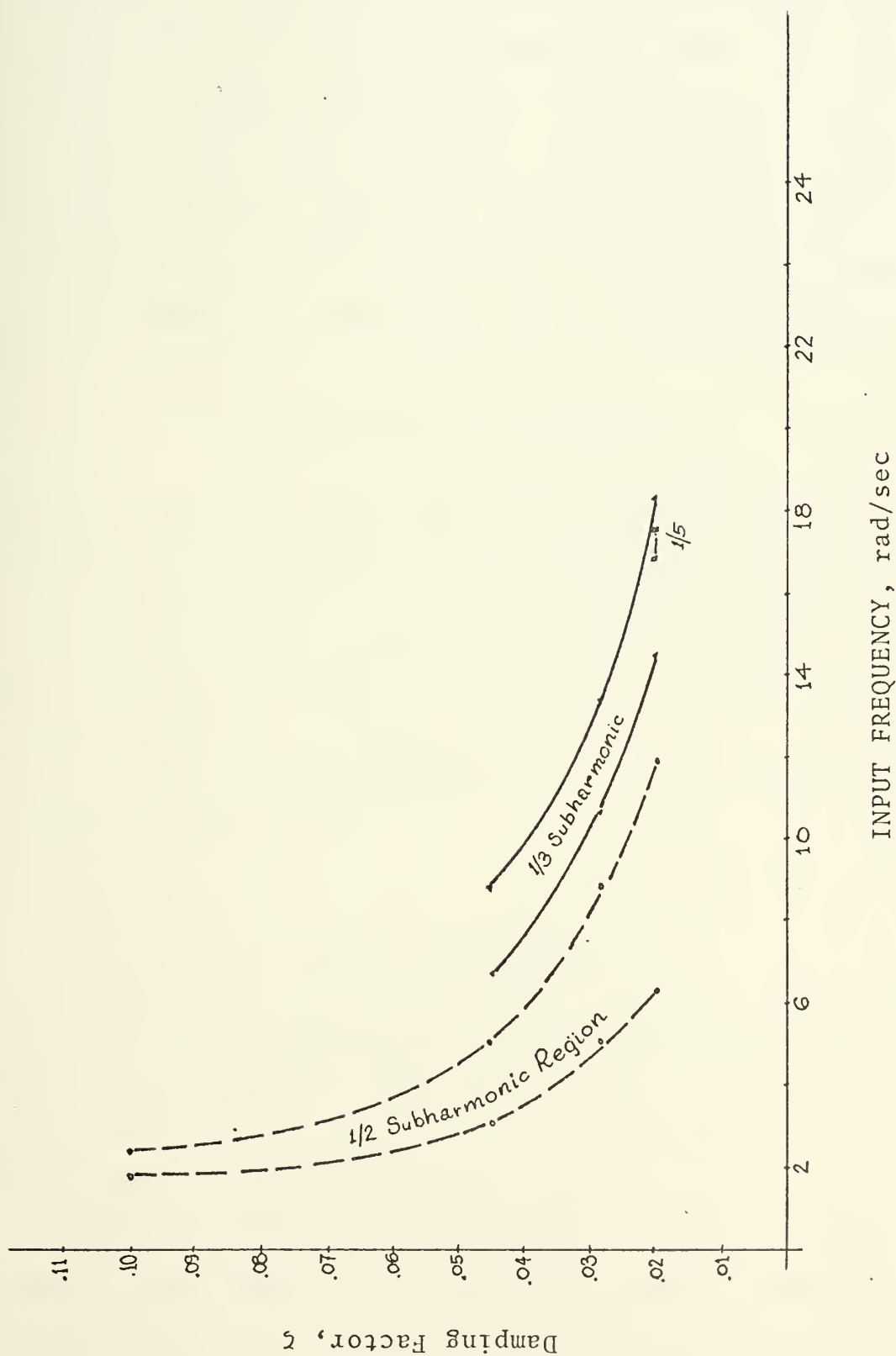


FIGURE V-6: Domains of subharmonic for a symmetrical saturation input amplitude = 6 volts.



The amplitude and frequency of possible 1/3 order subharmonic oscillation is found as follows. Assume that the amplitude, A of the input signal is known. For the system to oscillate continuously at a frequency equal to one-third of the input frequency, the overall open loop gain must be unity. Then the conditions for continuous oscillations may be evaluated by means of the describing function technique. The input to the nonlinear element is

$$A \cos 3\omega t + B \cos (\omega t + \theta)$$

Know the value of A, the describing function loci that correspond to this value of A are superimposed on the open loop frequency response locus of the linear system. Referring to Figures V-7a and V-7b this shows the describing function loci for A = 4 and A = 8, respectively. The open loop frequency response locus of the linear portion with a transfer function of

$$G(j\omega) = \frac{50}{j\omega(j\omega + 0.4)}$$

is superimposed. The point at which they pass through the point representing the frequency response at the subharmonic frequency determines the value of B, which is the amplitude of the subharmonic oscillation.

Figure V-8 shows the output amplitude for 1/3 subharmonic oscillation for a second order system with saturation nonlinearity where the saturation level is  $\pm 1$ . The curves were obtained from the results of the analog





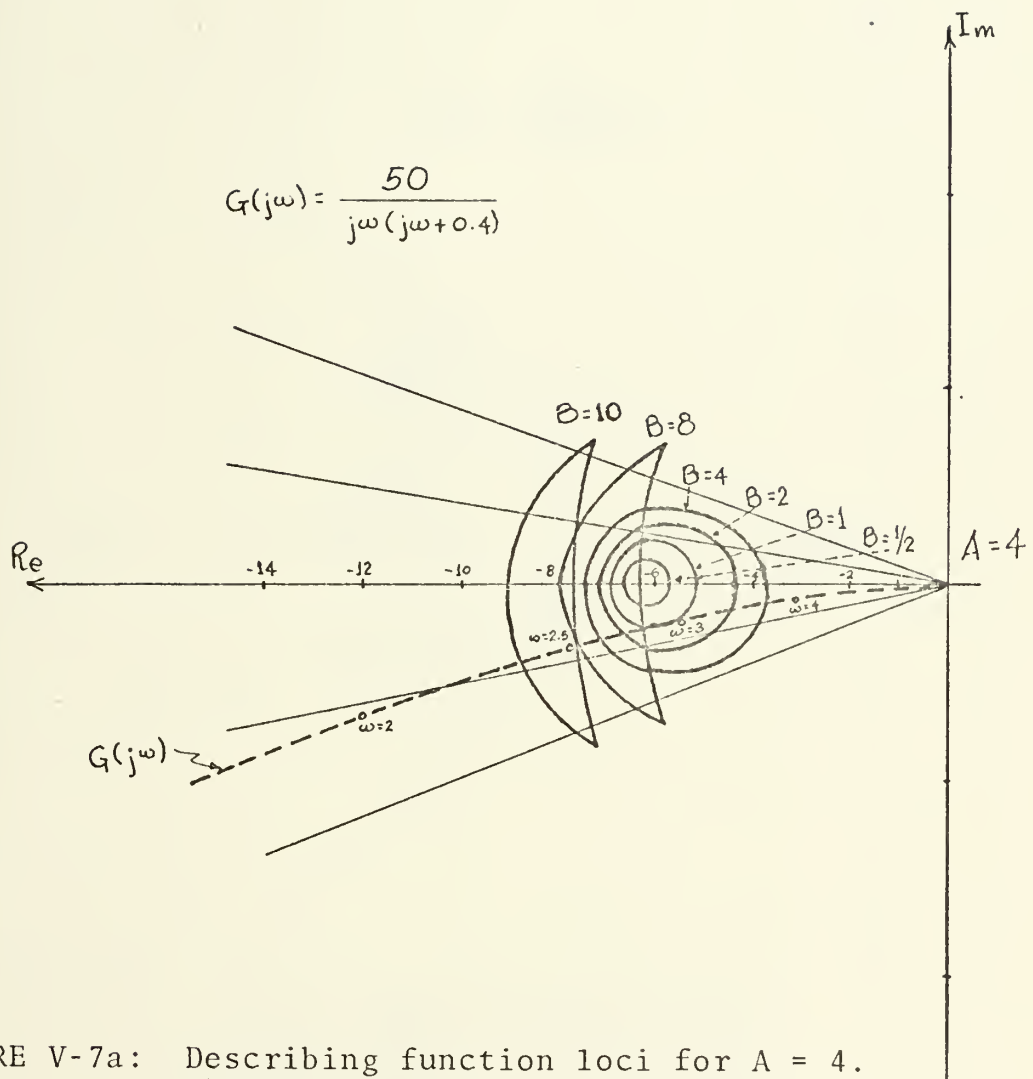


FIGURE V-7a: Describing function loci for  $A = 4$ . Shows response of saturation nonlinearity to a sinusoidal signal of amplitude  $B$  and of signal  $AE$  three times this frequency and of amplitude  $A$ . [Ref. 12].



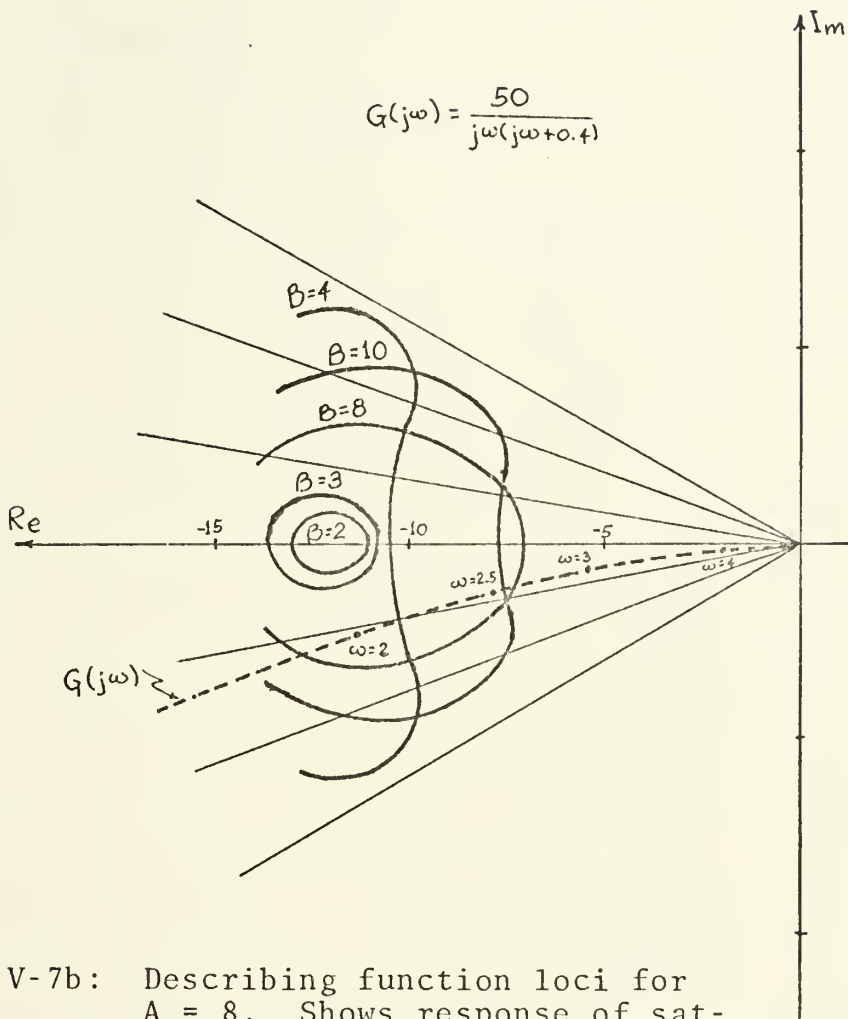


FIGURE V-7b: Describing function loci for  $A = 8$ . Shows response of saturation nonlinearity to a sinusoidal signal of amplitude  $B$  and of signal at three times this frequency and of amplitude  $A$ . Open-loop frequency response locus of linear system superimposed. [Ref. 12.]



$A_{input}$	8 volts		4 volts		2 volts		1 volt	
Input Fre- quency, rad	$A_{out}$	$A_{err}$	$A_{out}$	$A_{err}$	$A_{out}$	$A_{err}$	$A_{out}$	$A_{err}$
5.02	25.0	32.0						
5.65	19.0	25.0						
6.28	16.0	21.5	16.0	19.0				
6.91	12.5	18.0	12.5	15.5				
7.54	10.5	16.0	10.5	12.5	10.5	12.5		
8.16			9.0	11.0	9.0	10.5		
8.79			7.5	9.5	7.75	9.0		
9.42			6.5	8.5	6.75	8.0		
10.05			5.5	8.0	5.5	7.5	6.0	6.5
10.68			5.0	7.5	5.0	6.0	5.0	5.5
11.3					4.5	5.5	4.5	5.0
11.93					4.0	5.0	4.0	4.5
12.56					3.5	4.5	3.75	4.1
13.19					3.0	4.25	3.25	4.0
13.82					2.5	4.0	3.0	3.5
14.13					2.5	3.75	2.5	3.0
15.07							2.35	2.75
15.7							2.0	2.5
16.33							2.0	2.25
16.96							1.8	2.25
18.21							1.6	2.1
18.84							1.4	2.0

Table V-3: Amplitude of system response and error signal for system with saturation level  $\pm 1$ .



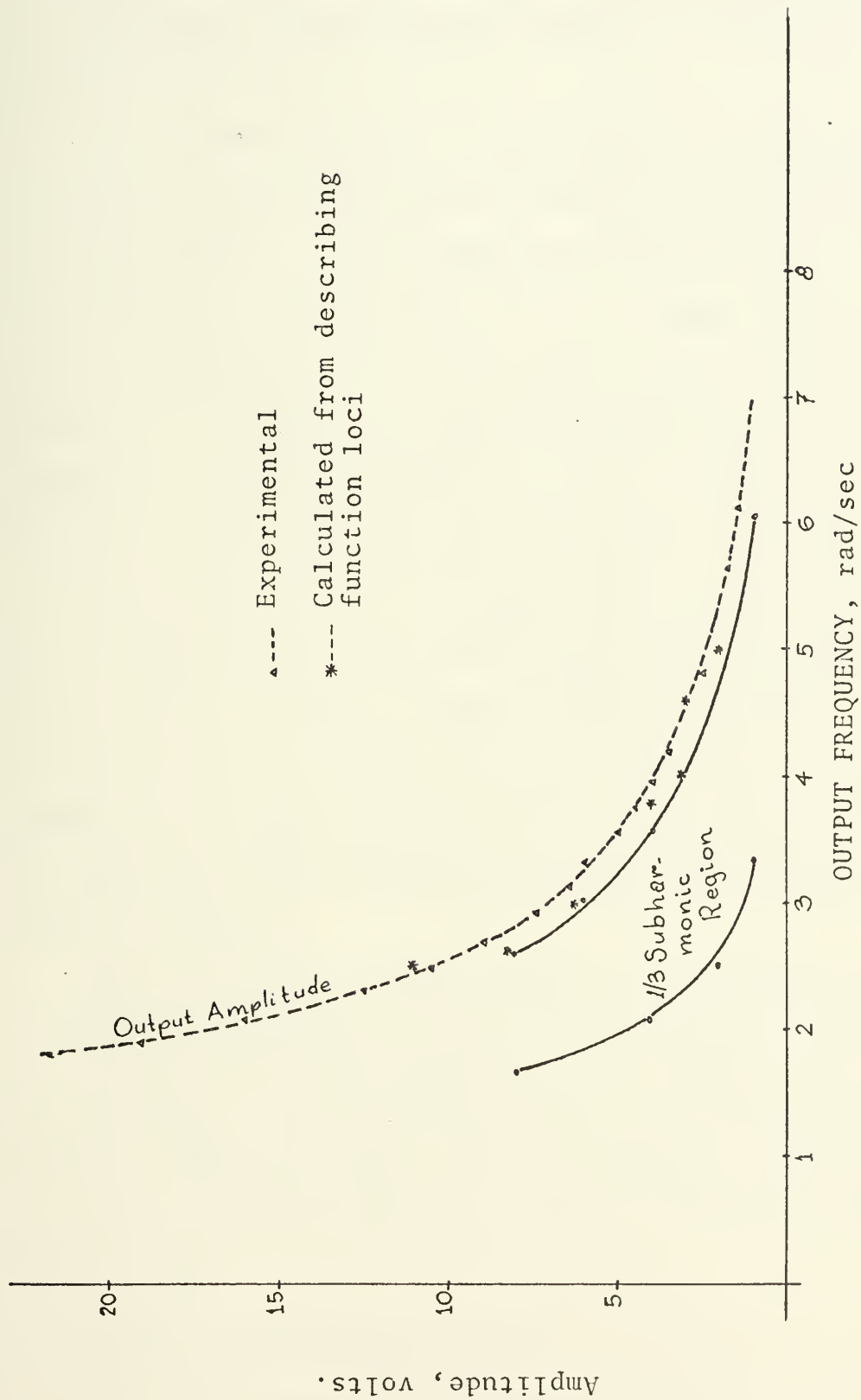


FIGURE V-8. Amplitude of 1/3 subharmonic oscillation for saturation level =  $\pm 1$ .





computer study. Also indicated are points calculated using the describing function loci of Figure V-7 and those tabulated in Ref. 12.

The difficulty with the dual-input describing function technique is the derivation of the dual-input describing function itself. If the nonlinear characteristic can be expressed as a simple power series or simple output-input relationship such as the cubic nonlinearity considered in Chapter II, the dual-input describing function can be determined by simple algebraic analysis. However, in the case of practical feedback systems where the nonlinearity is rarely expressible as a simple power series, like in the case of saturation, relay, and backlash, the algebraic analysis of the nonlinear element becomes difficult. Graphical methods are possible but very laborious. Due to the complexity of these nonlinearities, the use of computers for determining the relevant dual-input describing function is necessary.

For the purpose of this study, the derivation of the dual-input describing function for the nonlinearities are not included. The DIDF derivation can be treated as a separate problem and the results can then be applied to any form of linear systems to study the effect of the nonlinearity.

#### B. SYSTEM WITH NON-IDEAL RELAY

The other second order system simulated to observe the occurrence of subharmonic oscillation contained a



double valued nonlinearity. Figure III-4a shows a second order system with a relay with hysteresis. Referring to this figure, the nonlinearity can be defined by the following equations. Assume the input to the nonlinearity is

$$e_i = A \sin \omega t$$

then

$$e_o = -a \quad 0 < \omega t < \beta$$

$$e_o = a \quad \beta < \omega t < \pi + \beta$$

where

$$\beta = \sin^{-1} \frac{c}{A}$$

The conventional describing function [Ref. 9] is

$$G_D = \frac{4a}{\pi A} \sin^{-1} \frac{c}{A}$$

and the plot of the inverse of this describing function for  $a = 1$  (constant) and three different values of  $c$ , where  $2c$  is the amount of hysteresis, is shown in Figure V-9. Superimposed on the  $-1/G_D$  curve is the plot for  $G(j\omega)$  of the linear portion of the system. The figure shows that for a particular amount of hysteresis, the point of intersection between the  $G(j\omega)$  curve and the relevant  $-1/G_D$  curve represents a limit cycle whose amplitude and frequency can be determined easily. For example, consider  $c = 0.2$ , the limit cycle frequency is approximately 1.8 rad/sec with an amplitude of 0.46. The Bode plot of the simple linear portion is shown in Figure V-10.



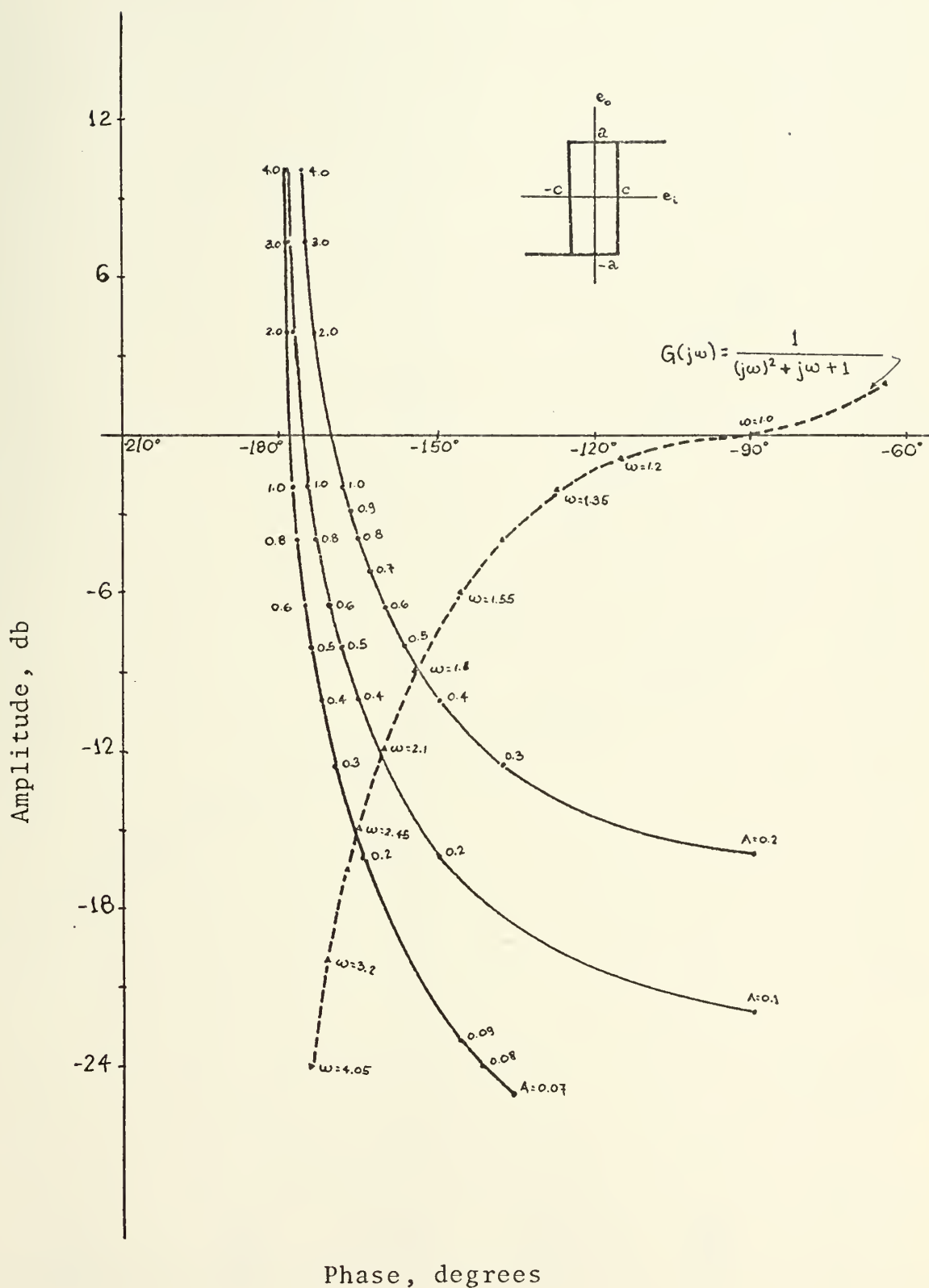


FIGURE V-9: Describing function for relay with hysteresis.



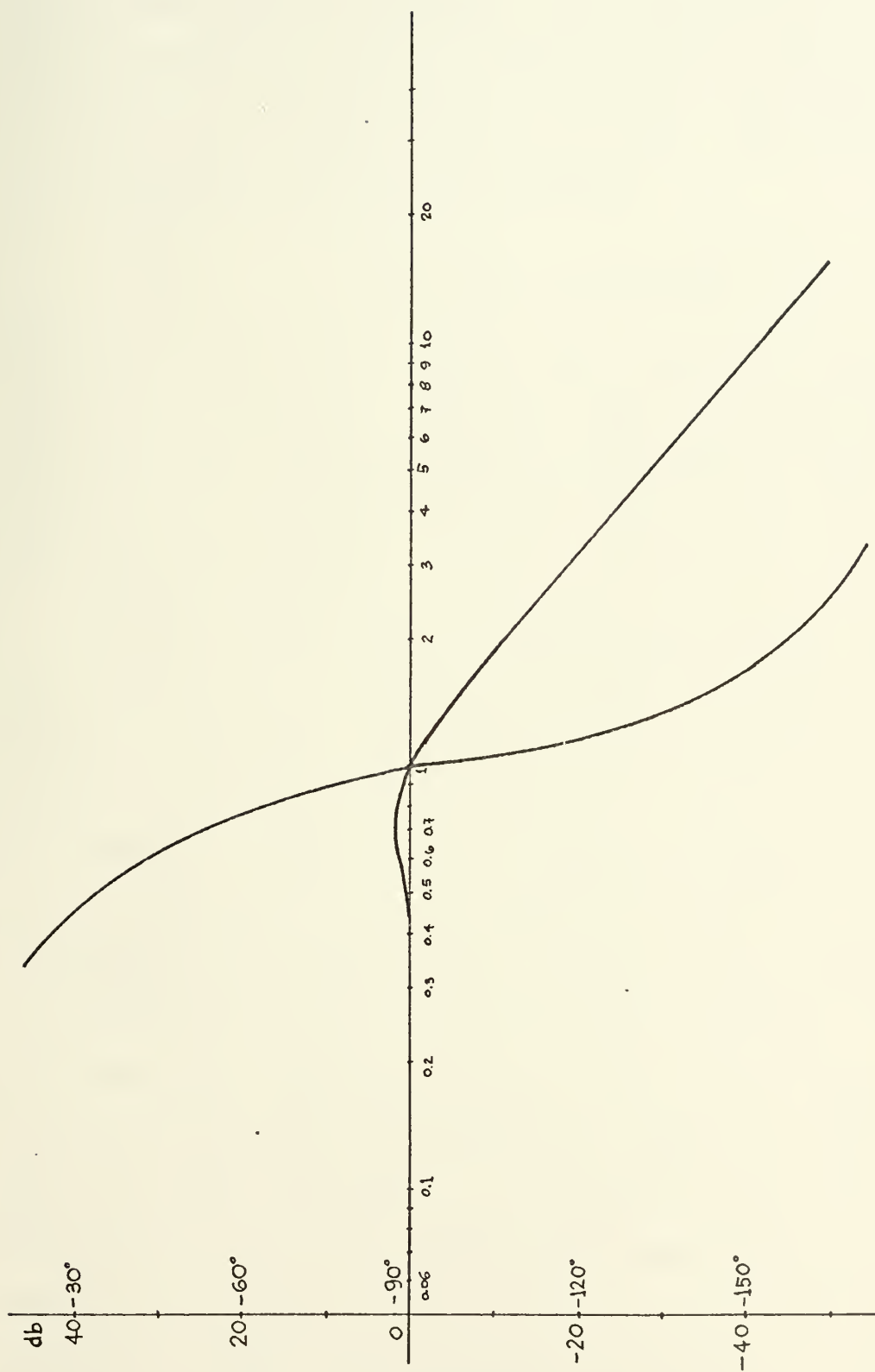


FIGURE V-10: Bode plot of  $G(s) = \frac{1}{s^2 + s + 1}$





The system in Figure III-4a has a sinusoidal input of known amplitude and frequency. The output of the relay,  $f(t)$  is assumed to lose its higher frequency components due to the low pass characteristics of  $G(s)$ . Then, the input to the nonlinearity can be written as

$$A \cos n\omega t + B \cos (\omega t + \theta)$$

where  $A \cos n\omega t$  is the primary input signal of known amplitude and frequency. The dual-input describing function of subharmonic oscillation developed by West, Douce and Livesly [Ref. 12] can be used if the dual-input describing function is available.

In the analog computer study for the system, subharmonic oscillation as high as 1/2 order and as low as 1/13 order were observed. The subharmonic oscillation once initiated is stable and stays "locked on" a reasonable range of frequency. There is an overlapping of domains of different subharmonic order, as shown in Figure V-11. The subharmonic oscillation that is stable is the subharmonic order initiated first. It can be seen from Figure V-11 that odd-order subharmonics have a much larger domain than even-order subharmonics and that the domain decreases for lower odd-order subharmonics. The figure also shows the amplitude of the output which is the amplitude of the subharmonic oscillation. This is the amplitude curve for all subharmonic modes. If the output oscillates at a frequency of 2.45 rad/sec, then the output amplitude is 0.225 regardless of the subharmonic mode.



Input Ampli- tude	0.1		0.12		0.18		0.21		0.27	
Order	$\omega_{in}$	A out	$\omega_{in}$	A out	$\omega_{in}$	A out	$\omega_{in}$	A out	$\omega_{in}$	A out
1/2	3.77	.45	3.77	.40	3.77	.375	3.77	.375	3.77	.375
	4.08	.40	4.08	.35					4.08	.338
1/3	5.02	.538	5.02	.543	5.02	.52	5.02	.55	5.02	.513
	5.65	.40	5.65	.40	5.65	.4	5.65	.40	5.65	.40
	6.28	.338	6.28	.35	6.28	.325	6.28	.325	6.28	.325
					6.91	.25	6.91	.275	6.91	.26
					7.22	.225	7.54	.213	7.54	.213
							8.15	.175	8.16	.175
									8.79	.15
									9.42	.125
									10.05	.113
									10.68	.10
									11.3	.088
									11.93	.075
1/4	6.91	.475	6.91	.475	7.54	.4	8.05	.363	8.16	.325
	7.53	.40	7.53	.4	7.85	.35				
1/5	8.16	.538	8.16	.525	8.16	.538	8.16	.55	8.79	.45
	8.79	.45	8.79	.45	8.79	.45	9.42	.375	9.42	.375
	9.42	.375	9.42	.375	9.42	.388	10.05	.31	10.05	.33
			10.05	.325	10.05	.338	10.68	.28	11.3	.265
								.26	11.93	.24
								.23	12.56	.2
								.2	13.19	.188
									13.82	.175
									14.44	.163
									15.07	.15
									15.7	.125
1/6	10.05	.5	10.68	.425	11.3	.4	11.62	.375		
	10.67	.44	11.3	.375	11.93	.34	11.93	.34		
	11.3	.38					12.56	.31		
1/7	11.93	.49	11.93	.49	11.93	.49	12.87	.4	15.7	.26
	12.56	.44	12.56	.44	12.56	.43	13.82	.35	16.33	.25
	13.19	.39	13.19	.39	13.19	.39	14.44	.33	16.96	.225
	13.82	.35	13.82	.35	13.82	.35	15.07	.29	17.58	.21
					14.44	.31	15.7	.26	18.21	.2
					15.07	.3	16.33	.25	18.84	.19
					16.01	.25	16.96	.24	20.1	.15
									21.35	.14

Table V-4: Simulation Data for Non-Ideal Relay;  
a = 1, c = 0.2



INPUT AMPLITUDE		0.1		0.12		0.18		0.21		0.27	
Order		$\omega_{in}$	$A_{out}$	$\omega_{in}$	$A_{out}$	$\omega_{in}$	$A_{out}$	$\omega_{in}$	$A_{out}$	$\omega_{in}$	$A_{out}$
1/8		14.44	.43	14.44	.43	15.7	.35	16.01	.35		
		15.07	.39	15.07	.39	16.33	.33	17.27	.28		
				15.7	.35	16.96	.3	18.21	.26		
						17.58	.28	18.84	.24		
1/9		15.7	.46	16.33	.43	16.96	.39	18.21	.34		
		16.33	.43	16.96	.4	17.58	.36	19.15	.3		
		16.96	.38	17.58	.36	18.84	.31	20.1	.26		
		17.58	.35	18.21	.35	19.47	.29	20.72	.25		
						20.41	.25	21.35	.23		
1/10		18.21	.43	18.84	.39						
		18.84	.39								
		19.47	.36								
1/11		20.09	.44								
		20.72	.39								
		21.35	.36								

INPUT AMPLITUDE		0.3		0.375		0.4		0.45		0.51	
Order											
1/3		4.7	.72	5.02	.58	4.71	.63	4.71	.63	4.9	.53
		5.02	.55	5.65	.4	5.02	.53	5.02	.55	5.15	.45
		5.65	.43	6.28	.33	5.65	.4	5.65	.38	5.27	.44
		6.28	.33	6.91	.28	6.28	.33	6.28	.33	5.4	.41
		7.54	.21	7.54	.21	6.91	.25			5.53	.39
		8.79	.15	8.16	.17	7.54	.2				
		10.05	.11								
		11.3	.09								
		12.56	.07								
		13.19	.06								
1/5		9.42	.38								
		10.05	.34								
		10.68	.3								
		13.82	.18								
		15.07	.14								
		16.33	.12								
		16.96	.11								

Table V-5: Simulation Data for Non-Ideal Relay (continuation)



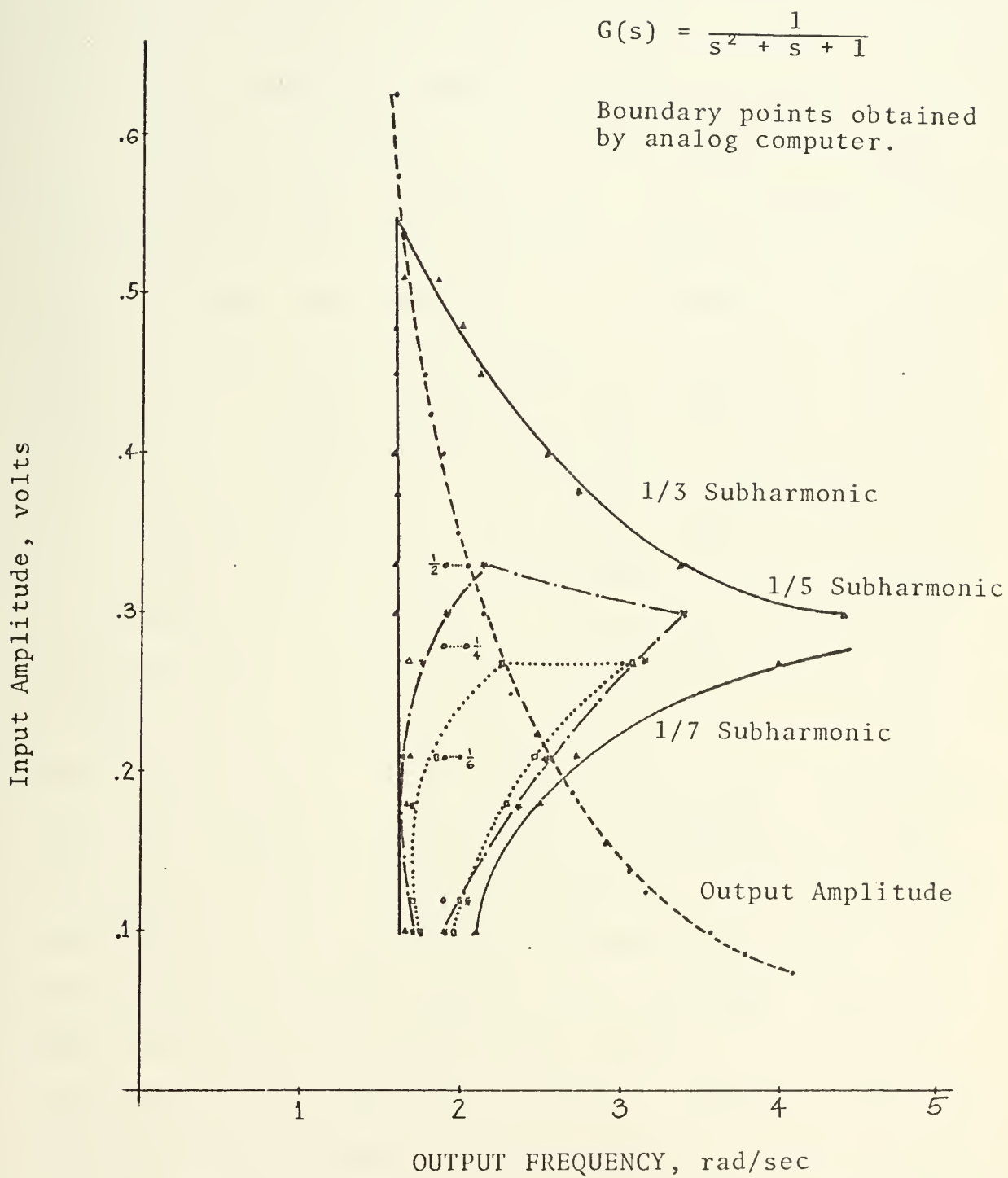


FIGURE V-11: Domains for subharmonic output for system with relay:  $a = 1$ ,  $c = 0.2$ .





Figure V-12 shows the domain of subharmonic oscillations for  $a = 1$  and  $c = 0.1$  adapted from the work of Sawaragi and Akashi [Ref. 8]. The points plotted represent data that were obtained from the analog computer experiment.

Figures C-6 through C-16 show the simulation results for the system with non-ideal relay. In the system with saturation nonlinearity, subharmonic generation was not self starting. The occurrence of subharmonic oscillation was dependent on the initial conditions, such as, the sudden change of input frequency or input amplitude. For the system with non-ideal relay nonlinearity, subharmonic oscillation was self starting. This can be seen in Figure C-6 which shows the system response changing from fundamental oscillation to  $1/3$  subharmonic oscillation. Figure C-6 also shows the relationship between the amplitude of the output when oscillating at the fundamental frequency and when oscillating at the subharmonic frequency. Figure C-10 shows the change from subharmonic to fundamental oscillation, i.e., from  $1/5$  order subharmonic to fundamental. The amplitude of the output at the fundamental frequency is practically negligible compared with the output amplitude when oscillating at a subharmonic frequency. Figures C-7 through C-16 show the changing modes of the subharmonic oscillation due to change in input frequency. There were instances when the output oscillates at two different subharmonic modes at the same input frequency. Figure C-16 shows the output oscillating at two different subharmonic modes; namely,  $1/11$  order and  $1/13$  order at the same input frequency.



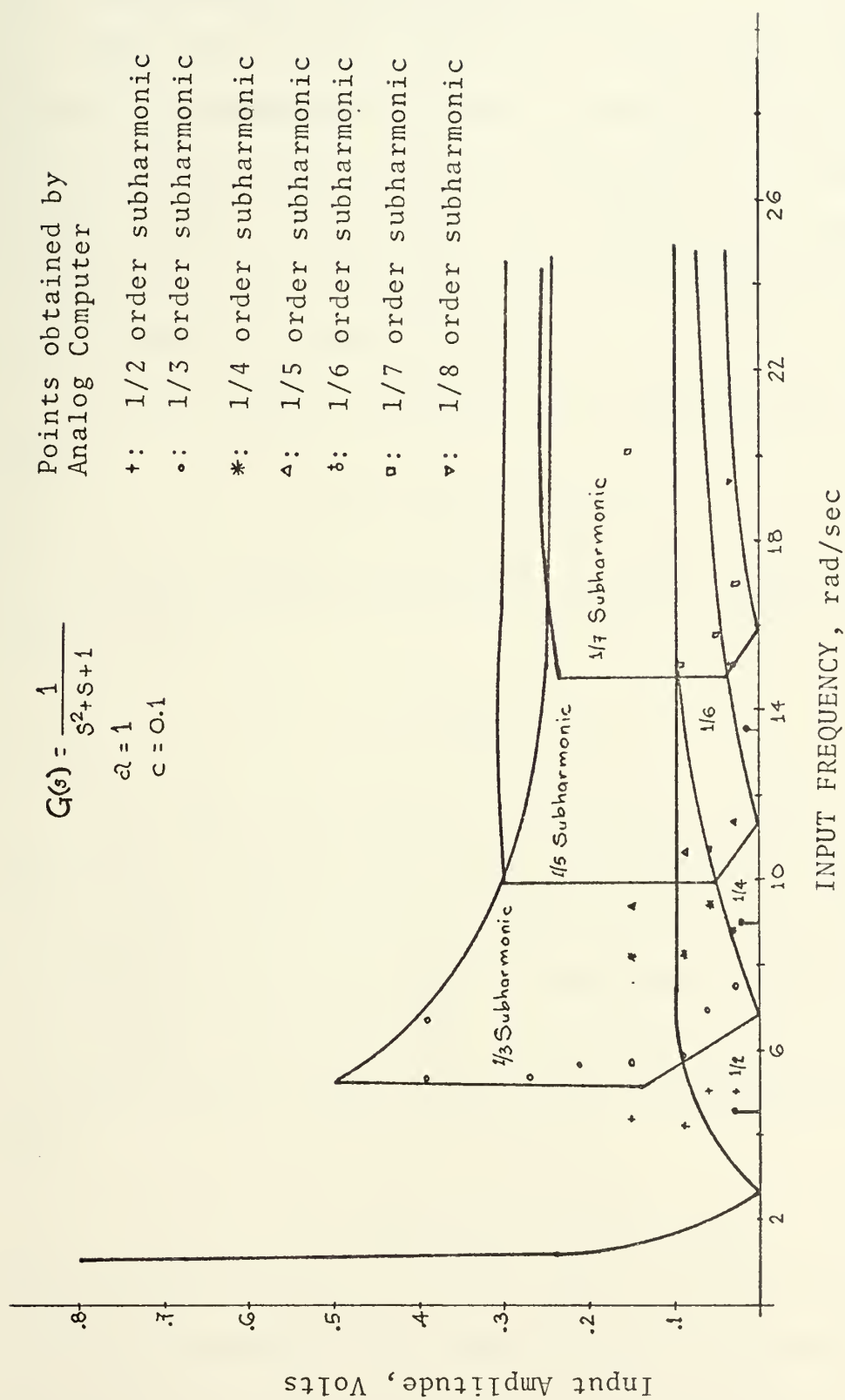


FIGURE V-12: Domain of subharmonic output. (adapted from Sawaragi and Akashi, Ref. 7)



### C. SYSTEM WITH TWO NONLINEARITIES

The third system simulated to investigate the occurrence of subharmonic oscillation contained saturation and friction controlled backlash nonlinearities as shown in Figure III-5a. It is a two loop system with a tachometer feedback for the inner loop to provide the necessary damping to make the system stable.

Using standard procedure, the characteristic equation is

$$s^2 + K_m K_t s + K_m = 0$$

It is clear that the damping factor,  $\zeta$  is dependent on  $K_m$  and  $K_t$ , i.e.,

$$\zeta = \frac{K_t}{2} \sqrt{K_m}$$

Han [Ref. 4] presented a procedure to predict the existence of limit cycles in a system with two nonlinearities such as the system shown in Figure III-5a. For the purpose of observing the occurrence of subharmonic oscillation in the system, assume that the system oscillates with a limit cycle so that the input to the first nonlinearity is of the form

$$A \cos n\omega t + B \cos (\omega t + \theta)$$

where  $A \cos n\omega t$  is the primary input signal of known amplitude and frequency. The linear frequency dependent element,  $G(s)$  is a low-pass filter which is assumed to adequately



attenuate the higher frequencies so that harmonics can be neglected in  $e_{in}$ . It also follows that the input to the second nonlinearity is a sinusoid.

The analog computer simulation was performed for different values of  $K_m$  and  $K_t$  and the results are tabulated in Table V-6 and V-7. Figures C-17 through C-23 show the signal waveforms obtained. Figure C-17 and C-18 show the waveforms for 1/3 and 1/5 orders, respectively. It can be seen that the signal  $e_{in}$  which is the input to the backlash nonlinearity oscillates at the subharmonic frequency, i.e., in Figure C-17,  $e_{in}$  is oscillating at a frequency that is 1/3 of the input frequency and in Figure C-18, at 1/5 of the input frequency. The system output,  $\theta_c$  oscillates at the same frequency as  $e_{in}$  with a phase difference of  $180^\circ$ . This shows that the subharmonic oscillation is due to the effect of the saturation nonlinearity. The effect of the backlash nonlinearity can be analyzed by using the conventional describing function since the input to the backlash nonlinearity,  $e_{in}$  is only composed of one sinusoidal signal. Figure C-19 shows the change of fundamental oscillation to 1/3 subharmonic oscillation and Figures C-20 and C-21 show the build up of subharmonic oscillations. It can be seen also from these figures that the subharmonic oscillations are self starting as compared with the system with saturation nonlinearity only.

The domains of subharmonic oscillation as a result of the simulation study are shown in Figures V-13, V-14, and





V-15. The domain of the  $1/3$  subharmonic oscillation is of the order of the natural frequency. For lower order subharmonic modes, i.e.,  $1/4$ ,  $1/5$ ,  $1/6$ ,  $1/7$ , ..., subharmonic oscillation occurs at a higher input frequency.



Input Amplitude		3.0		9.0		21.0		30.0	
Order	$\omega_{in}$	Out-put, v	$\omega_{in}$	Out-put, v	$\omega_{in}$	Out-put, v	$\omega_{in}$	Out-put, v	
1/2	20.41	4.75	11.93	15.0					
	20.72	4.75	12.56	14.0					
	21.35	4.5	13.82	13.0					
	25.12		15.07	12.0					
			16.33	12.0					
			17.58	11.75					
1/3	22.61	15.5	11.3	66.7	7.54	135.0	8.16	130.	
	23.86	13.0	12.56	60.	8.16	125.0	8.79	125.	
	25.12	11.75	13.82	48.	8.79	105.	9.42	90.	
	26.38	10.	15.02	39.	9.42	85.	10.68	72.5	
	27.63	8.88	16.33	32.	10.05	80.	11.93	60.0	
	28.89	8.25	17.58	27.	10.68	75.	13.19	50.	
	30.14	7.5	18.84	22.	11.93	57.5	13.82	42.0	
	31.4	6.1	20.1	20.	12.56	50.	15.07	37.5	
	36.66	6.0	21.35	17.5	13.82	45.			
	33.91	5.5	22.61	15.0	15.07	37.5			
	35.17	4.5	23.86	13.0	16.33	30.0			
			28.26	9.5	17.58	25.0			
			29.52	8.0	18.84	20.0			
1/4	35.8		30.14	10.0	18.12		15.7	27.5	
			31.4	9.0	18.79		16.33	27.	
			34.54	8.5	20.1		16.96	25.0	
					21.98		17.58	23.	
							18.21	22	
1/5			37.68	9.0	22.61		11.93		
							13.19		
					to		14.44	117.5	
					28.26		15.7	97.5	
							16.96	80	
							18.21	72.5	
							20.1	62.5	
							21.35	52.5	
							22.61	47.5	

Table V-6: Domain of subharmonic for system with two nonlinearities,  $\zeta = 0.283$ ,  $\omega_n = 14.14$



Input Amplitude $\zeta$	Order	3.0		9.0		9.6		21.0		25.5		30.0	
		Frequency Range rad/sec	Frequency Range rad/sec	Frequency Range rad/sec	Frequency Range rad/sec	Frequency Range rad/sec	Frequency Range rad/sec	Frequency Range rad/sec	Frequency Range rad/sec	Frequency Range rad/sec	Frequency Range rad/sec	Frequency Range rad/sec	Frequency Range rad/sec
0.1	1/2	12.56	15.7					5.02	5.65	5.02	5.65	5.02	
	1/3	15.7	22.61	6.28	13.81	7.54	12.56	7.54	11.3	6.28			
	1/4	23.86	27.0	10.05		12.56	13.82	11.93		8.79	9.42		
	1/5	28.26	34.54	11.3	21.98	9.42	17.58	12.56	15.7				
	1/6	37.08											
	1/7	40.8	43.96	25.12		18.84							
0.2	1/3	11.93	23.86	8.79	17.58	6.91	16.33	6.28	11.93	5.65	10.36	7.54	10.05
	1/4	24.49	28.89	17.58	20.72	17.58	18.84	11.93	15.07	10.05	10.68	9.73	11.3
	1/5	30.14	37.68	23.86	28.58	16.96	26.38	17.5	18.84	13.5	16.96	12.56	16.33
	1/6	37.68	39.56										
	1/7	44.44	43.96	31.4	37.68	35.8		28.26					
	1/8	47.1											
	1/9	53.38											
0.3	1/3	17.58	22.61	11.3	21.35	7.54	15.07	6.28	15.07	6.28	11.3	5.65	10.68
0.435	1/3			13.19	16.96	9.42	13.82	7.54	12.56	6.91	10.08	5.65	10.05
0.545	1/3			14.26		11.3	13.82	9.42	12.56	7.54	10.68	6.91	10.08
0.65	1/3							10.68	11.93	9.42	11.3	8.16	10.05

Table V-7: Range of input frequency for subharmonic oscillation (two nonlinearities)  $\omega_n = 10$



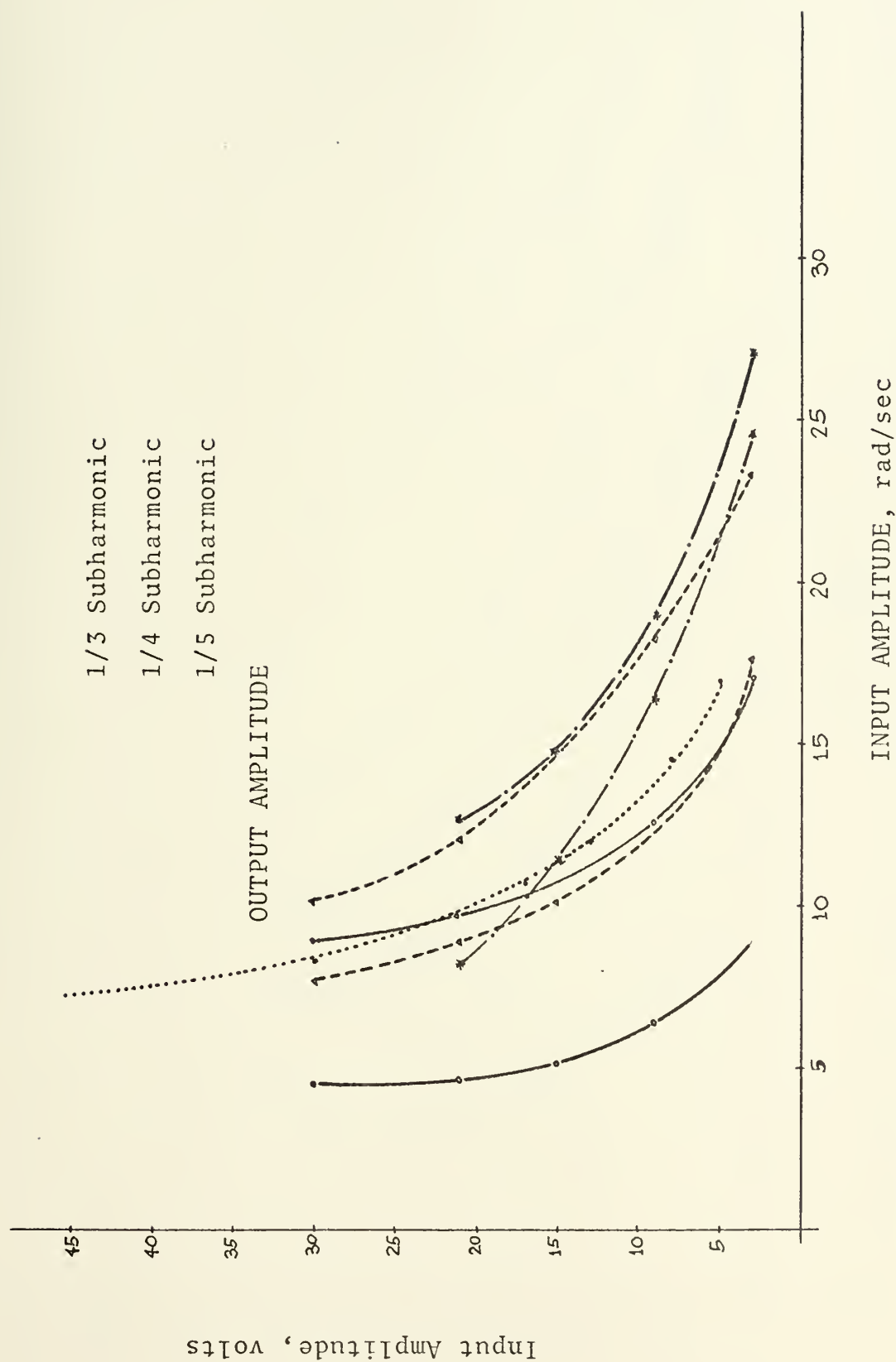


FIGURE V-13: Domain of subharmonic oscillation for system with saturation and backlash.  $\zeta = 0.212$ ,  $\omega_n = 7.07$ .





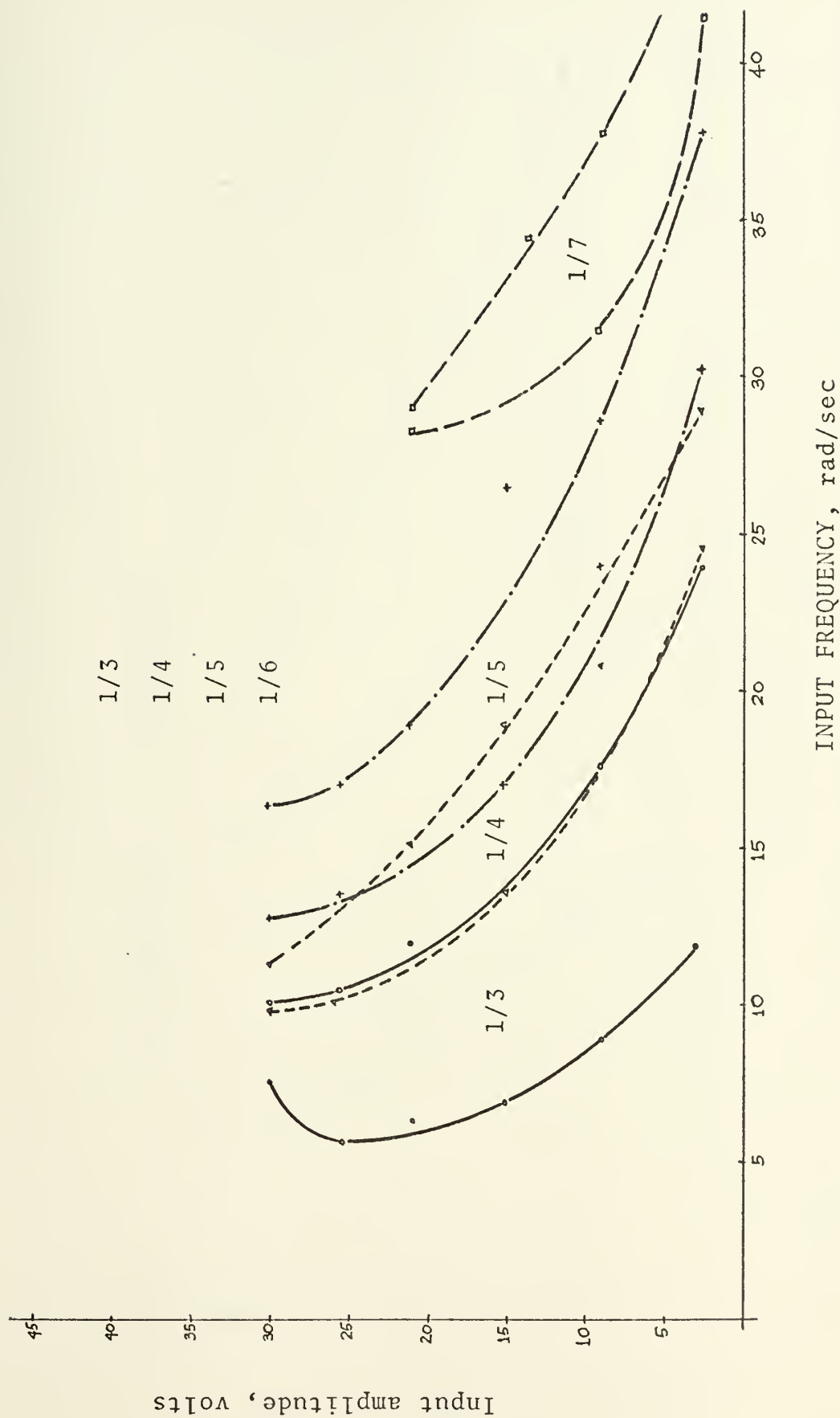


FIGURE V-14: Domains of subharmonic for system with saturation and backlash  
 $\zeta=0.2$ ,  $\omega_n = 10.0$



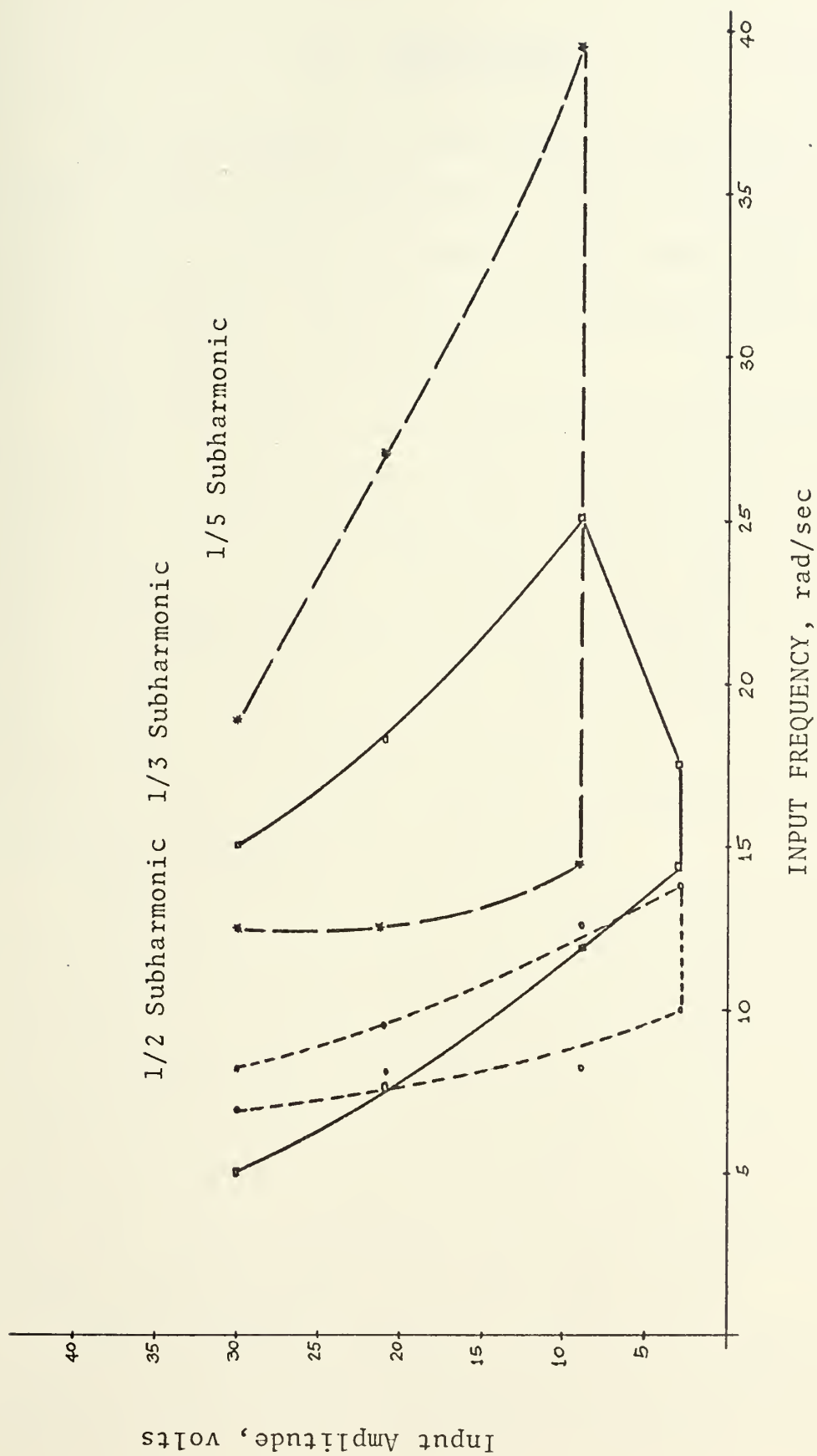


FIGURE V-15: Domains of Subharmonic oscillations for system with two nonlinearities  
 $\zeta = 0.141$ ;  $\omega_n = 14.14$  rad/sec



## VI. CONCLUSIONS

The investigation of subharmonic oscillation in nonlinear systems was undertaken by means of an analog computer study on three nonlinear second order feedback control systems. The following conclusions are summarized from the result of this study.

When the output of the system with saturation nonlinearity is oscillating with the input frequency, subharmonic oscillation cannot occur unless some kind of sudden disturbance is given to the input. This sudden disturbance may be a sudden disturbance may be a sudden increase in input amplitude or frequency. This is not the case for the systems with hysteresis nonlinearity. In the system with non-ideal relay and backlash characteristics, subharmonic generation was self starting.

The possibility of the occurrence of subharmonic oscillation is great when the output-input amplitude ratio is large. In the case of saturation nonlinearity, there is a minimum output-input amplitude ratio for subharmonic oscillation to occur, i.e., the output-input amplitude ratio is greater or equal to 1.125. For the system with non-ideal relay, subharmonic oscillation can occur for output-input amplitude ratio less than unity.

The "28-degree criterion" introduced by Douce [Ref. 1] gives accurate results in predicting the possibility of



subharmonic responses in a system with saturation nonlinearity. This is a useful technique in the elimination of subharmonic oscillation for systems with a limiting nonlinearity.

Subharmonic oscillation once initiated is sustained over a reasonable range of frequency. There is an overlapping of these frequency ranges for different subharmonic modes. In the region where two or more orders of subharmonic oscillation can occur, the order that occurs first dominates and tends to continue and is quite stable. The frequency of the subharmonic oscillation has a minimum depending on its order. The frequency for 1/3 order subharmonic is usually in the neighborhood of the natural frequency of the system. Subharmonic oscillation is dependent on the input signal amplitude. It can occur only within a certain range of signal amplitude. It can be concluded that subharmonic oscillation can occur only with a certain range of input amplitude and frequency.

The system with a limiting nonlinearity is dependent on the damping factor for subharmonic oscillation to occur. The system has to be very lightly damped, i.e.,  $\zeta < 0.1$  in order for the system response to oscillate at a subharmonic frequency. If the input amplitude is increased, the system has to be much more lightly damped for subharmonic oscillation to occur.

The dual-input describing function technique developed by West, Douce, and Livesly [Ref. 12] appears to be a very



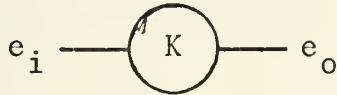


useful technique for predicting quantitatively the amplitude and frequency of subharmonic oscillation. Recommended for future study is the derivation of relevant dual-input describing functions (two sinusoidal input) and application of the results to any linear system with the relevant non-linearity. Quantitative analysis of the occurrence of subharmonic oscillations should be undertaken.



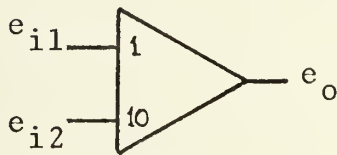
## APPENDIX A: PROGRAM SYMBOLS

### (1) Servo Set Potentiometer



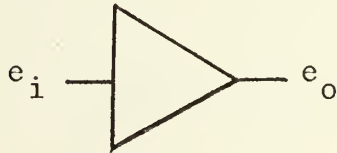
$$e_o = K e_i \text{ where } K < 1$$

### (2) Summer Amplifier



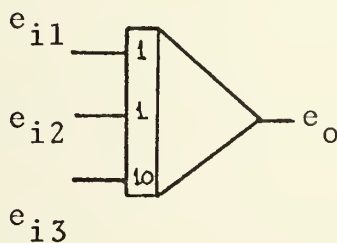
$$e_o = - (e_{i1} + 10e_{i2})$$

### (3) Inverter



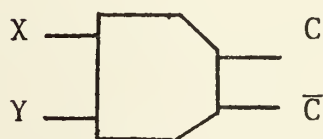
$$e_o = - e_i$$

### (4) Integrator



$$e_o = - (e_{i1} + e_{i2} + 10e_{i3}) dt$$

### (5) Comparator



Output Logic:

Algebraic sum of  $X + Y > 0$

$C = -6$  volts (true)

$\bar{C} = 0$  volt (false)

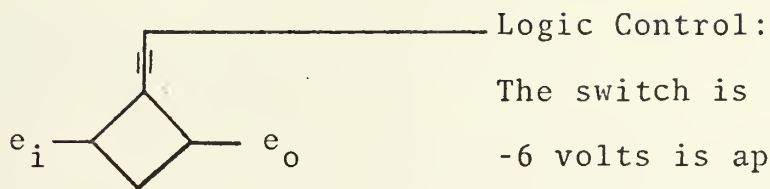
Algebraic sum of  $X + Y < 0$

$C = 0$  volt (false)

$\bar{C} = -6$  volts (true)

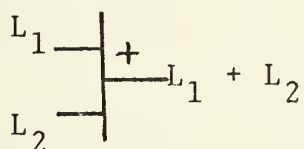


(6) Digital/Analog (D/A) Switch

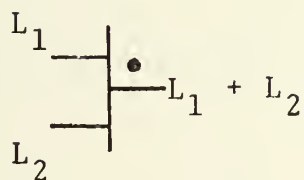


The switch is closed if either -6 volts is applied or the input is left open; the switch is open if 0 volt is applied.

(7) OR Gate



(8) AND Gate





## APPENDIX B: ANALOG SIMULATION

### 1. Nonlinearities

#### (a) Saturation

Figure B-1a shows the saturation characteristic curve and Figure B-1b is the circuit diagram for the simulation using the analog computer. Referring to Fig. B-1b, the simulation works as follows:

$$(1) \quad e_i < -a$$

Algebraic sum of  $C1 < 0 \rightarrow C1$  false,  $\overline{C1}$  true and also the algebraic sum of  $C2 < 0 \rightarrow C2$  false,  $\overline{C2}$  true such that the output of the AND gate = 0 and D/A1 is open. For  $\overline{C1}$  true, D/A2 is closed and for  $C2$  false, D/A3 is open, therefore,

$$e_o = +V_1$$

(2) Algebraic sum of  $C1 > 0 \rightarrow C1$  true,  $\overline{C1}$  false and the algebraic sum of  $C2 < 0 \rightarrow C2$  false and  $\overline{C2}$  true. The output of the AND Gate = -6 volts and D/A1 is closed. For  $\overline{C1}$  false, D/A2 is open and  $C2$  false, D/A3 is open, therefore,

$$e_o = -me_i$$

$$(3) \quad 0 < e_i < b$$

Algebraic sum of  $C1 > 0 \rightarrow C1$  true,  $\overline{C1}$  false and the algebraic sum of  $C2 < 0 \rightarrow C2$  false and  $\overline{C2}$





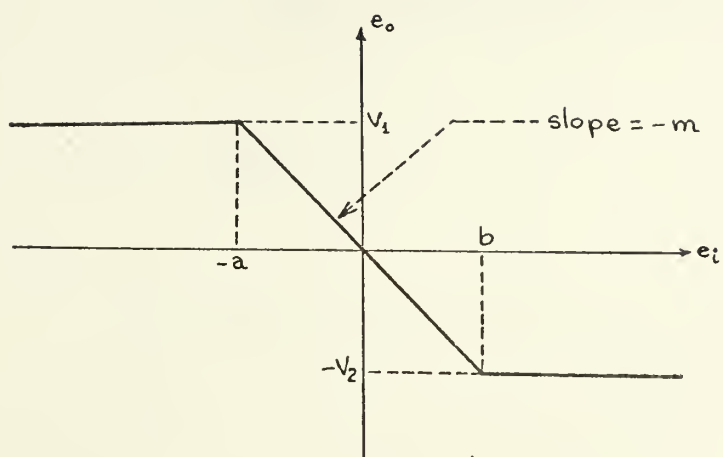


FIGURE B-1a: Saturation characteristic curve.

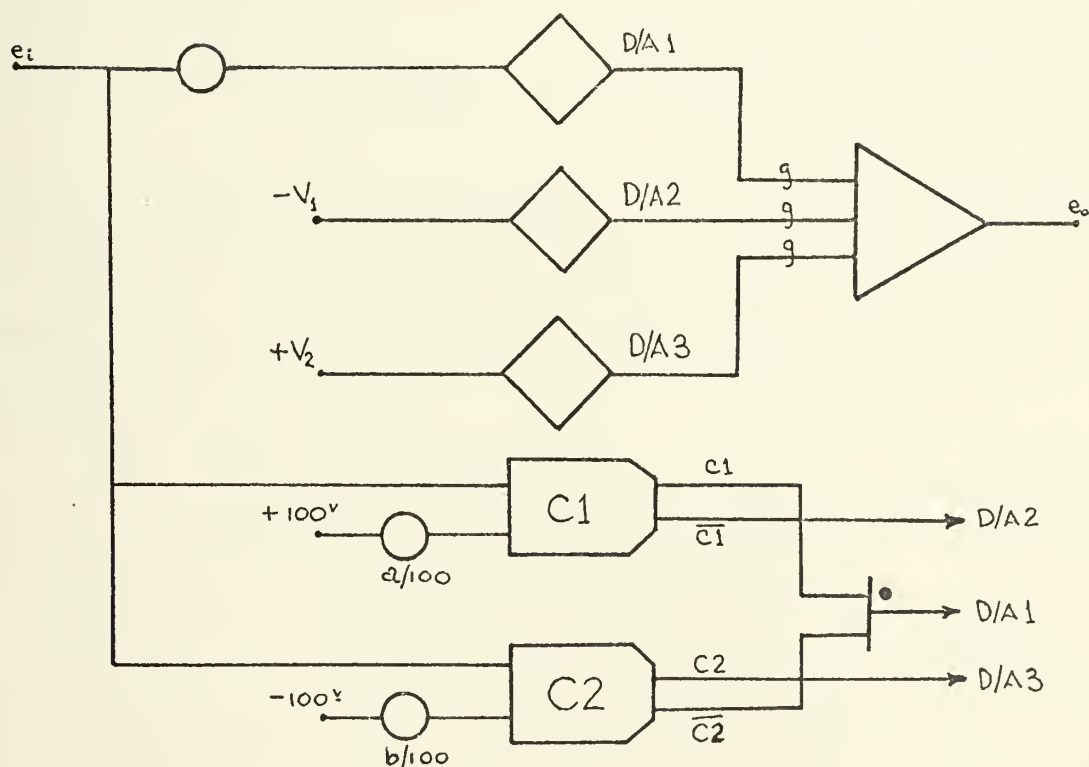


FIGURE B-1b: Analog simulation for saturation. The symbol "g" refers to frid of amplifier and 100 is the reference voltage of the computer being used.



true. The output of the AND Gate = -6 volts and D/A1 is closed. For  $\overline{C1}$  false, D/A2 is open and C2 false, D/A3 is open, therefore,

$$e_o = -me_i$$

$$(4) \quad e_i > b$$

Algebraic sum of  $C1 > 0 \rightarrow C1$  true,  $\overline{C1}$  false and the algebraic sum of  $C2 > 0 \rightarrow C2$  true and  $\overline{C2}$  false. The output of the AND Gate = 0 and D/A1 is open. For  $\overline{C1}$  false, D/A2 is open and for C2 true, D/A3 is closed, therefore,

$$e_o = -V_2$$

In the description of operation above, -6 volts represents a logical 1 and 0 volts represents a logical 0. The logic control for the D/A switches is the output of the comparator or of the AND Gate.

#### (b) Relay with Hysteresis

Figure B-2a is the characteristic curve of a non-ideal relay with hysteresis and Figure B-2b is the diagram for analog simulation. The Track-Track (T/T) unit is composed of two D/A switches with a common G terminal. Figure B-2c is the analog circuit for the T/T unit. Switch T is closed and  $\overline{T}$  is open when a logical 1 is applied to the input or the input is left open. When the input is a logical 0, the switch states are reversed. When the switches are open, the resistor switch ends are grounded.



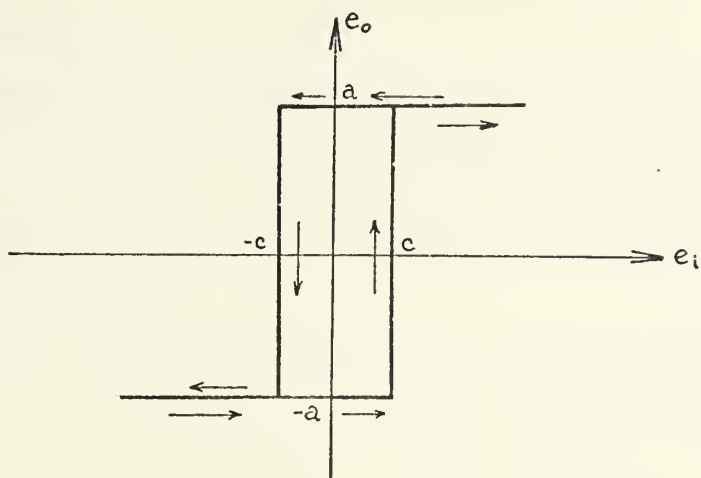


FIGURE B-2a: Characteristic curve of relay with hysteresis.

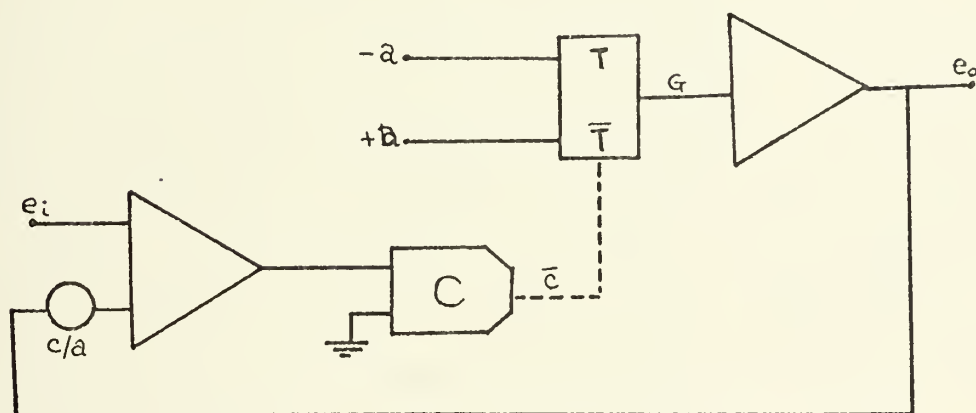


FIGURE B-2b: Analog simulation of relay with hysteresis.

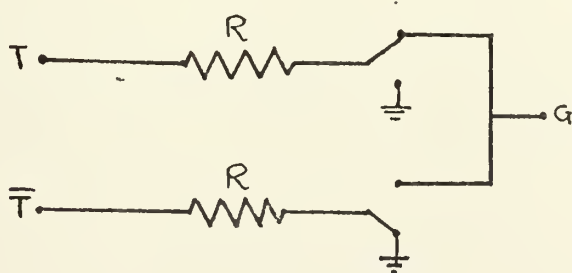


FIGURE B-2c: Analog circuit of track-track (T/T) unit.



### (c) Backlash

The backlash characteristic curve is shown in Figure B-3a and the analog simulation circuit diagram is shown in Figure B-3b. The backlash characteristic is achieved as follows:

As  $e_i$  increases from zero nothing happens to  $e_o$  until  $(e_i - e_o) = e' > a$ . At that point the integrator output will begin to change at the rate  $m(e_i - e_o)$ , and  $e_o$  will approach  $(e_i - a)$  through the feedback correction of the loop. As soon as  $e_i$  changes direction,  $(e_i - e_o)$  becomes less than  $a$  resulting in  $e'$  going to zero and the output of the integrator holding its value. As  $e_i$  continues to decrease,  $e_o$  remains unchanged until  $e'$  becomes less than  $b$ , at which time, the output of the integrator begins to change at the rate  $m(e_i - e_o)$ . Again when  $e_i$  changes direction,  $e'$  goes to zero and the output of the integrator remains at some steady voltage.

The results of the simulation for the three nonlinearities considered are shown in Figure III-2.

### 2. Scaling

When simulating problems on an analog computer, scaling is quite important. There are many approaches to this technique. What is of interest here is to point out that it is necessary to perform magnitude and frequency scaling on the analog simulation of the nonlinearities simulated in this study. This is true for the two nonlinearities with hysteresis. The simulation for the saturation nonlinearity only requires amplitude scaling.





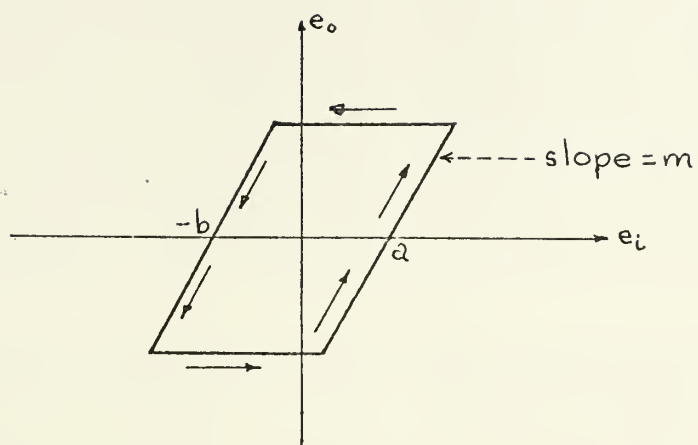


FIGURE B-3a: Backlash characteristic curve.

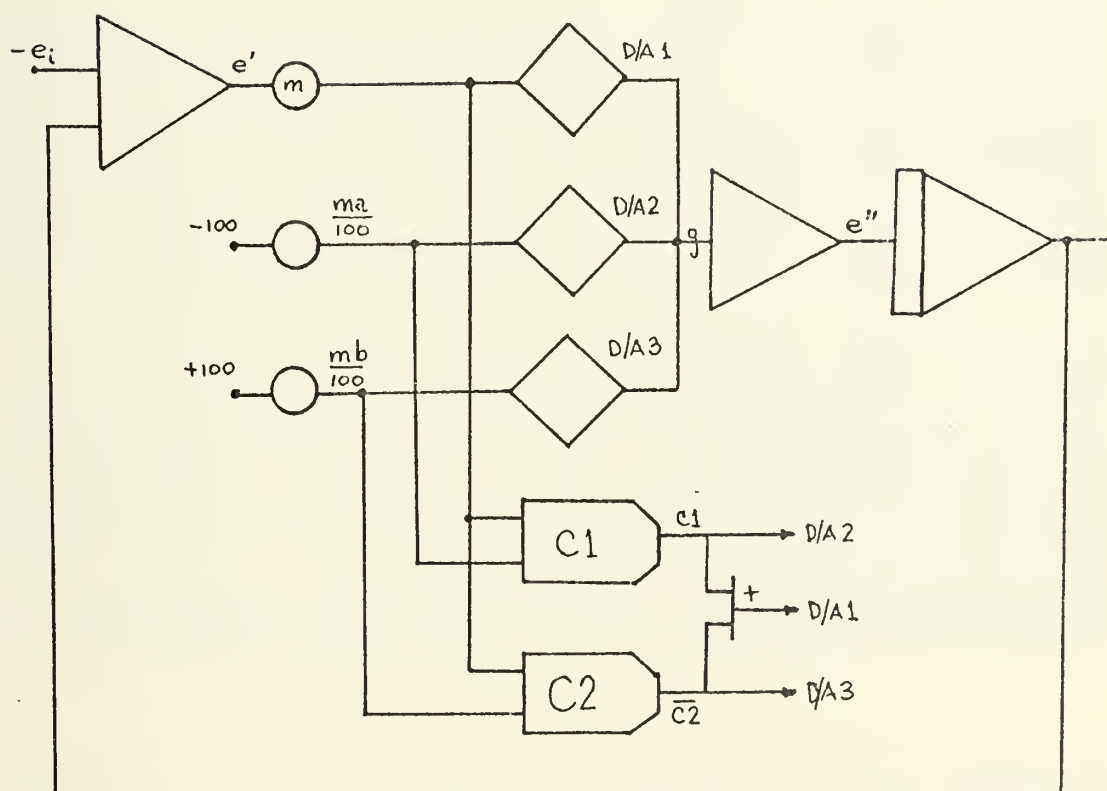


FIGURE B-3b: Analog simulation for backlash.



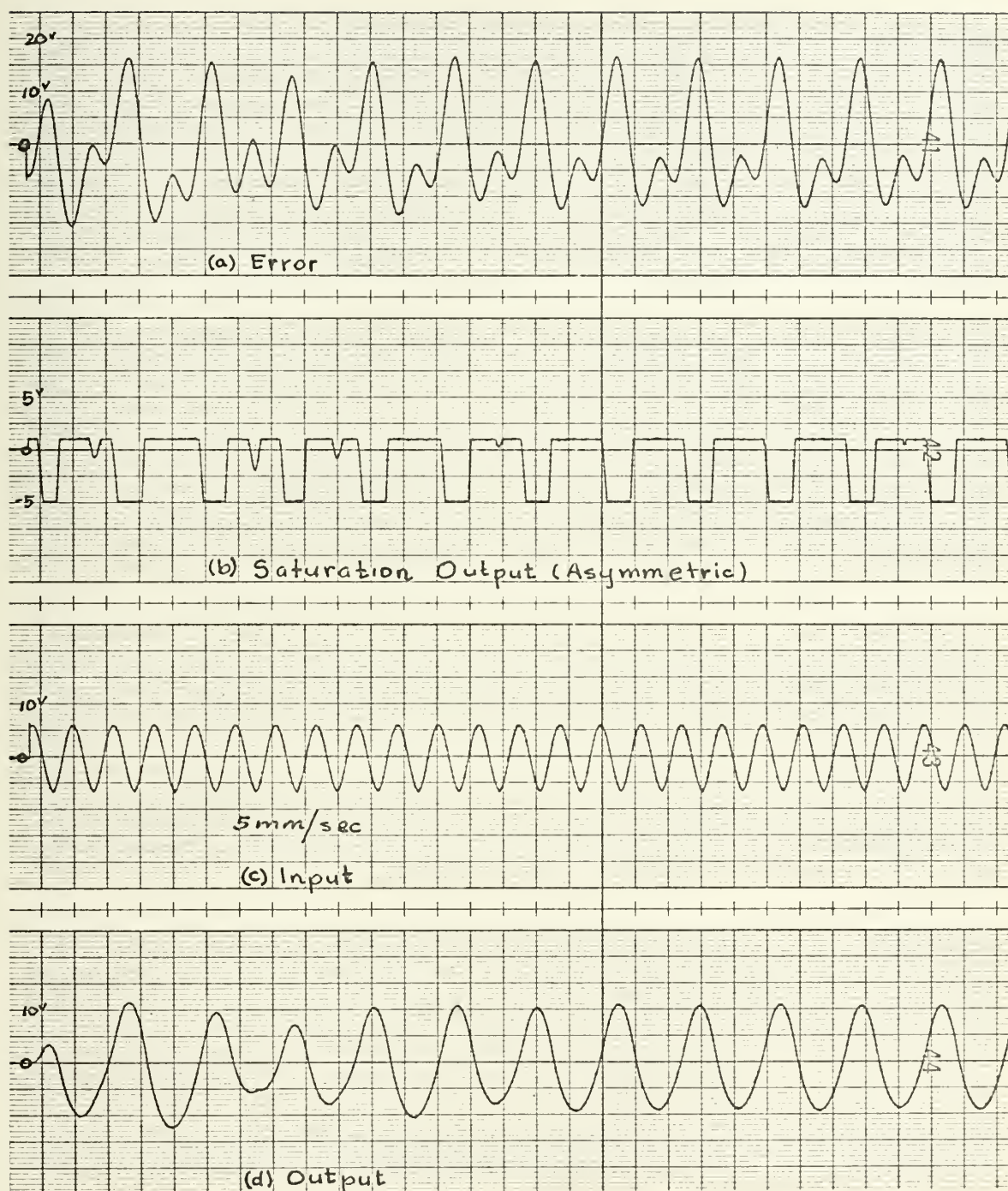


FIGURE C-1:  $1/2$  subharmonic oscillation due to asymmetric saturation input =  $6 \sin 1.6\pi t$ ;  $K_m = 20$



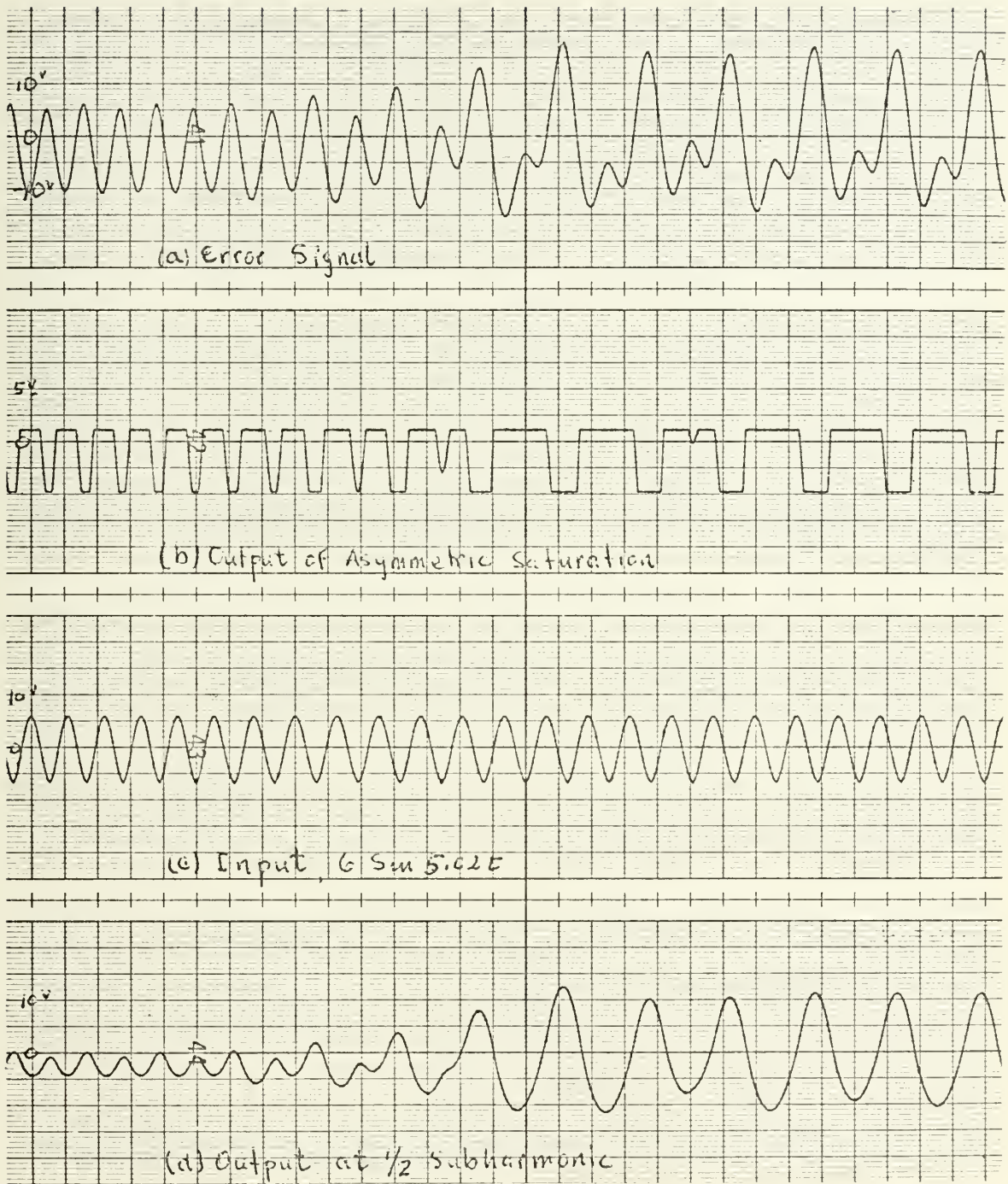


FIGURE C-2: Fundamental to  $1/2$  subharmonic due to asymmetric saturation,  $\text{smm/sec}$ .





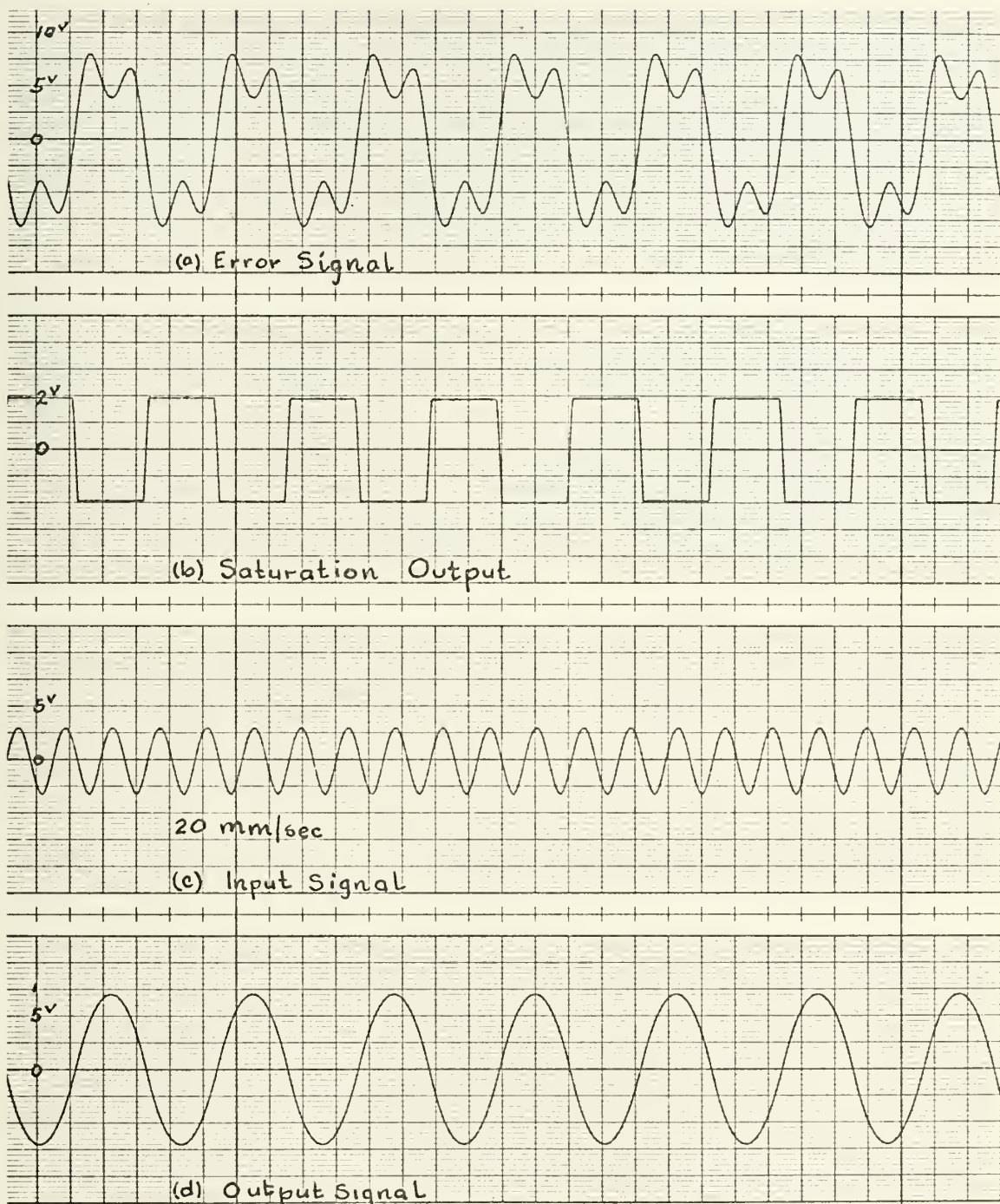


FIGURE C-3:  $1/3$  subharmonic oscillation due to symmetrical saturation input =  $3 \sin 5.6\pi t$ ,  $K_m = 100$





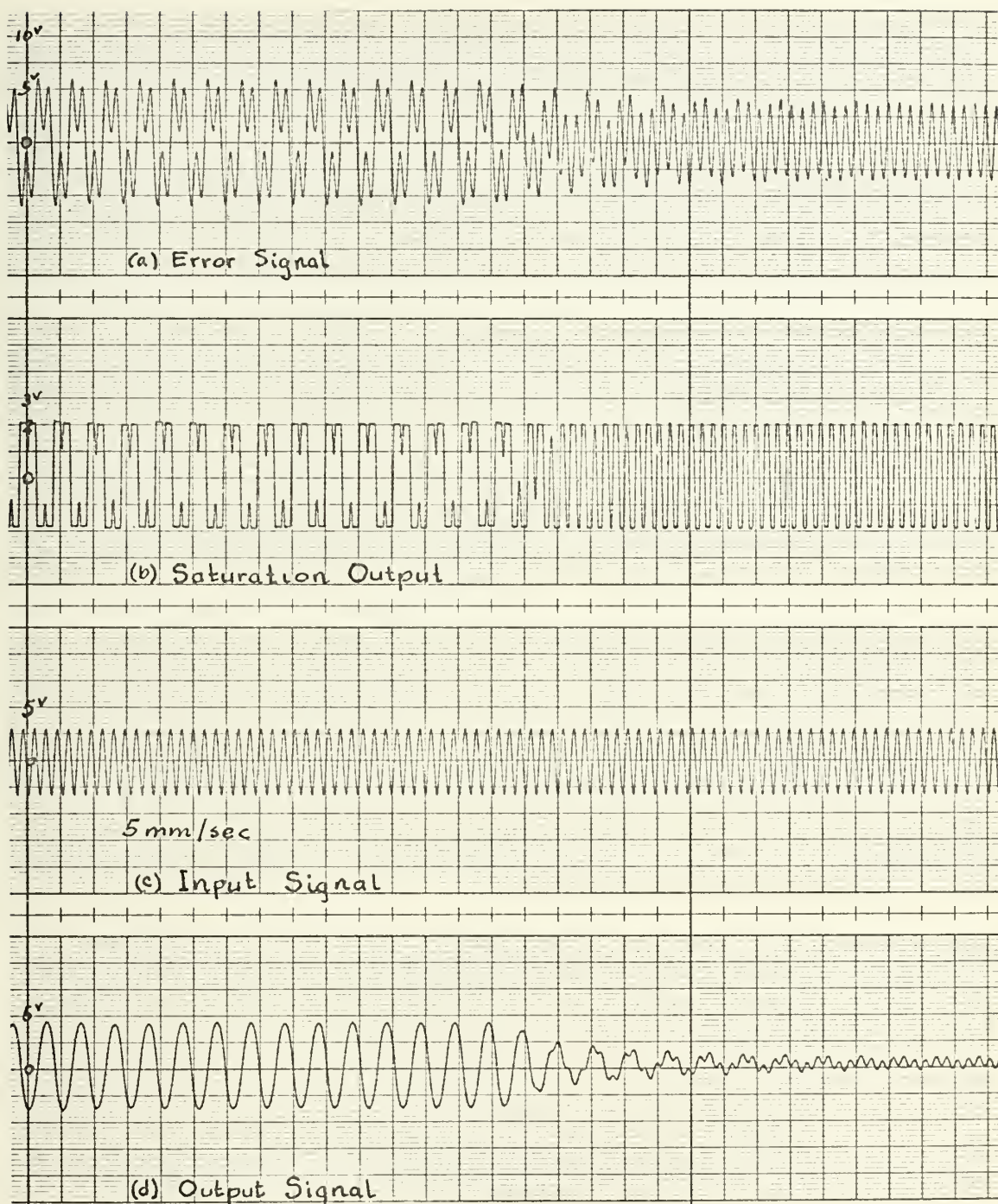


FIGURE C-4: 1/3 subharmonic oscillation to fundamental oscillation input frequency from 2.9hz to 3.0hz  
 $K_m = 70$ .



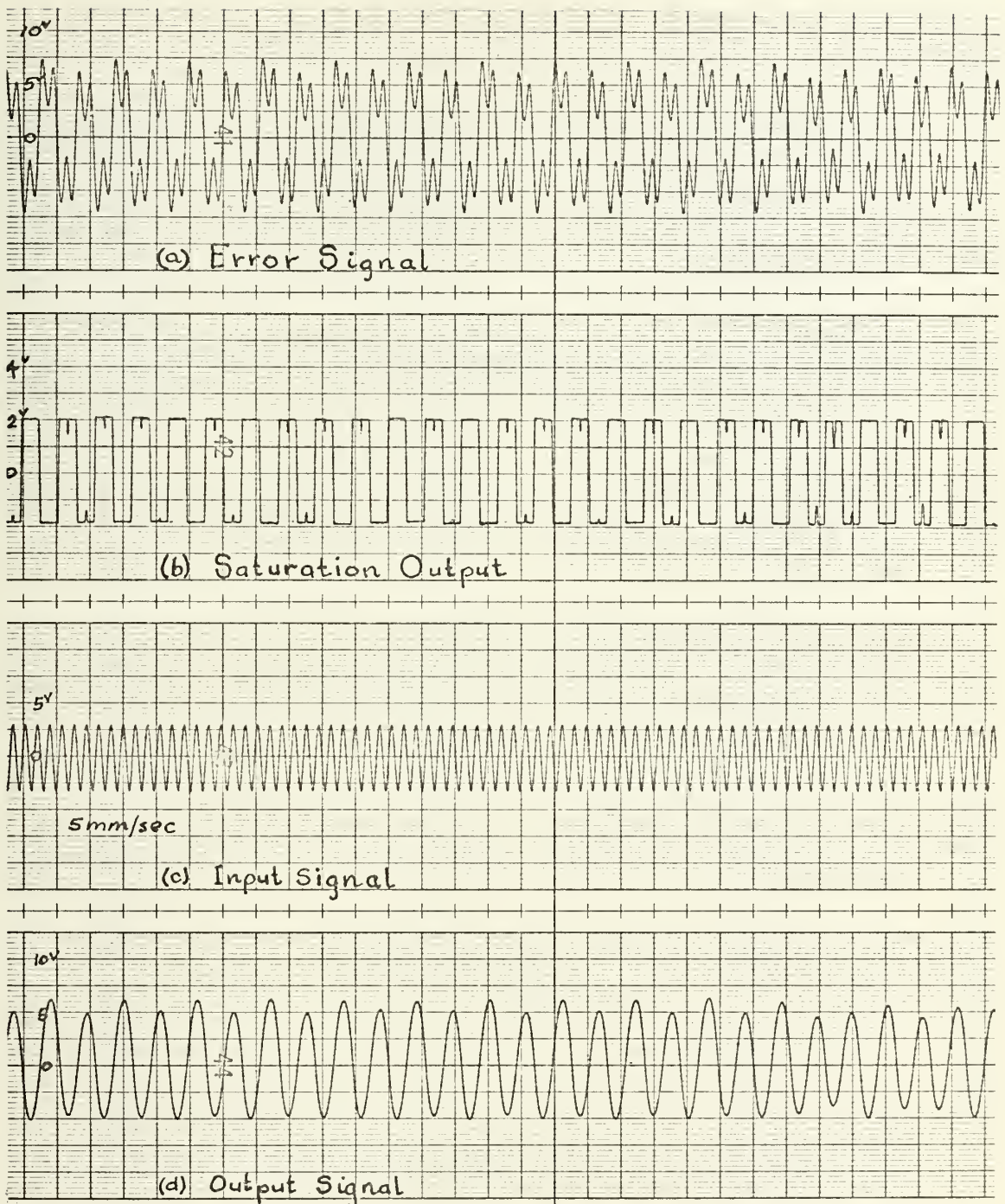


FIGURE C-5:  $1/3$  subharmonic oscillation due to saturation  
input =  $3 \sin 5.2\pi t$ ,  $K_m = 70$





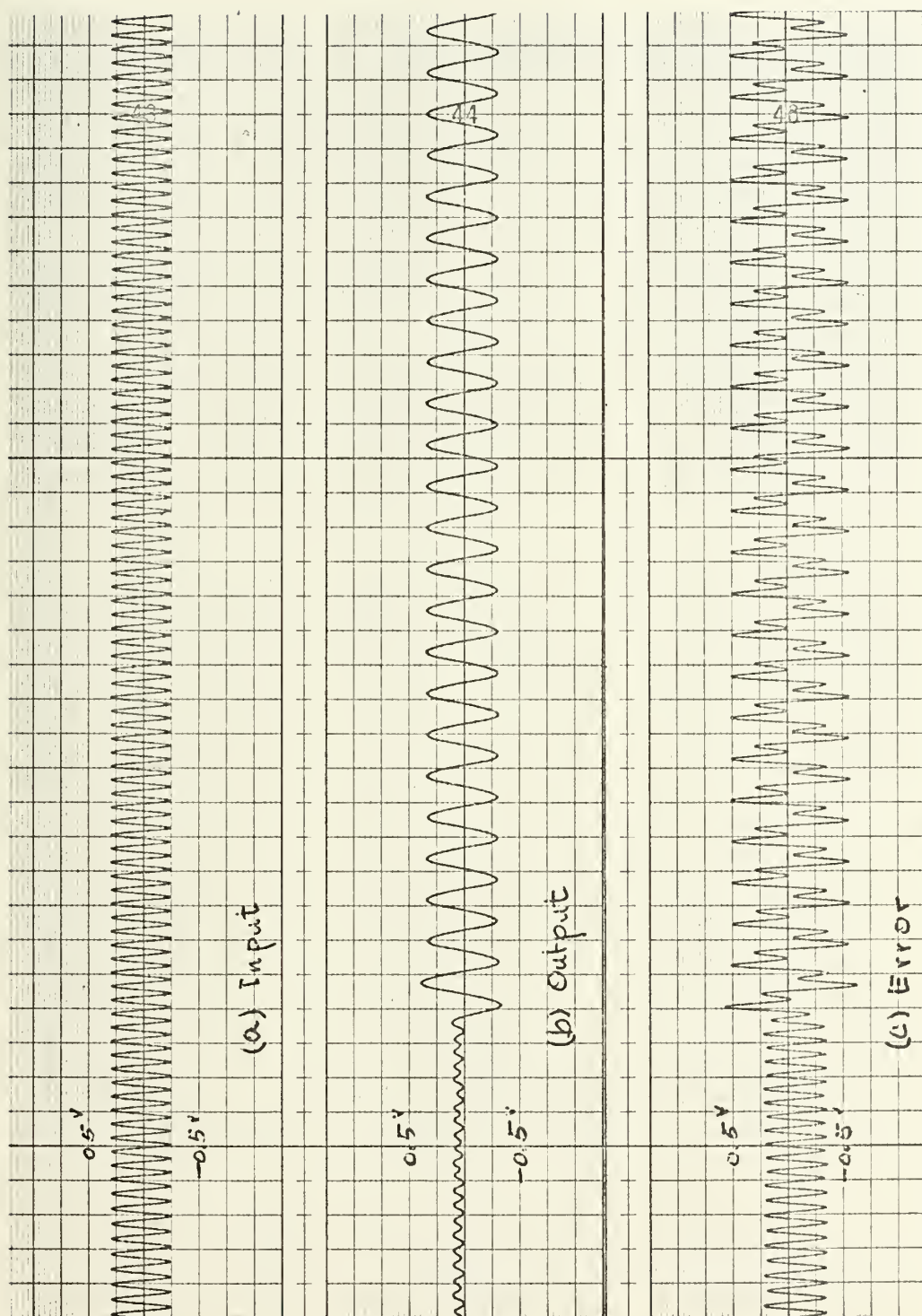


FIGURE C-6: Fundamental oscillation to  $1/3$  subharmonic oscillation for relay.  
Input =  $0.27 \sin 2\pi t$



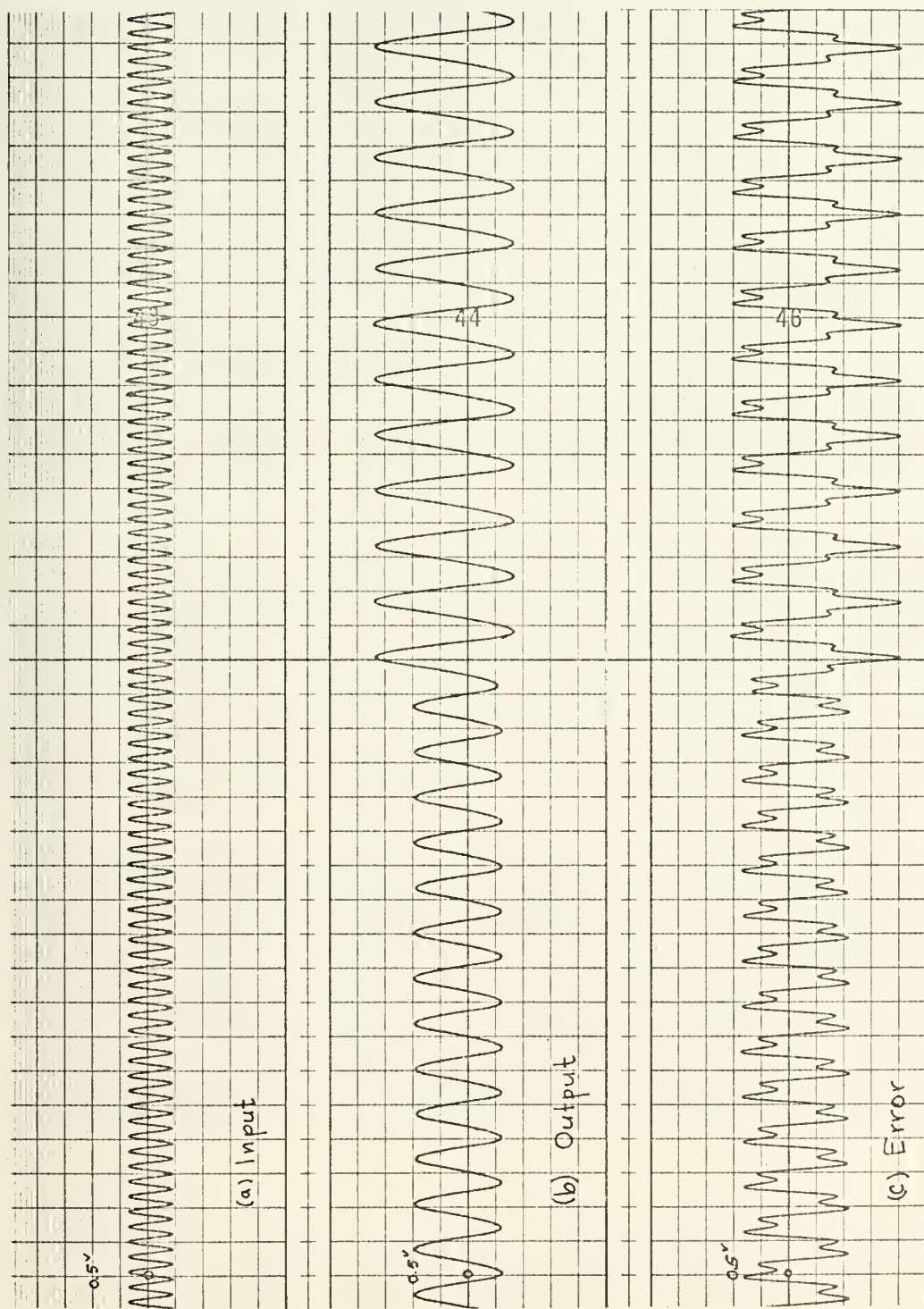


FIGURE C-7: 1/3 to 1/4 subharmonic oscillation due to relay with hysteresis.  
 $a = 1$ ,  $c = 0.3$ ; input =  $0.2 \sin 1.8\pi t$  to  $0.2 \sin 2\pi t$ .





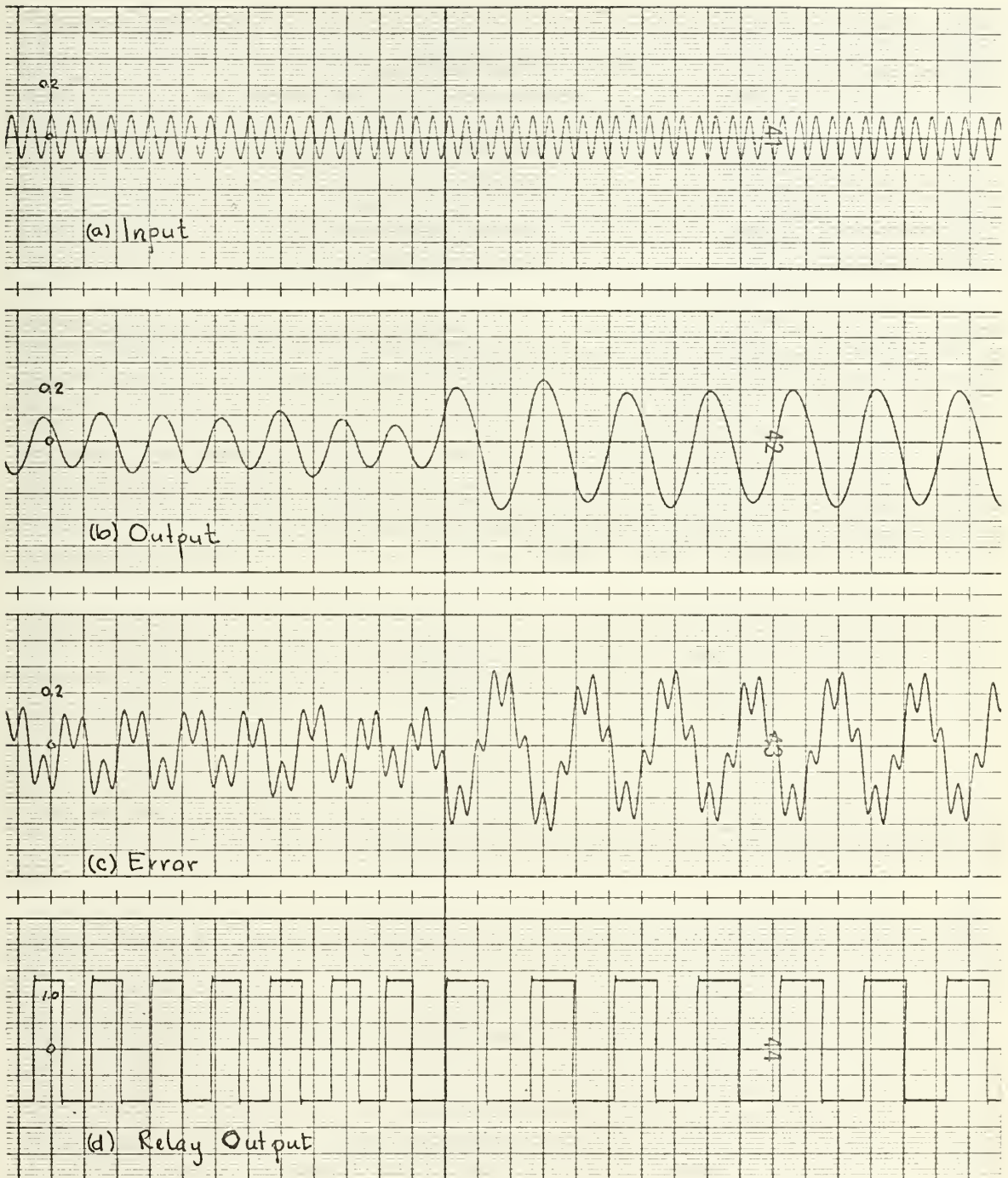


FIGURE C-8:  $1/3$  to  $1/5$  order subharmonic for system with relay;  $a = 1$ ,  $c = 0.1$ . Input frequency from 1.8 hz to 1.9 hz.



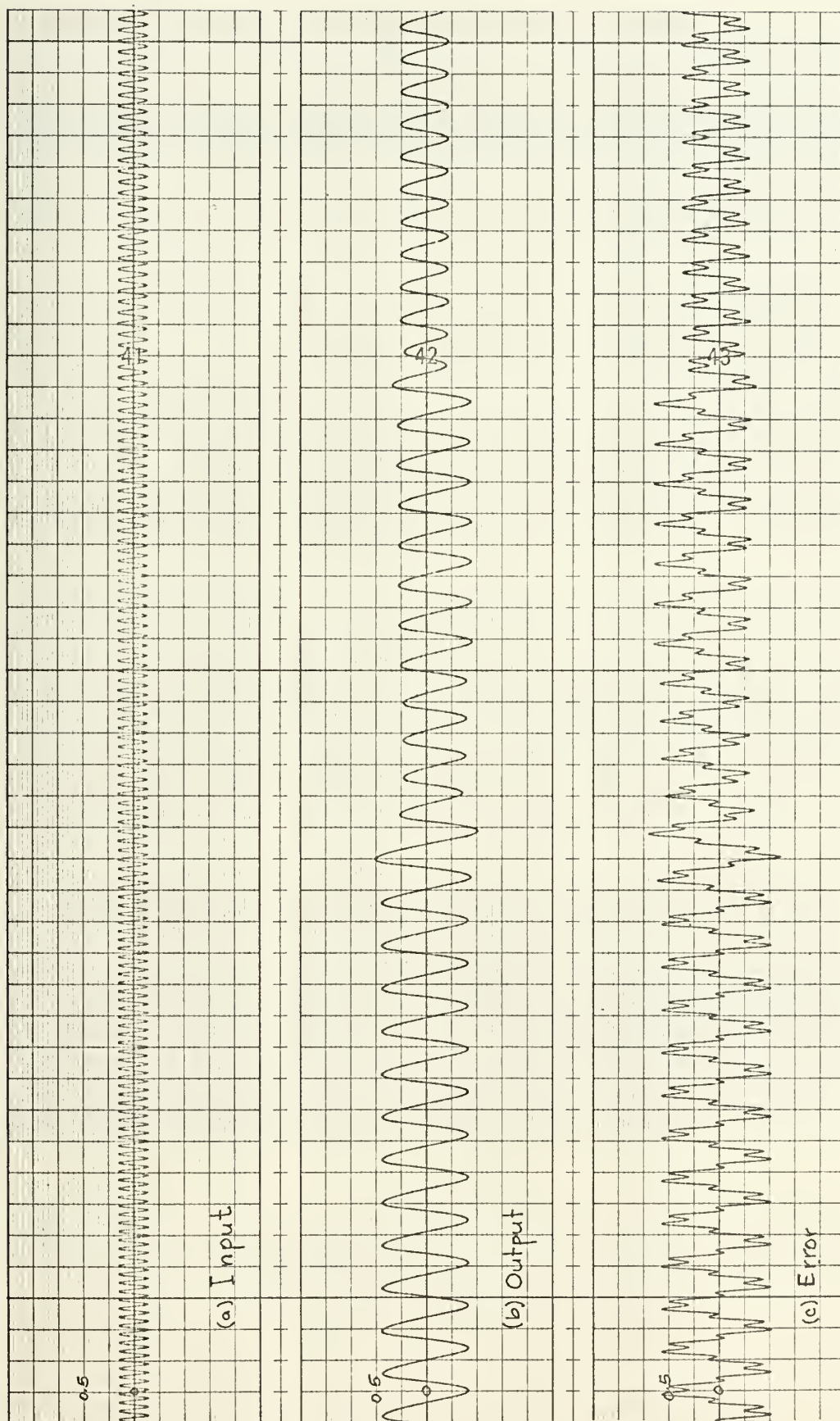


FIGURE C-9: Change of input frequency from 1.5hz to 1.3hz to 1.2hz resulting in a change of subharmonic oscillation from  $1/5$  to  $1/4$  to  $1/3$ .  $a = 1$ ,  $c = 0.1$ .





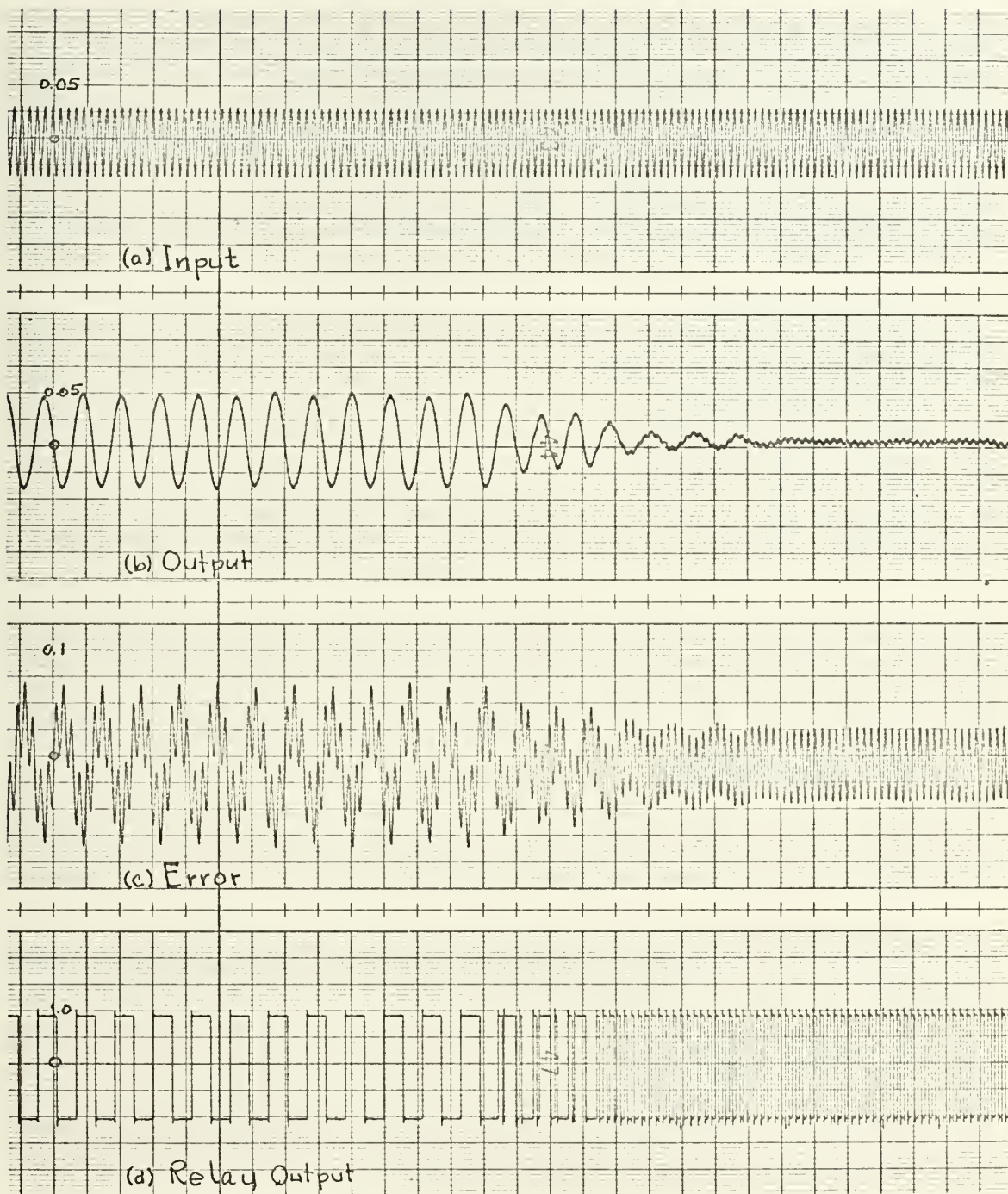


FIGURE C-10:  $1/5$  subharmonic oscillation to fundamental oscillation.  $a = 1$ ,  $c = .01$ . Input frequency from 4.0 hz to 4.6hz.



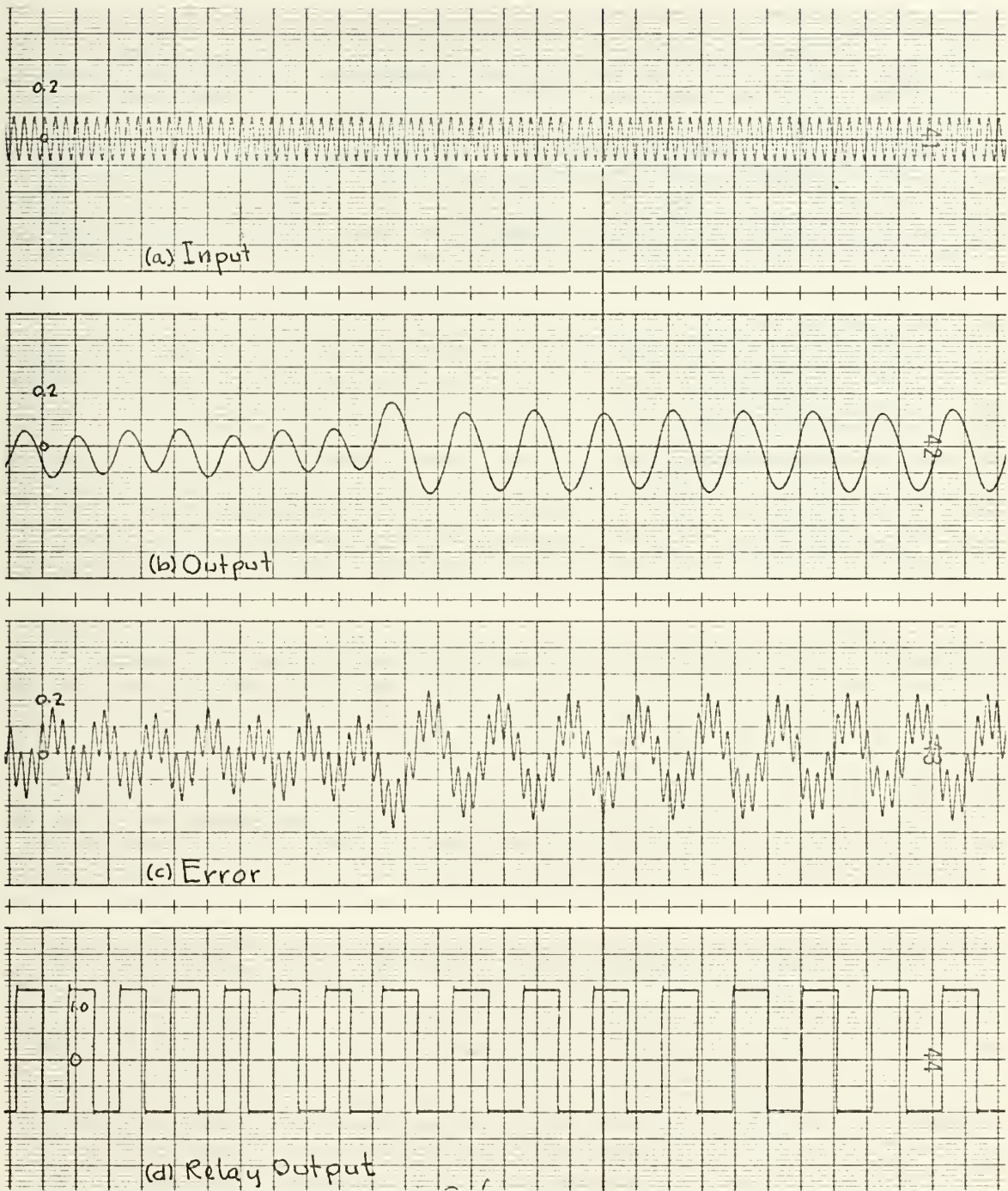


FIGURE C-11:  $1/5$  to  $1/7$  subharmonic oscillation for relay  $a = 1$ ,  $c = 0.1$ . Input frequency from 3.1hz to 3.2hz.





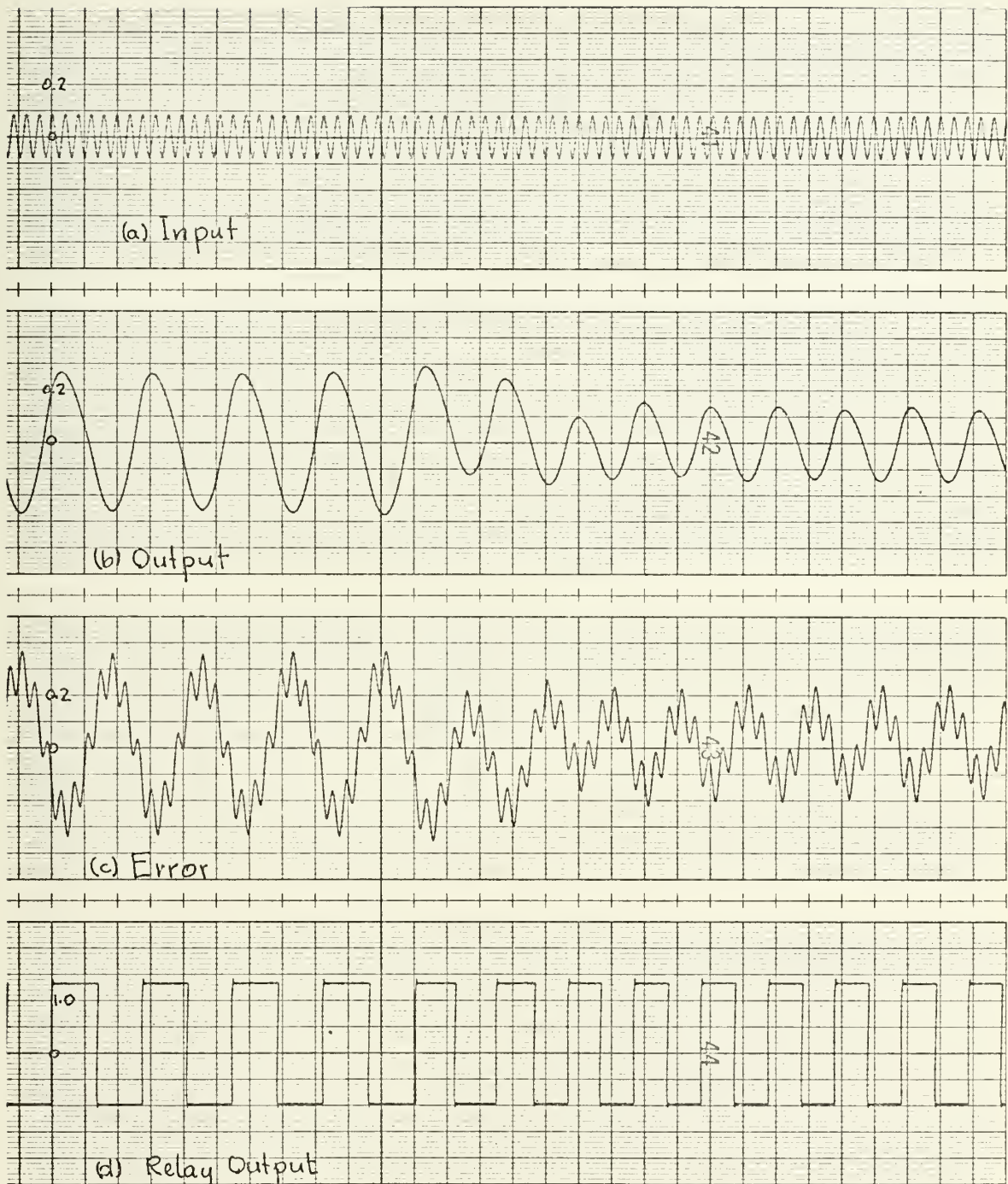


FIGURE C-12:  $1/7$  to  $1/5$  subharmonic oscillation. Input frequency from 2.5hz to 2.4hz,  $a = 1$ ,  $c = 0.1$ .



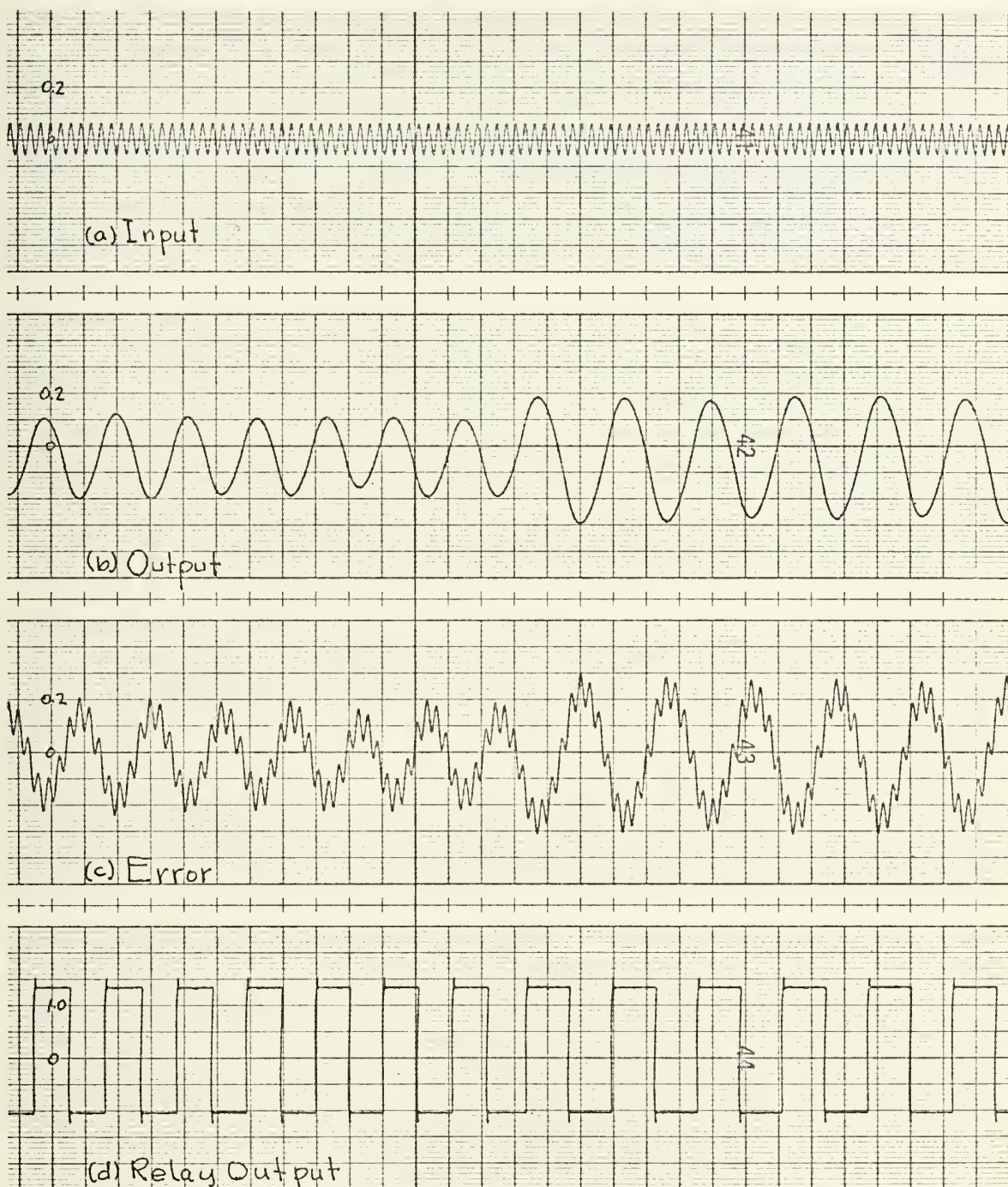


FIGURE C-13: Change of input frequency from 3.2hz to 3.4hz causing change of subharmonic oscillation from  $1/7$  to  $1/9$ ;  $a = 1$ ,  $c = 0.1$ .





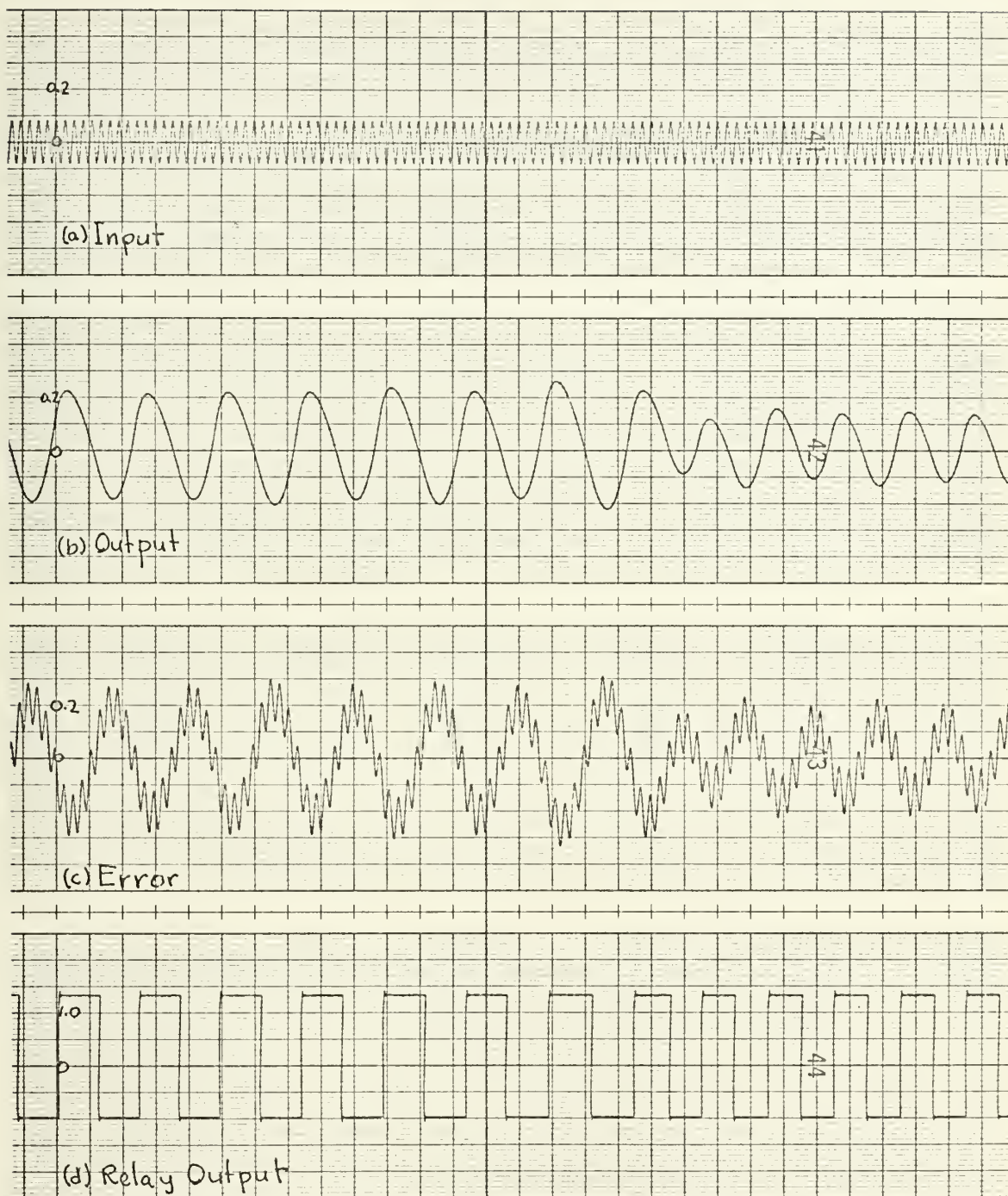


FIGURE C-14:  $1/9$  to  $1/7$  subharmonic for relay,  $a = 1$ ,  $c = 0.1$ .  
Input frequency from 3.5hz to 3.4 hz.



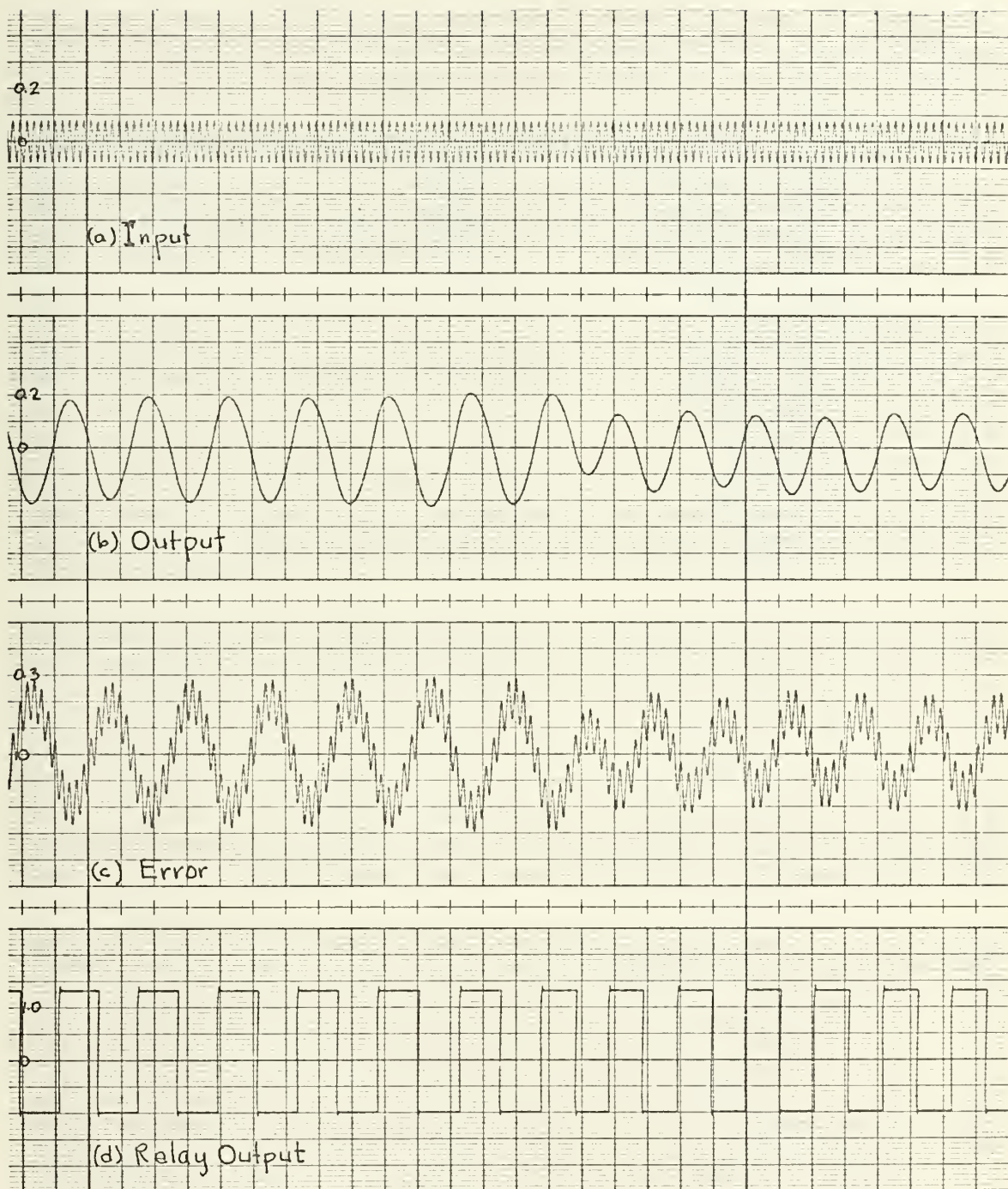


FIGURE C-15:  $1/11$  to  $1/9$  subharmonic oscillation. Input frequency from 4.3hz to 4.2hz.  $a = 1$ ,  $c = 0.1$ .





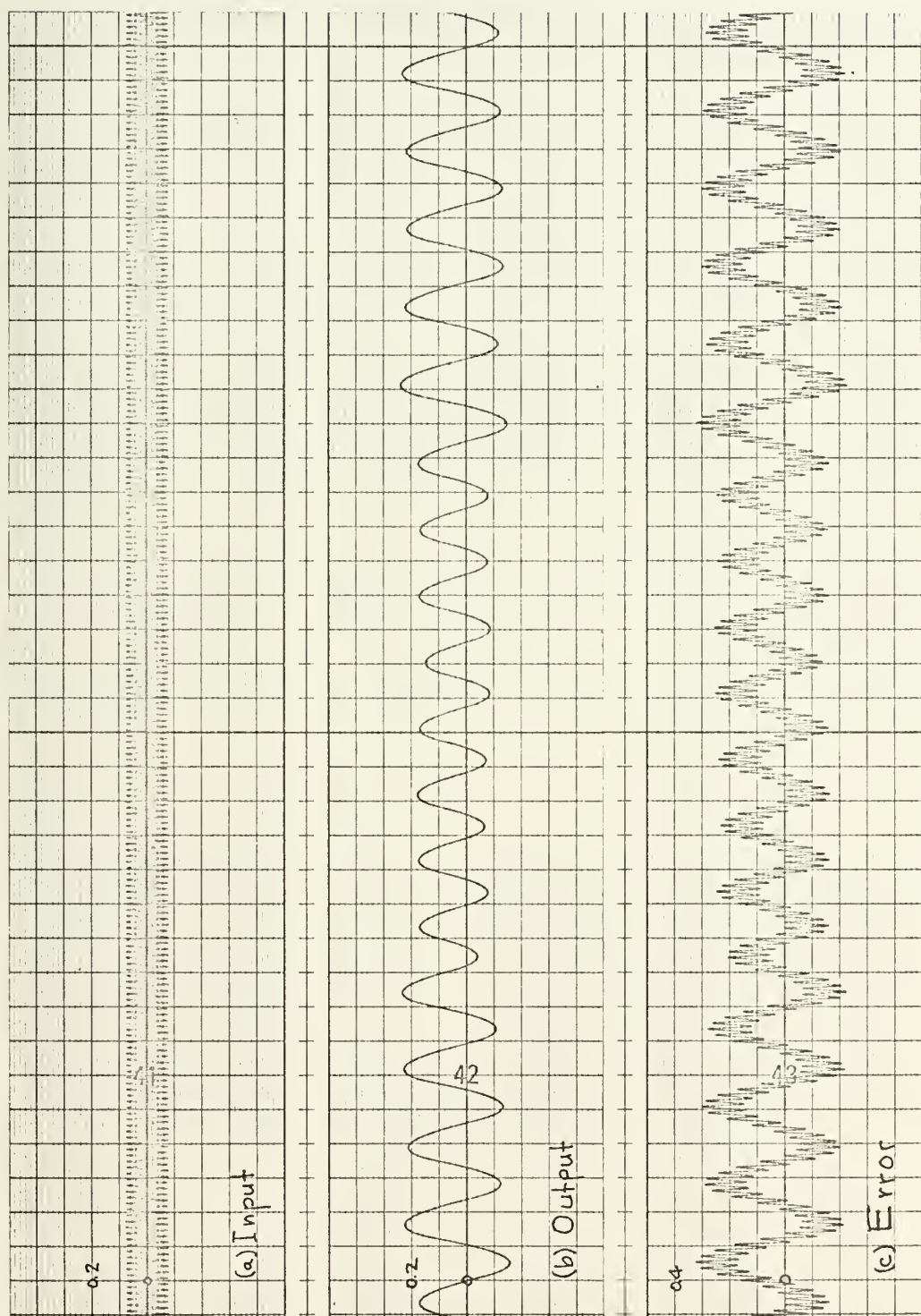


FIGURE C-16: Output oscillating at two different subharmonics  $1/11$  and  $1/13$  at same input frequency of  $5.5\text{hz}$ .  $a = 1$ ,  $c = 0.1$ .



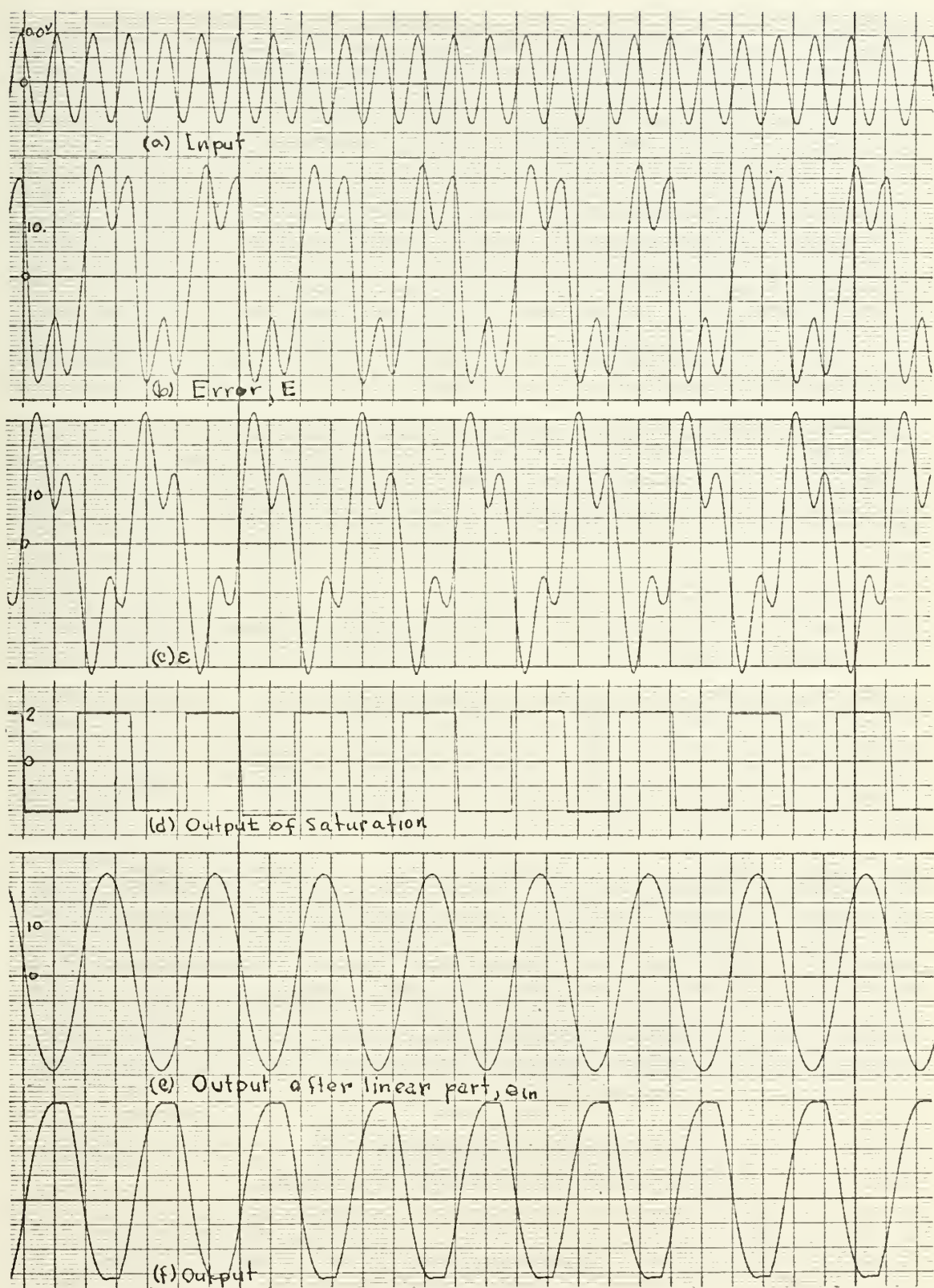


FIGURE C-17: Signal waveform of system with two nonlinearities  $\zeta = 0.387$ .

- |                               |                               |
|-------------------------------|-------------------------------|
| (a) Input = $9\sin 3.44\pi t$ | (d) Output of $N$ , $f(t)$    |
| (b) Error Signal, $E$         | (e) Input to $N_2$ , $e_{in}$ |
| (c) Input to $N_1$ , $E$      | (f) System Output $in$        |





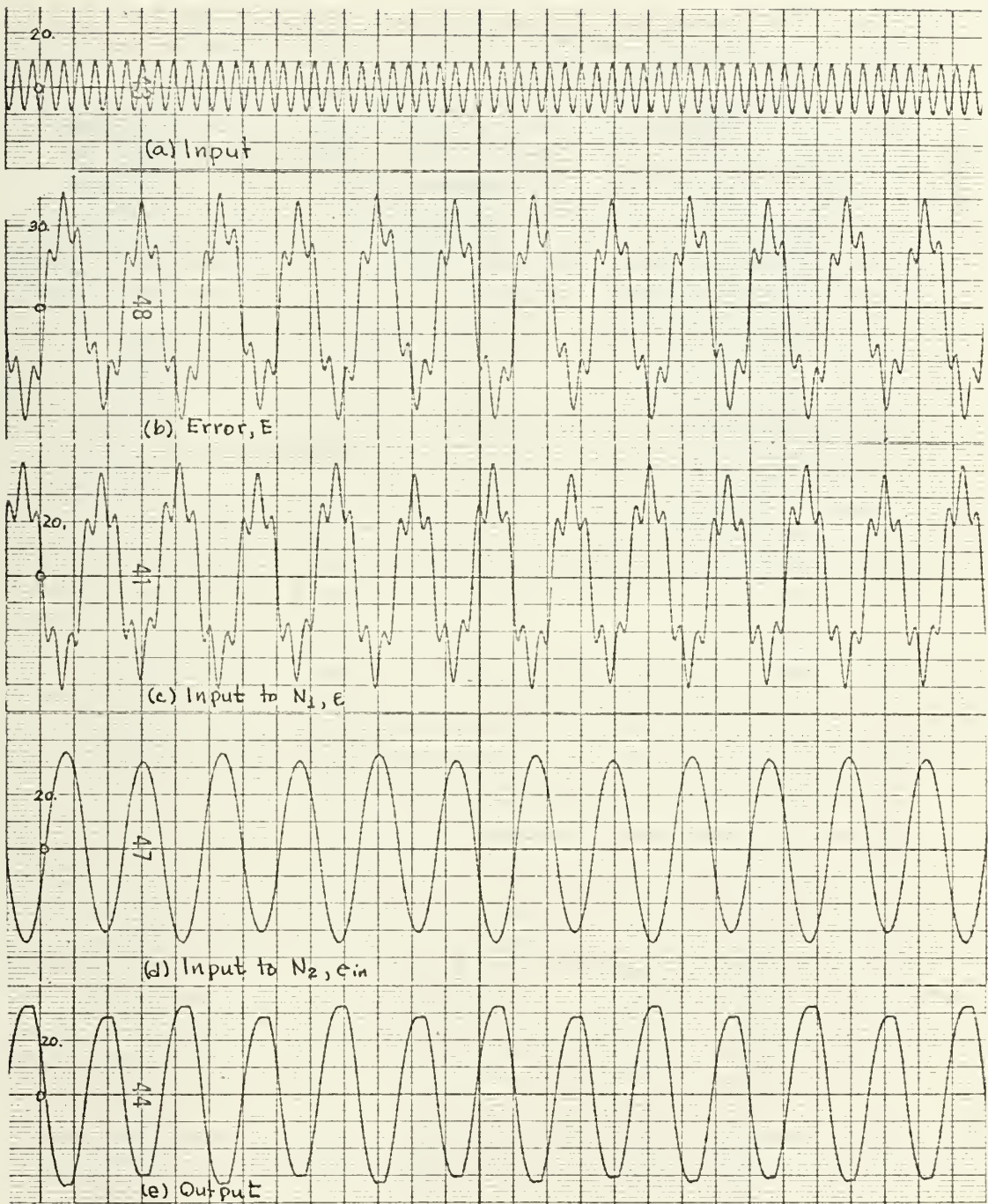


FIGURE C-18: Singal waveforms for  $1/5$  subharmonic oscillation. Input =  $95\sin 44 t$ ;  $K_m=50$ ,  $k_t=0.04$ .

- |                                 |                                  |
|---------------------------------|----------------------------------|
| (a) Input signal                | (d) Input to second nonlinearity |
| (b) Error signal                | (e) System output                |
| (c) Input to first nonlinearity |                                  |



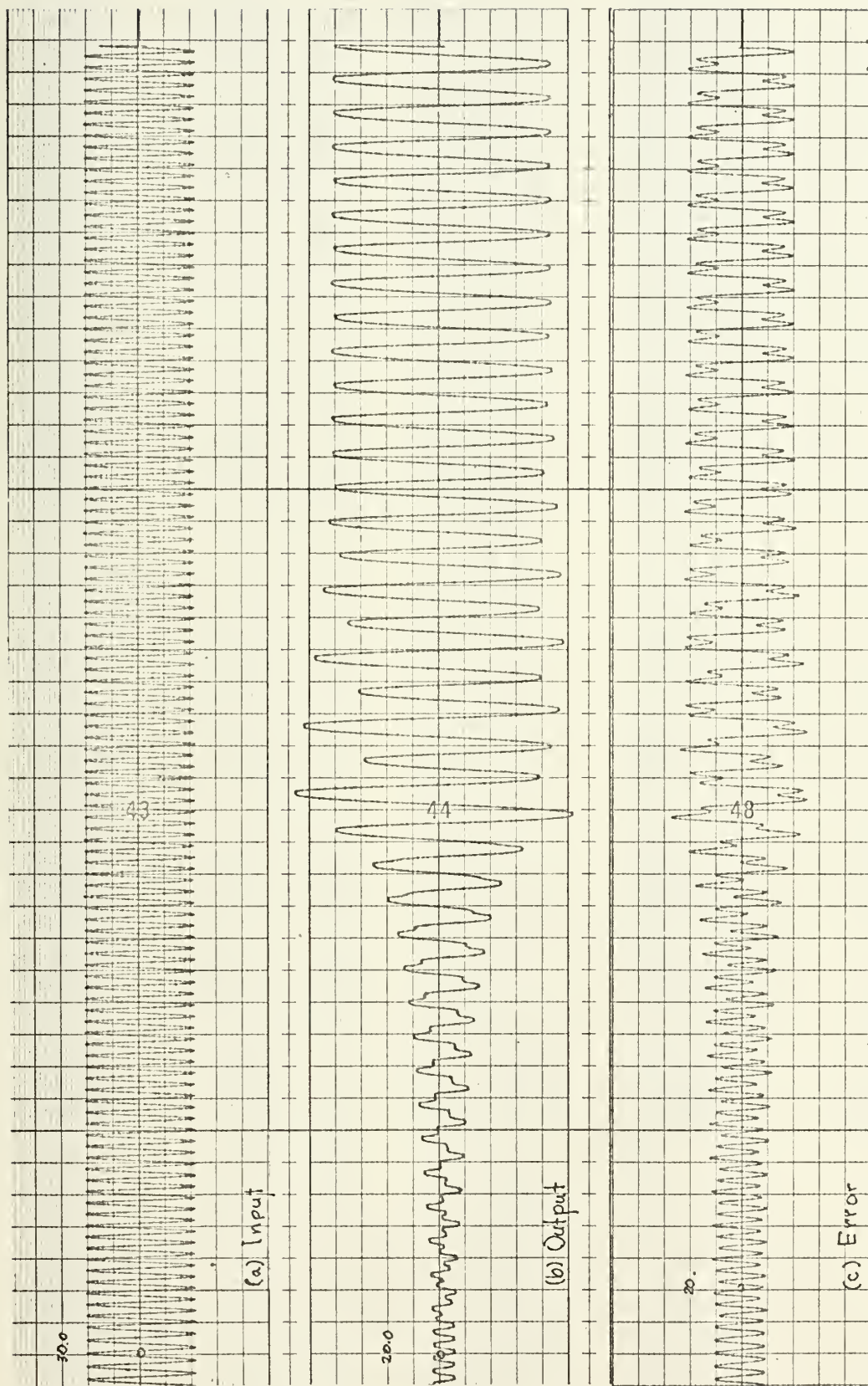


FIGURE C-19: Fundamental oscillation to 1/3 subharmonic oscillation for system with saturation and backlash.  $K_t = 0.04$ ,  $K_m = 50$ .





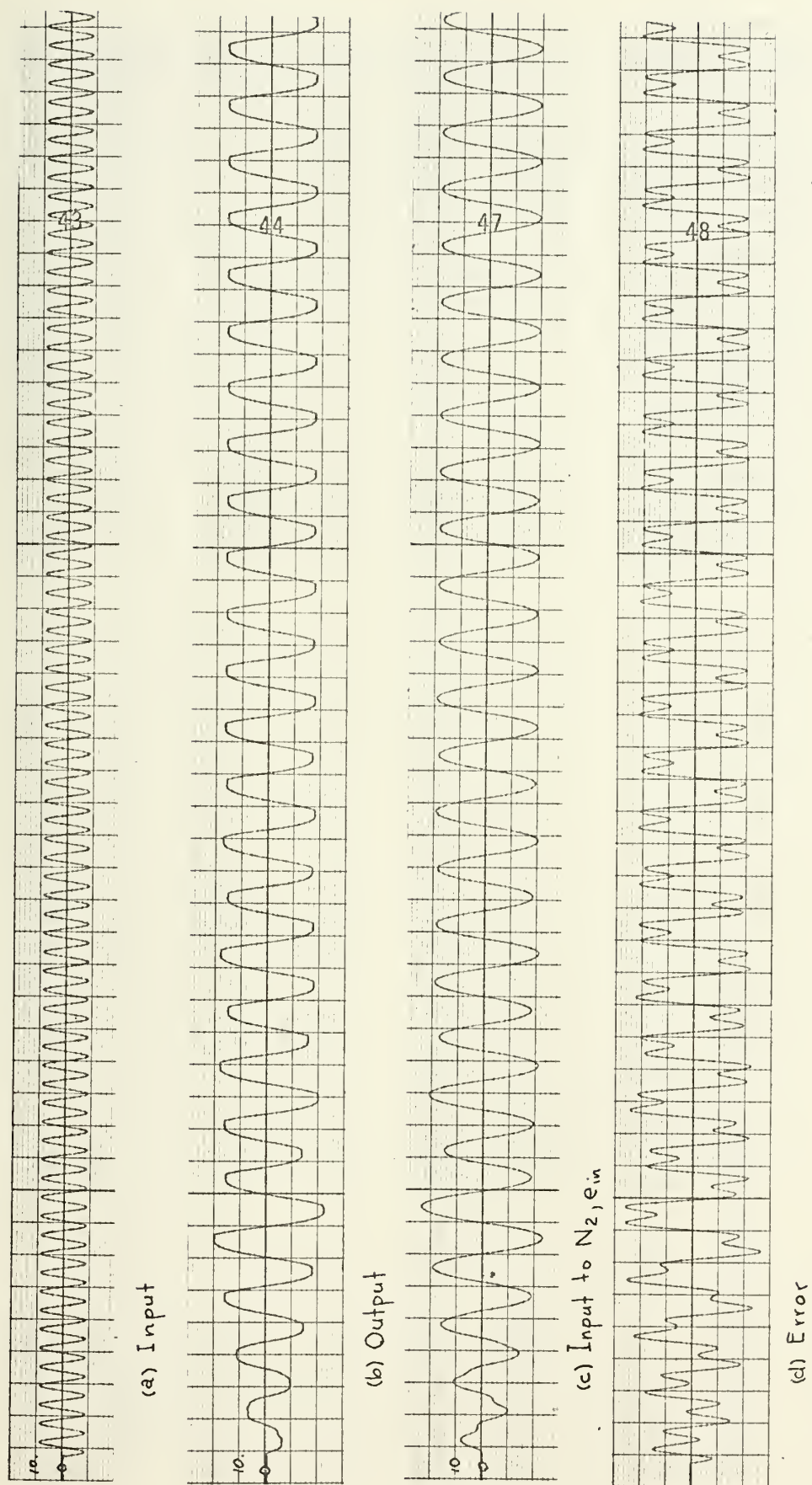


FIGURE C-20:  $1/3$  subharmonic oscillation build up with input =  $9\sin 6.6\pi t$  for saturation and backlash,  $K_t = 0.06$ ,  $K_m = 200$



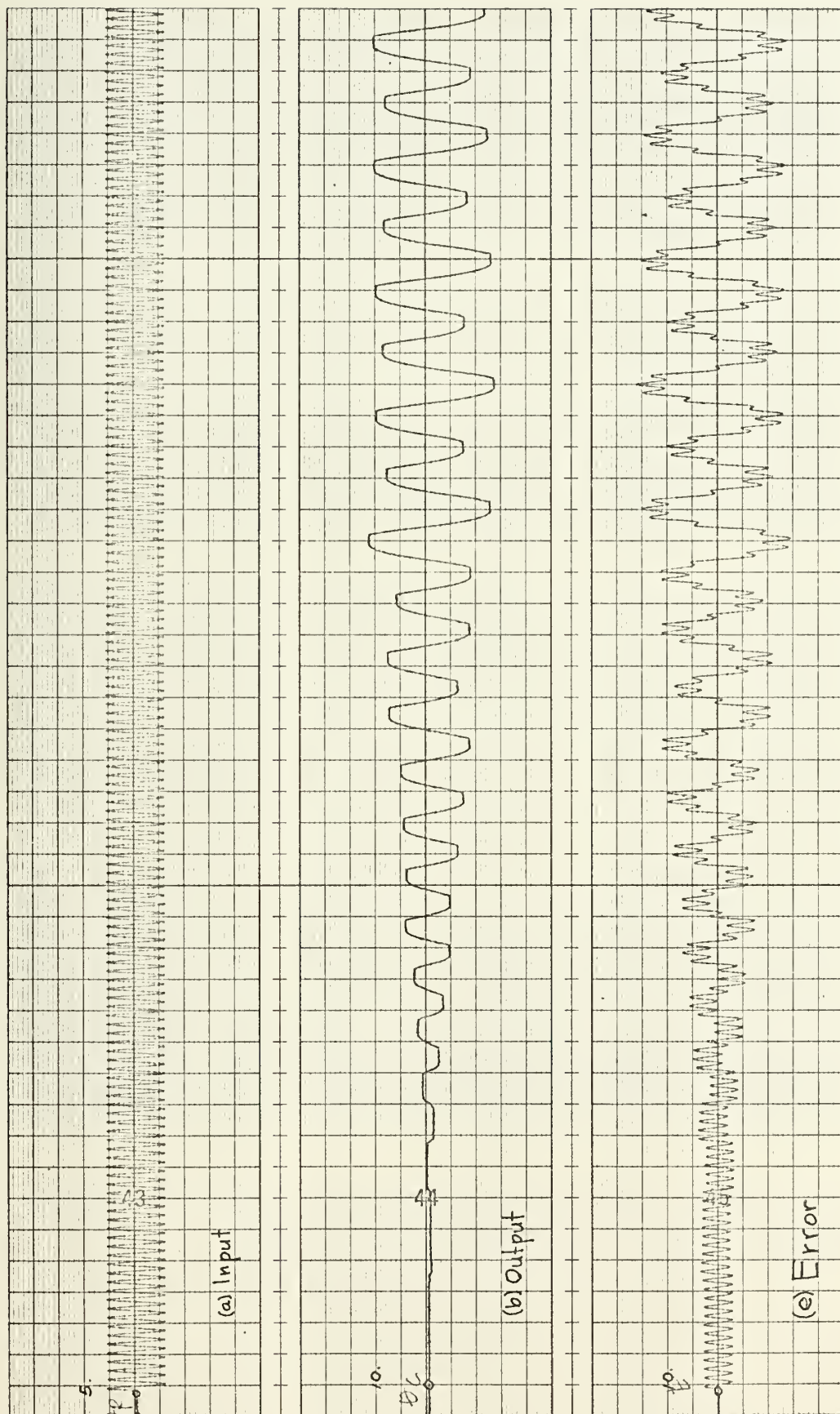


FIGURE C-21: Build up of 1/7 subharmonic saturation and backlash.  $K_t = 0.02$ ,  $K_m = 100$ .



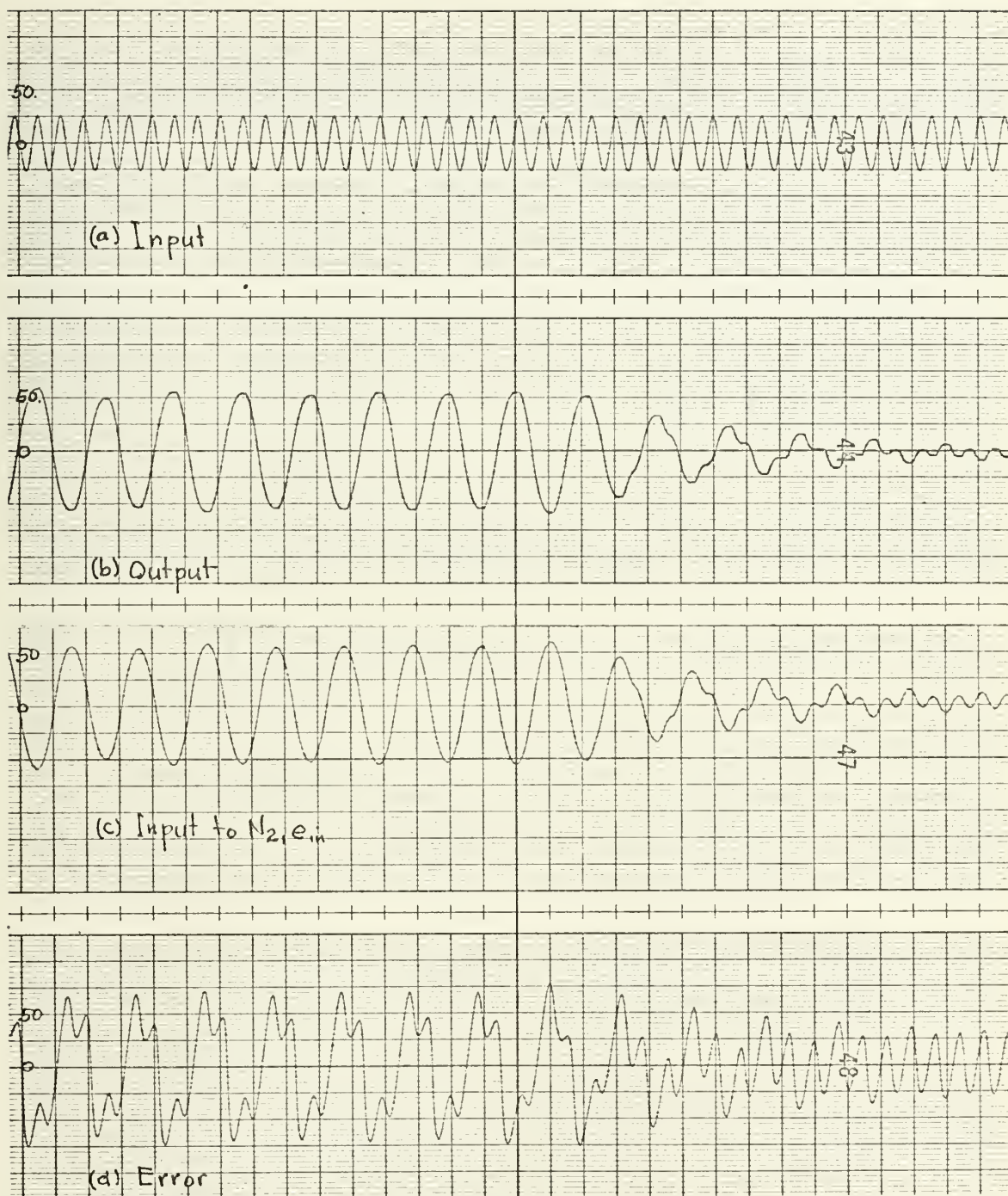


FIGURE C-22: 1/3 subharmonic oscillation fading to fundamental oscillation due to change of input frequency from 1.3 to 1.4 hz. Saturation and backlash:  $K_t = 0.13$ ,  $K = 100$ .





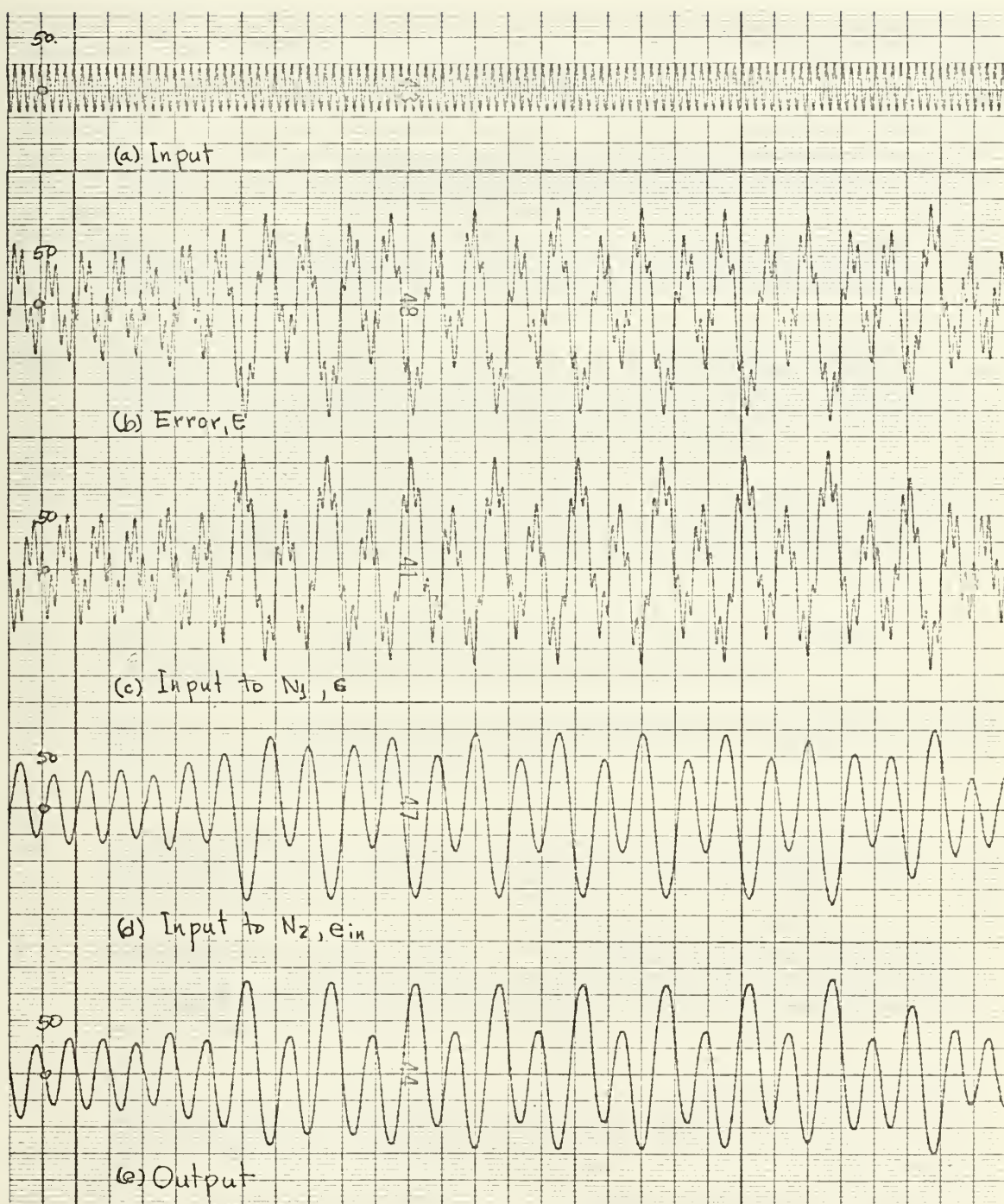


FIGURE C-23: Signal waveform showing change of subharmonic mode from  $1/4$  to  $1/5$ .

- |                               |                    |
|-------------------------------|--------------------|
| (a) Input = $21\sin 3.2\pi t$ | (d) Input to $N_2$ |
| (b) Error signal              | (e) System Output  |
| (c) Input to $N_1$            |                    |





## LIST OF REFERENCES

1. Douce, J. L., Discussion of a Paper by Ogata, Trans. ASME, vol. 80, no. 8, p. 1808, November 1958.
2. Gelb, A. and Vander Velde, W. E., Multiple-Input Describing Function and Nonlinear System Design, McGraw-Hill Book Company, 1968.
3. Gibson, J. E. and Sirdhar, R., A New Dual-Input Describing Function and an Application to the Stability of Forced Nonlinear Systems, Trans. AIEE, pt. II, Appl. Ind., p. 65-70, May 1963.
4. Han, K. W., Analysis and Design of Nonlinear Systems by Critical Curve and Critical Surface Methods, Project Report in connection with Nonlinear Control Systems Course, Naval Postgraduate School, 1962.
5. Hayashi, C., Nonlinear Oscillations in Physical Systems, McGraw-Hill Book Company, 1964.
6. Ogata, K., Subharmonic Oscillations of Nonlinear Feedback Control Systems, Trans. ASME, vol. 80, no. 8, p. 1802-1808, November 1958.
7. Oldenburger, R. and Nichols, R., Stability of Subharmonic Oscillations in Nonlinear Systems, Proc. JACC, Minneapolis, Minn., p. 675-680, June 1963.
8. Sawaragi, Y. and Akashi, H., Condition for the Subharmonic Oscillation in Relay Control Systems, The Science and Engineering Review of Doshisha University, vol. 3, no. 1, p. 19-35, May 1962.
9. Thaler, G. J. and Pastel, M. P., Analysis and Design of Nonlinear Feedback Control Systems, McGraw-Hill Book Company, 1962.
10. West, J. C. and Douce, J. L., The Mechanism of Subharmonic Generation in a Feedback System, Proc. IEEE, vol. 102, part B, no. 5, p. 569-574, September 1955.
11. West, J. L., Analytical Techniques for Nonlinear Control Systems, D. Van Nostrand Company, Inc., 1960.
12. West, J. C., Douce, J. L., and Livesly, R. K., The Dual-Input Describing Function and its Use in the Analysis of Nonlinear Feedback Systems, J. IEEE, London, vol. B-103, p. 463-472, July 1956.



# INITIAL DISTRIBUTION LIST

	No. Copies
1. Defense Documentation Center Cameron Station Alexandria, Virginia 22314	2
2. Library, Code 0212 Naval Postgraduate School Monterey, California 93940	2
3. Flag Officer In Command, Philippine Navy Roxas Boulevard, Manila Philippines	1
4. Professor G. J. Thaler (thesis advisor) Department of Electrical Engineering Naval Postgraduate School Monterey, California 93940	2
5. Department of Physical Sciences Philippine Military Academy Fort Del Pilar, Baguio City Philippines	1
6. Commanding Officer Ship Repair Yard Cavite Naval Base, Cavite City Philippines	1
7. Lt. (jg) Hasan Kocaoglu Dervis Ali mah. Kefeve sok. no. 12 Karagumruk, Istanbul Turkey	1
8. Lcdr. Emerson C. Tangan 2671 Int. 11 Juan Luna Gagalangin, Manila Philippines	2



UNCLASSIFIED

Security Classification

## DOCUMENT CONTROL DATA - R &amp; D

(Security classification of title, body of abstract and indexing annotation must be entered when the overall report is classified)

ORIGINATING ACTIVITY (Corporate author)		2a. REPORT SECURITY CLASSIFICATION	
Naval Postgraduate School Monterey, California 93940		UNCLASSIFIED	
		2b. GROUP	
REPORT TITLE			
Investigation of Subharmonic Oscillations in Nonlinear Second Order Systems.			
DESCRIPTIVE NOTES (Type of report and, inclusive dates)			
Master's Thesis, December 1970			
AUTHOR(S) (First name, middle initial, last name)			
Emerson Carag Tangan			
REPORT DATE	7a. TOTAL NO. OF PAGES	7b. NO. OF REFS	
December 1970	105	12	
a. CONTRACT OR GRANT NO.	9a. ORIGINATOR'S REPORT NUMBER(S)		
b. PROJECT NO.			
c.	9b. OTHER REPORT NO(S) (Any other numbers that may be assigned this report)		
d.			
DISTRIBUTION STATEMENT			
This document has been approved for public release and sale; its distribution is unlimited.			
11. SUPPLEMENTARY NOTES		12. SPONSORING MILITARY ACTIVITY	
		Naval Postgraduate School Monterey, California 93940	
3. ABSTRACT			

A nonlinear control system sometimes oscillate at a frequency that is an integral submultiple of the driving frequency in response to a sinusoidal input. Such a response is undesirable. An analog computer study is undertaken to investigate the occurrence of subharmonic oscillation in second order systems with nonlinearities characterized by saturation and hysteresis effects.



14. KEY WORDS	LINK A		LINK B		LINK C	
	ROLE	WT	ROLE	WT	ROLE	WT
Dual-Input Describing Function Subharmonic Resonance Limit Cycle						





Thesis  
T136  
c.1

Tangan

126117

Investigation of  
subharmonic oscilla-  
tions in nonlinear  
second order systems.

Thesis  
T136  
c.1

Tangan

126117

Investigation of  
subharmonic oscilla-  
tions in nonlinear  
second order systems.

thesT136

Investigation of subharmonic oscillation



3 2768 001 01379 0

DUDLEY KNOX LIBRARY